

POSITIONAL CLONING OF THE GCT1 GRANULOSA
CELL TUMOUR SUSCEPTIBILITY LOCUS IN SWR
INBRED MICE

KERRI NICOLE SMITH

POSITIONAL CLONING OF THE GCT1 GRANULOSA CELL TUMOUR
SUSCEPTIBILITY LOCUS IN SWR INBRED MICE

by

© Kerri Nicole Smith, B.Sc. (Hons)

A thesis submitted to the
School of Graduate Studies
in partial fulfillment of the
requirements for the degree of
Master of Science in Medicine

Faculty of Medicine
Memorial University of Newfoundland

July 2011

St. John's

Newfoundland

Abstract

Female mice of the SWR/Bm (SWR) inbred strain are susceptible to the spontaneous initiation of juvenile-onset granulosa cell (GC) tumours of the ovary at the onset of puberty. The mouse GC tumours share histological, endocrinological and malignant features with juvenile-type GC tumours found in infants and young girls, and thus the SWR strain represents a model system for the identification of susceptibility genes. Genetic mapping studies between the SWR strain and tumour-resistant strains have consistently associated the *Granulosa cell tumour susceptibility 1 (Gct1)* locus on distal mouse chromosome (Chr) 4 with the GC tumour phenotype. Mapping the trait for dehydroepiandrosterone (DHEA) induced GC tumour appearance in six congenic mouse sublines successfully resolved the *Gct1* locus to 1.51 Mb and a candidate list of 23 unique annotated protein coding genes, non-coding RNA genes, and other processed transcripts which may represent novel genes with biological activity. A qualitative assessment of prioritized genes within the refined *Gct1* interval did not exclude any from the ovarian compartment and therefore shared identity with *Gct1*. *Tnfrsf1b* was given top priority as a candidate gene given its described role in ovarian biology, but no conclusive sequence variation or expression differences unique to SWR were identified that indicated *Tnfrsf1b* is *Gct1*. Three other protein coding genes (*Dhrs3*, *Tnfrsf8*, and *Vps13d*) are present in the *Gct1* region and orthologous between mouse and human, and are promising candidates for *Gct1*.

Acknowledgments

First and foremost, I would like to thank my supervisor, Dr. Ann Dorward, for giving me this opportunity, having patience during my graduate training, and teaching me to think critically. I am also indebted to Dr. Dorward for helping to further my academic career by allowing me to attend conferences and apply for funding and scholarships. Her tireless efforts and great attitude towards research have not gone unnoticed, and I look forward to the next four years in the Dorward laboratory as I start my PhD program.

I would like to thank my supervisory committee, Dr. Sevtap Savas and Dr. Laura Gillespie. Their valuable comments and criticisms were greatly appreciated. Thanks also to the MacPhee laboratory, for welcome feedback throughout my graduate program.

Thank you to the members of the Dorward lab, past and present, for technical help: Heidi Wells, Chris Hough, Sarah Halfyard, Danielle Jackson, Clare Lewis, Ed Yaskowiak, and others. Thanks especially to Katie Macdonald, for being a great friend as well as a lab mate.

I would like to acknowledge the funding agencies that have financially supported me and this project: the Canadian Institutes of Health Research, Newfoundland and Labrador's Department of Innovation, Trade and Rural Development, and Memorial University of Newfoundland's School of Graduate Studies. Thanks also to the Faculty of Medicine's Office of Research and Graduate Studies, the Canadian Cancer Society and the Beatrice Hunter Cancer Research Institute for travel funds.

Finally, thank you to my friends, family, and loved ones. Your support and encouragement has been immeasurable

Table of Contents

Abstract.....	ii
Acknowledgments	iii
Table of Contents	v
List of Tables	vii
List of Figures.....	viii
List of Abbreviations	x
List of Appendices.....	xiv
1. Introduction	1
1.1 Ovarian Physiology	1
1.2 Ovarian Cancer	13
1.2.1 Granulosa Cell Tumours of the Ovary	15
1.3 Animal Models of Granulosa Cell Tumourigenesis	19
1.3.1 The SWR/Bm Mouse Model of Juvenile GC Tumourigenesis	23
1.4 Hypothesis and Research Objectives.....	40
2. Materials and Methods.....	41
2.1 Animal Husbandry	41
2.2 Phenotypic Mapping.....	42
2.2.1 Genotyping by Simple Sequence Length Polymorphisms.....	46
2.2.2 Genotyping by Single Nucleotide Polymorphisms.....	49
2.3 Serum Analysis	54
2.4 Gene Expression Analyses	55
2.4.1 Qualitative Gene Expression Analysis	61
2.4.2 Quantitative Gene Expression Analysis	63
2.5 Candidate Gene Sequencing.....	67
3. Results	69

3.1 Phenotypic Mapping of <i>Gct1</i>	69
3.1.1 Development of the Line 4-3 Recombinant Subcongenic Lines.....	69
3.1.2 Refining the Genetic Boundaries of <i>Gct1</i>	71
3.2 The Refined <i>Gct1</i> Interval.....	76
3.2.1. <i>In silico</i> Data.....	76
3.2.2 Qualitative Gene Expression Analysis.....	81
3.2.3 Quantitative Gene Expression Analysis.....	82
3.2.4 <i>Tnfrsf1b</i> Sequencing.....	85
4. Discussion.....	90
4.1 <i>Gct1</i> Resides Within a 1.51 Mb Interval.....	91
4.2 Prioritizing <i>Gct1</i> Candidates: Qualitative Expression Analysis.....	92
4.3 The <i>Gct1</i> Interval in Mouse and Human.....	93
4.4 Summary.....	101
4.5 Future Directions.....	102
5. References.....	104

List of Tables

Table 1.1	Genetically engineered mouse models of sex cord-stromal tumours	21
Table 1.2	Autosomal and X-linked loci associated with GC tumour susceptibility in SWR mice.....	27
Table 1.3	Descriptions of inbred and congenic mouse strains.....	39
Table 2.1	SSLP and SNP genotyping markers	47
Table 2.2	Qualitative expression analysis primers	62
Table 2.3	<i>Tnfrsf1b</i> sequencing primers.....	68
Table 3.1	SSLP and SNP genotyping markers	72
Table 3.2	Annotated and novel SNPs identified within gene candidates	74
Table 3.3	Annotated and novel SNPs identified within the fragment amplified by <i>D4kns1</i>	75
Table 3.4	Summary of the genetic determinants within the 1.51 Mb <i>Gct1</i> interval.....	79
Table 3.5	Relative gene expression in the mouse gonad	80
Table 3.6	Qualitative expression of the <i>Gct1</i> transcripts within the 1.51 Mb interval.....	83
Table 3.7	Serum DHEA levels in SWR and Line 4-T mice treated with DHEA or empty capsules.....	84
Table 3.8	Nucleotide changes in SWR <i>Tnfrsf1b</i> cDNA versus B6 and Line 4-T	88
Table 4.1	Relative gene expression in human and mouse gonads	96

List of Figures

Figure 1.1	Ovarian anatomy and cellular components	2
Figure 1.2	The hypothalamic-pituitary-gonadal axis.....	3
Figure 1.3	Sex determination in the bipotential gonad.....	5
Figure 1.4	Ovarian folliculogenesis.....	9
Figure 1.5	The two-cell, two-gonadotropin theory of follicle hormone regulation and production	11
Figure 1.6	Bilateral GC tumours isolated from a genetically susceptible female mouse	24
Figure 1.7	Impact of the allelic constitution at <i>Gct1</i> and the endocrine environment on GC tumour susceptibility in female mice.....	30
Figure 1.8	The steroid biosynthetic pathway for the conversion of substrate cholesterol to androgens and estrogens.....	31
Figure 1.9	Isolating <i>Gct1</i> in a congenic strain	34
Figure 1.10	Creating subcongenic strains to map <i>Gct1</i>	36
Figure 1.11	Chr 4 haplotypes of SWR and Line 4-T subcongenic mouse lines at <i>Gct1</i>	38
Figure 2.1	Phenotypic mapping paradigm for GC tumour susceptibility versus resistance.....	43
Figure 2.2	Sample collection paradigm for quantitative gene expression in the ovary and serum analysis.....	44
Figure 2.3	Quantitative <i>Tnfrsf1b</i> expression analysis paradigm.....	64
Figure 3.1	Chr 4 haplotypes of SWR, Line 4-3, and the SWR.SJL-X.CAST-4 recombinant subcongenic mouse lines at <i>Gct1</i>	70

Figure 3.2	Chr 4 haplotypes of SWR, Line 4-3, and the SWR.SJL-X.CAST-4 recombinant subcongenic mouse lines at the refined <i>Gct1</i> interval77
Figure 3.3	Ensembl screenshot of the 1.51 Mb <i>Gct1</i> interval78
Figure 3.4	Fold change in <i>Tnfrsf1b</i> mRNA relative to <i>Actb</i>86
Figure 3.5	Alignment of the SWR, Line 4-T and B6 <i>Tnfrsf1b</i> amino acid sequences87
Figure 4.1	Ensembl screenshot of the mouse <i>Gct1</i> interval and the orthologous human region on Chr 1p36.2294

List of Abbreviations

°C	degrees Celsius
α	Type I error
β	Type II error
μ g	microgram
μ L	microliter
μ M	micromolar
<i>Actb</i>	mouse beta-actin gene
AMH	anti-Müllerian hormone
<i>Amhr2</i>	mouse AMH receptor type 2 gene
<i>Ar</i>	mouse androgen receptor gene
B6	C57BL/6
BCL	B cell lymphoma/leukemia
BMP2	bone morphogenetic protein 2
bp	base pair
<i>BRCA1</i>	human breast cancer 1, early onset gene
<i>BRCA2</i>	human breast cancer 2, early onset gene
C	CAST allele
CAST	Castaneus
CD99	Cluster of Differentiation 99
cDNA	complementary DNA
Chr	chromosome
c-IAP1	cellular inhibitor of apoptosis 1
c-IAP2	cellular inhibitor of apoptosis 2
cm	centimeter
CO ₂	carbon dioxide
CT	threshold cycle
<i>Ctmb1</i>	mouse catenin (cadherin associate protein), beta 1 gene
Cys	cysteine
d	day
dbSNP	Single Nucleotide Polymorphism Database
DHEA	dehydroepiandrosterone
<i>Dhrs3</i>	mouse dehydrogenase/reductase (SDR family) member 3 gene
<i>DHRS3</i>	human dehydrogenase/reductase gene (SDR family) member 3 gene
DHT	dihydrotestosterone
DNA	deoxyribonucleic acid
DNase	deoxyribonuclease
dNTP	deoxynucleotide triphosphate
E	embryonic day
<i>E</i>	primer efficiency

E ₂	17β-estradiol
EDTA	ethylenediaminetetraacetic acid
ELISA	enzyme-linked immunosorbent assay
F	filial generation
<i>Fancd2</i>	mouse fanconi anemia, complementation group D2 gene
FIGO	International Federation of Gynecology and Obstetrics
<i>FOXL2</i>	human forkhead box L2 gene
FOXL2	human forkhead box L2 protein
FSH	follicle-stimulating hormone
<i>Fshr</i>	mouse follicle-stimulating hormone receptor gene
g	gram
GC	granulosa cell
<i>Gct</i>	granulosa cell tumour susceptibility
GDF9	growth differentiation factor 9
gDNA	genomic DNA
GnRH	gonadotropin-releasing hormone
H	height
h	hour
hCG	human chorionic gonadotropin
HCl	hydrochloric acid
HPG	hypothalamic-pituitary-gonadal
<i>Inha</i>	mouse inhibin-alpha gene
Iso-Hi-pH1	isotonic high pH1
J	SJL allele
JNK	Jun N-terminal kinase
kg	kilogram
KIT	kit ligand receptor
KITL	kit ligand
<i>KRAS</i>	human v-Ki-ras2 Kristen rat sarcoma viral oncogene homolog gene
L	length
LH	luteinizing hormone
<i>Lhb</i>	mouse luteinizing hormone beta gene
Line 4-3	SWR.SJL-X.CAST-4-3
Line 4-T	SWR.SJL-X.CAST-4-T
M	molar
MAPK	mitogen-activated protein kinase
Mb	megabase
<i>Men1</i>	mouse multiple endocrine neoplasia 1 gene
mg	milligrams
MGD	Mouse Genome Database
min	minute
mL	milliliter
mm	millimeter
mM	millimolar

MMLV-RT	Moloney murine leukemia virus reverse transcriptase
mo	month
mRNA	messenger RNA
<i>Mthfr</i>	mouse 5,10-methylenetetrahydrofolate gene
n	sample size
N	backcross generation
NCBI	National Center for Biotechnology Information
NF- κ B	nuclear factor kappa B
ng	nanograms
nm	nanometer
<i>Nobox</i>	mouse newborn ovary homeobox gene
<i>Nbbp</i>	mouse natriuretic peptide type B gene
OMIM	Online Mendelian Inheritance in Man
<i>P</i>	p-value
PCR	polymerase chain reaction
PGC	primordial germ cell
Phe	phenylalanine
pmol	picomole
<i>PTEEN</i>	human phosphatase and tensin homolog gene
qPCR	quantitative real time polymerase chain reaction
RA	retinoic acid
RI	recombinant inbred
RNA	ribonucleic acid
RNase	ribonuclease
rRNA	ribosomal RNA
RSPO1	R-spondin 1
RT	room temperature
s	second
SCST	sex cord-stromal tumour
SDR	short-chain dehydrogenase/reductase
Ser	serine
SJL	SJL/Bm
<i>Smad1</i>	mouse MAD homolog 1 gene
<i>Smad5</i>	mouse MAD homolog 5 gene
SNP	single nucleotide polymorphism
<i>Sohlh1</i>	mouse spermatogenesis and oogenesis helix-loop-helix 1 gene
<i>Sohlh2</i>	mouse spermatogenesis and oogenesis helix-loop-helix 2 gene
<i>SOX9</i>	(sex-determining region Y)-box gene 9 gene
<i>SRY</i>	sex-determining region on the Y chromosome gene
SSLP	simple sequence length polymorphism
<i>STK11</i>	human serine/threonine kinase 11 gene
SW	SWR allele
SWR	SWR/Bm
SWXJ	(SWR x SJL)

T	testosterone
Taq	<i>Thermus aquaticus</i>
TBE	tris borate ethylenediaminetetraacetic acid
TE	tris ethylenediaminetetraacetic acid
TGF β	transforming growth factor beta
TNF α	tumour necrosis factor alpha
<i>Tnfrsf1a</i>	mouse tumour necrosis factor receptor superfamily, member 1a gene
<i>Tnfrsf1b</i>	mouse tumour necrosis factor receptor superfamily, member 1b gene
<i>Tnfrsf1b</i>	mouse tumour necrosis factor receptor superfamily, member 1b protein
<i>Tnfrsf8</i>	mouse tumour necrosis factor receptor superfamily, member 8 gene
<i>TP53</i>	human tumour protein 53 gene
TRAF2	TNF receptor associated factor 2
Trp	tryptophan
<i>Trp53</i>	mouse transformation related protein 53 gene
UBA	ubiquitin-associated domain
UTR	untranslated region
V	volt
<i>Vps13d</i>	mouse vacuolar protein sorting 13 D (yeast) gene
<i>VPS13D</i>	human vacuolar protein sorting 13 D (yeast) gene
W	width
w/v	mass concentration
wk	week
WNT4	wingless-type MMTV integration site family, member 4

List of Appendices

Appendix A	Contributions.....	115
Appendix B	Copyright permission	116
Appendix C	Harvard PrimerBank IDs for primer sequences used in the qualitative gene expression analysis	119
Appendix D	Alignment of the SWR, Line 4-T, and B6 <i>Tnfrsf1b</i> cDNA nucleotide sequences.....	120

1. Introduction

1.1 Ovarian Physiology

Overview

The mammalian ovary is a highly specialized reproductive organ with two primary roles, the first of which is gametogenesis, or the production and release of developmentally competent haploid oocytes. Secondly, the ovary is an endocrine organ, and steroid hormone production by ovarian cells is critical for germ cell fertilization and embryo implantation, as well as other long term physiologic functions necessary for development of the adult organism. The mature ovary is enclosed within the ovarian bursa, and consists of an inner zone, the medulla, and an outer zone, the cortex (Figure 1.1). The medulla is highly vascularized and contains lymphatic vessels, nerves, and connective tissue. The cortex is covered by a layer of specialized surface epithelium, and immediately beneath this layer is the tunica albuginea, a dense strip of interstitial cells. Ovarian development is a complex process that begins with the specification and differentiation of primitive germ cells in the early embryo, followed by the organization of germ cells and somatic cells into ovarian follicles. The follicles, which reside in the cortical region, are the functional unit of the ovary that support the growing oocyte and are the source of estrogens and androgens. The hypothalamic-pituitary-gonadal (HPG) axis plays a critical role in normal follicle development (Figure 1.2). The hypothalamus secretes gonadotropin-releasing hormone (GnRH), which stimulates the gonadotrope

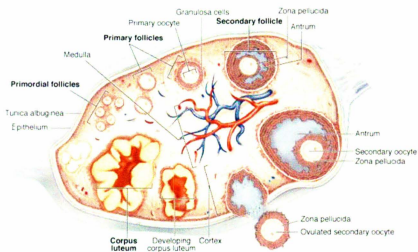


Figure 1.1 Ovarian anatomy and cellular components

The ovarian cortex is covered by a layer of surface epithelium, immediately above the dense tunica albuginea. Follicles composed of a single oocyte surrounded by the somatic granulosa and thecal cells reside amongst the interstitial cells in the cortical region. The inner medulla is highly vascularized and contains lymphatic vessels, nerves, and connective tissue (Copyright © 2010 by The McGraw-Hill Companies, Inc, used with permission).

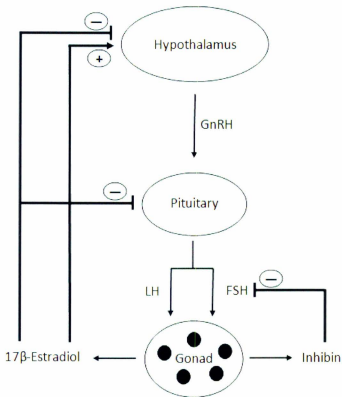


Figure 1.2 The hypothalamic-pituitary-gonadal axis

The hypothalamus secretes GnRH, which stimulates the gonadotrope cells of the anterior pituitary to release follicle-stimulating hormone (FSH) and luteinizing hormone (LH). Positive and negative feedback by steroids from the ovarian follicles stimulates and represses the secretion of FSH and LH depending on the follicle's phase of growth.

cells of the anterior pituitary to release FSH and LH. These gonadotropin hormones are cyclically regulated through both positive and negative feedback from the ovarian follicles following the pubertal transition, stimulating follicular growth and ultimately resulting in the preparation of mature oocytes for ovulation.

Ovarian Development

The gonads develop as bilateral thickenings of coelomic epithelium at the genital ridge, a region on the ventromedial surface of the embryonic kidney, or mesonephros, during week (wk) four of gestation in humans or embryonic day (E) 9.5 in the mouse (van Wagenen and Simpson 1965, Kaufman 1991). The primitive gonad is sexually undifferentiated and bipotential; it may differentiate into the testes or ovaries, depending on the presence or absence of the Y chromosome (Chr), and specifically the *Sex-determining region on the Y chromosome (SRY)* gene (Figure 1.3; Sinclair *et al.* 1990, Koopman *et al.* 1991). The indifferent gonad initially contains only somatic cells derived from the coelomic epithelium and mesonephros. Primordial germ cells (PGCs), the precursors of mature oocytes, are initially identical in XX and XY gonads. Prior to gonad formation, PGCs in the mouse differentiate from a clustered cohort of approximately 45 proximal epiblast progenitor cells, adjacent to the extraembryonic ectoderm at the base of the allantois (Gardner and Rossant 1979, Lawson and Hage 1994). Following the breakdown of the PGC cluster, individual PGCs migrate to the genital ridge during the fifth wk of gestation in humans and from E9.5 to E11.5 in the

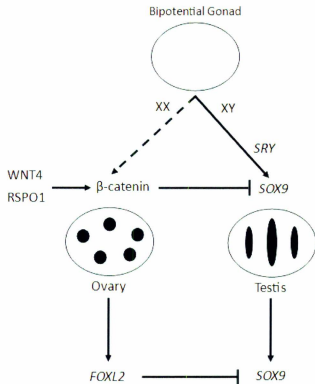


Figure 1.3 Sex determination in the bipotential gonad

WNT4 (Wingless-type MMTV integration site family, member 4) and RSPO1 (R-spondin 1) stabilize β -catenin in the embryonic XX gonad, preventing the *SRY*-induced expression of *SOX9* and subsequent testis formation. Following ovarian development, *FOXL2* (Forkhead box L2) actively maintains ovarian somatic cell differentiation. Adapted from Uhlenhaut *et al.* (2009).

mouse (Everett 1943, Mintz and Russell 1957, Kurilo 1981). Dorsal PGC migration from the allantois through the hindgut is directed by the chemoattractant signaling action of KIT ligand (KITL) and its receptor KIT (Farini *et al.* 2007). KITL/KIT signaling is also required for PGC survival during migration (reviewed by Saga 2008). Throughout migration and colonization of the gonad, the PGCs undergo mitotic proliferation which expands the population to around 26,000 cells in the mouse (Bowles and Koopman 2007). At this point in embryogenesis, the gonad is still indifferent and PGC differentiation, migration, and proliferation are identical between XY and XX embryos. However, around the time of gonad colonization, XY gonads express *SRY*, which acts through its target gene, (*Sex-determining region Y*)-box gene 9 (*SOX9*) to trigger the differentiation of the gonad towards a testis fate (Hacker *et al.* 1995, Jeske *et al.* 1995, Sekido *et al.* 2004). PGCs in XX gonads differentiate into oogonia; once thought to be a passive, default pathway due to the absence of *SRY*, female gonad differentiation is now known to be an active process regulated by WNT4 (Wingless-type MMTV integration site family, member 4) and RSPO1 (R-spondin 1). As shown in Figure 1.3, WNT4 and RSPO1 stabilize β -catenin, inhibiting *SOX9* expression in the female gonad (Maatouk *et al.* 2008). The transcription factor Forkhead box L2 (FOXL2) is required to actively suppress the differentiation of ovarian somatic cells to the male fate post-gonad differentiation (Uhlenhaut *et al.* 2009). When XX gonad colonization is complete, further mitotic proliferation increases the germ cell pool, and by 20 wk gestation in humans approximately seven million oogonia are present (Baker 1963). Mitotic PGC proliferation is characterized by incomplete cytokinesis, which results in clusters of

daughter cells connected by intracellular bridges, termed germ cell cysts (Pepling and Spradling 2001). The end of germ cell production, at wk 24 in humans or E13.5 in the mouse, is marked by the initiation of meiosis, a process initiated by retinoic acid (RA), a form of vitamin A (Bowles *et al.* 2006, Koubova *et al.* 2006). The oogonia proceed through the leptotene, zygotene and pachytene stages of prophase I, but arrest at the diplotene stage. Now called primary oocytes, the diploid germ cells remain in a perpetual quiescent state until just before ovulation when they complete the first meiotic division. In the second trimester of human development and immediately after birth in the mouse, germ cell cysts begin to breakdown. The oocytes are subject to extensive apoptosis during cyst breakdown (Ruby *et al.* 1969, Pepling and Spradling 2001). This process, termed oocyte attrition, is thought to be controlled by the B cell lymphoma/leukemia (BCL) and caspase protein families (reviewed by Tilly 2004). The surviving oocytes constitute a finite and non-renewable ovarian reserve, although it has recently been postulated that *de novo* oocytes are able to differentiate from stem cells (Johnson *et al.* 2004).

Folliculogenesis

Follicular development is a tightly regulated process that relies on bi-directional communication between the oocyte and its surrounding somatic cells to coordinate follicle growth, recruitment and selection in concert with follicle death (Eppig *et al.* 2002). Following breakdown of the germ cell cysts, the remaining oocytes become

organized into primordial follicles consisting of an oocyte surrounded by a single layer of somatic-derived, squamous pre-granulosa cells (GCs; Figure 1.4). A basement membrane separates the pre-GC layer from the surrounding stromal cells, excluding vascular networks from the inner follicle (Baker 1963, Hirshfield 1991). The process of follicular atresia, or death of the follicles by apoptosis, begins after the formation of primordial follicles and continues throughout life. Oocyte attrition and follicular atresia result in substantial germ cell loss, such that the human ovary contains approximately one million oocytes within resting primordial follicles at birth (Baker 1963). The pool of resting primordial follicles is depleted by follicle degeneration and the continuous initiation of follicle growth and ovulation. The exact molecular mechanisms that prompt initial recruitment into the growing population are still under speculation, although a number of genes have been implicated. Follicles in mice null for the *Newborn ovary homeobox (Nobox)* gene cannot progress past the primordial stage (Rajkovic *et al.* 2004). Mice with deletions of either the *Spermatogenesis and oogenesis helix-loop-helix 1 (Sohlh1)* gene or *Sohlh2* show a similar phenotype (Pangas *et al.* 2006, Choi *et al.* 2008, Hao *et al.* 2008). Furthermore, down-regulation of KITL during early mouse folliculogenesis results in a decreased pool of growing follicles compared to controls, as well as arrested growth at the primordial stage (Kuroda *et al.* 1988, Huang *et al.* 1993, Bedell *et al.* 1995). Primordial follicles that enter the growing pool progress to the primary stage, which is marked by growth of the oocyte and its surrounding GC layer, as well as the *FOXL2*-dependent transition of GCs from a squamous to cuboidal morphology (Schmidt *et al.* 2004, Uda *et al.* 2004). Cellular communication between

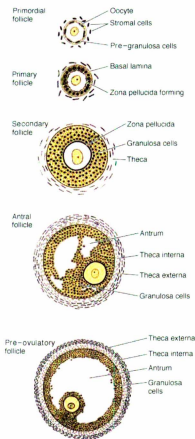


Figure 1.4 Ovarian folliculogenesis

Primordial follicles that are recruited for growth from the quiescent primordial pool progress to the primary stage. Multiple GC layers and the theca layer are characteristics of secondary follicles. Following antrum formation, select follicles are recruited for further growth, although only one or a subset of these are eventually ovulated in humans or mouse, respectively (Copyright © 2010 by The McGraw-Hill Companies, Inc, used with permission).

adjacent GCs is achieved via gap junctions composed of homologous connexin complexes organized to form a connexon structure with a central channel (Juneja *et al.* 1999). Follicles committed to the growth phase also acquire a zona pellucida between the oocyte and GC layer. GCs extend cytoplasmic projections through the zona pellucida to contact the oocyte through heterologous connexons (Simon *et al.* 1997). These gap junction networks provide bi-directional communication between the oocyte and GCs and are essential for growth of the follicle and germ cell maturation. The oocyte-specific Growth differentiation factor 9 (GDF9) is necessary for the progression of the follicle from the primary to secondary stage due to its promotion of GC proliferation (Dong *et al.* 1996, Elvin *et al.* 1999). Secondary, or pre-antral, follicles are characterized by a double layer of GCs around the oocyte, and an outer thecal cell layer that differentiates from surrounding stromal cells. The theca is vascularized and provides a connection with the body's circulatory system (Hirshfield 1991). Follicles progress to the antral stage when the aggregation of small fluid-filled cavities forms the antrum, accompanied by the differentiation of the theca into two distinct layers: theca interna and theca externa.

The stages of folliculogenesis prior to and including secondary follicle formation are independent of the pituitary gonadotropins FSH and LH, and the transition from pre-antral to antral at the pubertal onset marks the start of follicular regulation by the HPG axis. The recruitment of a small cohort of antral follicles for further growth, termed cyclic recruitment, occurs after the start of puberty. Cyclic follicle recruitment is initiated by FSH; antral follicles that are not recruited face death by atresia. Expression of the enzymes necessary for steroid hormone production by follicular cells is controlled by FSH and LH (Figure 1.5). GCs in antral follicles are capable of producing 17 β -estradiol

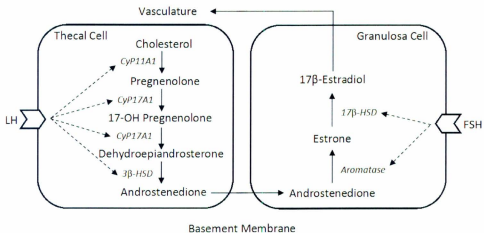


Figure 1.5 The two-cell, two-gonadotropin theory of follicle hormone regulation and production

LH stimulation of thecal cells results in the expression of the steroidogenic enzymes necessary for androgen synthesis from cholesterol precursors, as well as the transport of cholesterol into the inner mitochondrial membrane. FSH stimulates GCs and up-regulates the enzymes necessary for aromatization of androgens to estrogens, and is later essential for the expression of LH receptors on the GC surface.

(E₂) using androgenic substrates produced by the thecal cells in response to gonadotropin stimulation. Low levels of E₂ secreted by GCs exert negative feedback on GnRH secretion from the hypothalamus, as well as FSH and LH secretion from the pituitary, preventing the FSH-induced development of new antral follicles within the same cycle. Except in the case of dizygotic twins, a single follicle from the antral cohort is selected for ovulation and becomes the dominant follicle in humans, whereas in mice, selection for and ovulation of multiple oocytes occurs every cycle. The exact factors regulating specific follicle selection and dominance are undefined, but may be due to a threshold of FSH sensitivity (Fauser and van Heusden 1997). Shortly before ovulation, increasing E₂ levels peak and result in the positive regulation of GnRH. High E₂ levels result in dramatically increased levels of LH, known as the LH surge, whereas FSH secretion is negatively regulated by the GC-secreted peptide hormone inhibin. During this time, meiosis resumes within the dominant follicle germ cell, and the diploid primary oocyte becomes a haploid secondary oocyte. The LH surge results in a cascade of events leading to the rupture of the ovarian surface epithelium and extrusion of the oocyte and its surrounding GC layer. Following ovulation, the follicular remnants collapse and become luteinized through terminal differentiation, forming the corpus luteum, a transient and highly vascularized progesterone-secreting tissue. The processes of folliculogenesis in both species work continuously to recruit waves of follicle cohorts to the growing pool, so that following ovulation new follicles have reached the antral stage and can become destined for ovulatory dominance through cyclic recruitment. This repetitive process of initial recruitment, follicle growth, and cyclic recruitment, complemented by oocyte attrition and follicular atresia, create a balanced dynamic of life and death in the ovary

that eventually results in the complete depletion of the ovarian reserve at the close of reproductive life.

1.2 Ovarian Cancer

Ovarian cancer is the second most common gynecological malignancy, and ranks as the fifth deadliest cancer among Canadian women (Canadian Cancer Society 2011). Approximately 1 in 69 women will be diagnosed with and 1 in 92 women will succumb to the disease annually (Canadian Cancer Society 2011). Ovarian cancer symptoms are generally non-specific or absent and reliable biomarkers are lacking, two factors which contribute to the diagnosis of late stage tumours that show resistance to traditional chemotherapeutic methods and often recur. The overall five-year survival rate for such late stage cases is approximately 30%, though this figure increases to 80% for those diagnosed early (Jemal *et al.* 2008). The majority of women are diagnosed during the fifth and sixth decades of life, although ovarian cancer occurs in all age groups (Koonings *et al.* 1989).

Traditionally, human tumours of the ovary have typically been thought to arise from one of the three ovarian cell components, and as such are divided into three major classes. Tumours arising from the surface epithelium surrounding the ovary, termed epithelial ovarian tumours, account for 90% of ovarian cancers (Crum 1999). Approximately 7% of ovarian cancers are sex cord-stromal tumours (SCSTs) derived from cells specialized in steroid hormone production, including the granulosa and theca

cells surrounding ovarian follicles (Colombo *et al.* 2007). Finally, germ cell tumours derived from the oocytes represent 1-2% of malignant ovarian neoplasms (Pectasides *et al.* 2008). The remaining percentage of ovarian tumours are metastases from distant sites. All three classes of ovarian cancer are further divided into distinct subtypes based mainly on histology. Recent advances in the management of ovarian cancer have focused on recognizing and treating individual subtypes as separate diseases.

The single most common subtype of ovarian cancer in Canadian women is high-grade serous carcinoma, a subtype of the epithelial ovarian tumour class (Köbel *et al.* 2010). The etiology of malignant ovarian tumours is mechanistically undefined, and due to the high incidence of epithelial ovarian cancer, the majority of research has been focused on this tumour class. The most popular theory of ovarian cancer origin is that of “incessant ovulation” (Fathalla 1971), which posits that ovulation disrupts the ovarian surface epithelium, and its subsequent proliferative repair increases the risk for the accumulation of deleterious mutations. This hypothesis is supported by the protective roles of ovulation-blocking oral contraceptive use and pregnancy, and the increased risk associated with early menarche and late menopause (Casagrande *et al.* 1979, Purdie *et al.* 2003). Recently, researchers have proposed that some epithelial ovarian cancers are caused by the incorporation of dislodged fallopian tube epithelial cells into the ovary following ovulation, or are in actuality secondary cancers arising from malignant lesions in nearby tissues, particularly the fallopian tube (Kurman and Shih 2010). The observation that salpingo-oophorectomy (removal of the fallopian tubes and ovaries) reduces ovarian cancer risk, particularly in women with an increased risk due to familial

mutations in the *Breast cancer 1, early onset (BRCA1)* and *BRCA2* tumour suppressor genes, supports this hypothesis (Kauff *et al.* 2002). However, neither of these theories explain events leading to malignancy in the SCST or germ cell tumour types, which arise from distinct cell types below the ovarian surface. Furthermore, a number of somatic and germline mutations in human tumour suppressor genes and oncogenes have been associated with an increased risk of epithelial ovarian cancer initiation and progression, including *BRCA1* and *BRCA2*, *Tumour protein 53 (TP53)*, *v-Ki-ras2 Kristen rat sarcoma viral oncogene homolog (KRAS)*, and *Phosphatase and tensin homolog (PTEN)*; reviewed by Bast *et al.* 2009) – however, mutations in these genes are not generally associated with ovarian tumours derived from other cell types. Finally, the increased risk associated with ovulatory events over a woman’s lifetime is not applicable to juvenile forms of ovarian cancer, suggesting a strong predisposing genetic component for ovarian cancer susceptibility in such cases.

1.2.1 Granulosa Cell Tumours of the Ovary

Approximately 70% of SCSTs are GC tumours (Colombo *et al.* 2007), which according to the World Health Organization Classification of Gynecologic Tumours, are SCSTs composed of a 10-100% GC component (Tavassoli *et al.* 2003). GC tumours are divided into two clinicopathologic subtypes, adult and juvenile, based on histology and age at tumour diagnosis. Unlike epithelial ovarian cancers, GC tumours occur at either end of the reproductive spectrum. Adult GC tumours are more common, and typically

occur in peri- and post-menopausal women (Björkholm and Silfverswärd 1981). Juvenile GC tumours most commonly affect young girls from newborns through adolescence; Young *et al.* (1984) found 44% occurred in the first decade, 34% in the second, 18% in the third, and only 3% after age 30.

The rarity of juvenile GC tumours in the human population has precluded investigations into their etiology. A small number of cases have occurred in patients with Ollier disease and Maffucci syndrome (OMIM 166000), diseases characterized by the development of multiple enchondromas or enchondromas and hemangiomas, respectively (Young *et al.* 1984). Generally considered sporadic, these conditions have not been associated with any genetic determinants conferring susceptibility. GC tumours can develop in human females with Peutz-Jeghers syndrome (OMIM 175200), a hamartomatous disease caused by germline mutations in the tumour suppressor *Serine/threonine kinase 11 (STK11)* gene (formerly *LKB1*; Dozois *et al.* 1970, Hemminki *et al.* 1998). However, Kato *et al.* (2004) found no association between sporadic GC tumours and *STK11* mutations in patients without Peutz-Jeghers syndrome, but did find loss of heterozygosity near the *STK11* locus in 50% of sporadic GC tumours examined. Loss of the wild-type *STK11* allele may therefore be a consequence of tumour progression in sporadic cases. Recently, Shah *et al.* (2009) performed whole-transcriptome sequencing of adult GC tumours, and identified a recurrent, somatic c.402C>G mutation in the *FOXL2* gene, the transcription factor required to maintain female gonad identity and GC differentiation during folliculogenesis, in 97% of cases examined. Although the mechanism of this p.Cys134Trp mutation in adult GC tumour

initiation is still unknown, it was notably absent from juvenile GC tumours, indicating the two subtypes have distinct genetic etiologies (Al-Agha *et al.* 2011). Cytogenetic aberrations, including trisomy Chr 12 and monosomy Chr 22, have been detected in some human juvenile GC tumours, although these events likely represent a consequence of tumour progression rather than a requirement for tumour initiation (Schofield and Fletcher 1992, Shashi *et al.* 1994, Halperin *et al.* 1995, Lindgren *et al.* 1996).

The largest series of human juvenile GC tumours examined to date was reported by Young *et al.* (1984). The majority of juvenile GC tumours present with acute endocrine symptoms, with or without a palpable abdominal mass. Abdominal pain and swelling may also be present, and ascites are observed in approximately 10% of cases. Most tumours are estrogenic due to functioning GCs, with symptoms depending on the patient's age and reproductive status. Young *et al.* (1984) also found that 82% of female infants and pre-pubertal children present with isosexual pseudoprecocity, characterized by the growth of pubic and/or axillary hair, breast development, uterine bleeding, vaginal discharge, and accelerated somatic and skeletal growth. In adolescent girls and adult women, the most common endocrine symptoms of juvenile GC tumours are amenorrhea and irregular uterine bleeding due to estrogen stimulation of endometrial hyperplasia (Young *et al.* 1984). Rare cases of androgenic juvenile GC tumours resulting in virilization have been reported (Young *et al.* 1984, Nomellini *et al.* 2007), suggesting that the ability of the aberrant GCs to convert androgens to estrogens has been compromised. Most tumours secrete excessive levels of inhibin (Sivasankaran *et al.* 2009), and serum inhibin, E₂, and anti-Müllerian hormone (AMH) are used as tumour biomarkers

(Silverman and Gitelman 1996).

Macroscopic examination has revealed that the average diameter of juvenile GC tumours is 12.5 cm in patients. Most tumours are unilateral, although bilateral cases have been reported. The majority of tumours are uniformly solid and cystic, and usually vary in color from yellow to gray-white to pink. Localized areas of necrotic or hemorrhagic tissue may be present (Young *et al.* 1984, Scully *et al.* 1998). Microscopically, juvenile GC tumours show a distinct nodular or diffuse pattern of neoplastic GCs, often with large oval or round rudimentary follicles containing eosinophilic or basophilic fluid. The GCs and theca cells may be luteinized, and are present in a fibrothecomatous background. In contrast to adult GC tumours, the juvenile subtype shows GCs with immature and hyperchromatic nuclei (Young 2005). Mitotic activity is generally higher in juvenile GC tumours compared to the adult subtype (Scully *et al.* 1998, Young 2005). In addition to AMH and inhibin, juvenile GC tumours also show positive immunohistochemical staining for calretinin, CD99, and FOXL2 (Matias-Guiu *et al.* 1998, McCluggage and Maxwell 2001, Al-Agha *et al.* 2011).

The majority of juvenile GC tumours are diagnosed at FIGO (International Federation of Gynecology and Obstetrics) stage I; however, the disease is almost always fatal at advanced stages (Young *et al.* 1984). Treatment for early stage tumours is usually surgical debulking, with adjuvant platinum-based chemotherapy for advanced stage and recurrent cases. Tumours that recur tend to do so within three years, and metastatic recurrence is more common in the juvenile subtype compared to adult GC tumours (Young *et al.* 1984, Geetha and Nair 2010).

In the absence of a clear genetic etiology for juvenile GC tumours, the ability to predict susceptibility, accurately treat both primary and recurrent cases, and estimate patient survival is severely hindered. The knowledge that juvenile GC tumours initiate in infants and young girls with an intact ovarian reserve prior to normal follicle recruitment, as well as the absence of the somatic mutation in *FOXL2* reported in adult GC tumours, suggests that the two subtypes have different etiologies. To define the genetic determinants responsible for the initiation of these juvenile GC tumours, researchers have used model mammalian systems for genetic analyses.

1.3 Animal Models of Granulosa Cell Tumourigenesis

Sex cord-stromal tumours are the most common spontaneous ovarian neoplasms affecting laboratory rodents, including mice, gerbils, rats and guinea pigs (Greenacre 2004, Thayer and Foster 2007). GC tumours occur at variable frequencies in different inbred strains of mice, particularly in aged mice. CE/WyJ inbred mice are naturally susceptible to GC tumours, with 34% of females affected by 22 months (mo; Dickie 1954). Aged NZC/B1 inbred mice also spontaneously develop GC tumours at a 33% frequency (Bielschowsky and D'Ath 1973, Geary 1984). Furthermore, aged CF-1 and C3H/HeNtr inbred mice are spontaneously susceptible to ovarian tumours at 17% and 37% frequencies, respectively, although tumour subtype classifications have not been reported (Breslow *et al.* 1974, Frith *et al.* 1981). Despite the abundance of mouse strains spontaneously affected by GC tumours, no genes conferring resistance or susceptibility

have yet been identified. Furthermore, these late-onset GC tumour models are observed at a time when the ovary is at or near follicle depletion, and as such are reflective of the adult GC tumour condition rather than the juvenile condition.

In addition to the spontaneous models of GC tumourigenesis, a number of models have been engineered through genetic alterations of oncogenes and tumour suppressor genes, genes critical to normal endocrine function, and/or genes expressed exclusively in ovarian GCs (Table 1.1). Mice null for *Inhibin alpha (Inha)* lose the normal negative feedback regulation required to suppress FSH, and 90% of animals develop SCSTs as early as 1 mo of age (Matzuk *et al.* 1992). Targeted expression of the Simian virus 40 T-antigen under the control of the *Inha* promoter in ovarian stromal cells results in complete GC tumour penetrance in mice between 5 and 7 mo (Rahman *et al.* 1998). Risma *et al.* (1995) introduced a transgenic LH β -subunit into female mice, which resulted in an increased LH half-life and subsequently elevated levels of serum testosterone (T) and E₂. GC tumours develop in 100% of these transgenic mice at 5 mo, albeit in a strain-dependent manner, suggesting the influence of additional modifier genes (Keri *et al.* 2000). Danilovich *et al.* (2001) found that half of female mice null for the *FSH receptor (Fshr)* gene spontaneously develop SCSTs by 12 mo. Homozygous knockout of the *Fanconi anemia, complementation group D2 (Fancd2)* gene with heterozygosity for the *Transformation related protein 53 (Trp53)* gene results in tumours with GC components in 30% of mice aged 14-15 mo (Houghtaling *et al.* 2005). 129P2/OlaHsd and 129/Sv mice that are heterozygous for the *Multiple endocrine neoplasia 1 (Men1)* gene develop tumours in multiple endocrine organs, including SCSTs, with 50% affected by 19-26 mo

Table 1.1 Genetically engineered mouse models of sex cord-stromal tumours. KO: knockout

Tumour Type	Affected Gene	Chr Location (mouse)	Nature of Mutation	Age of GC Tumour Onset	GC Tumour Frequency	Reference
mixed SCST	<i>Inha</i>	1	KO	1 mo	90%	Matzuk <i>et al.</i> 1992
mixed SCST	<i>Fancd2</i>	6	KO (<i>Trp53</i> heterozygous)	14-15 mo	30%	Houghtaling <i>et al.</i> 2005
GC	<i>Lhb</i>	7	Transgenic <i>LH β</i> -subunit	5 mo	100%	Keri <i>et al.</i> 2000
GC	<i>Smad1/Smad5</i>	8/13	Double KO	3 mo	100%	Pangas <i>et al.</i> 2008
GC	<i>Ctnnb1</i>	9	Constitutive activation	7.5 mo	57%	Boerboom <i>et al.</i> 2005
mixed SCST	<i>Fshr</i>	17	KO	12 mo	50%	Danilovich <i>et al.</i> 2001
mixed SCST	<i>Men1</i>	19	Heterozygous KO	12-26 mo	0-50%	Bertolino <i>et al.</i> 2003

(Bertolino *et al.* 2003). Finally, the targeted mutation of genes specifically in ovarian GCs has been accomplished using *cre* recombinase expression driven by the *AMH receptor type 2 (Amhr2)* gene promoter. Boerboom *et al.* (2008) utilized this system and found that GC-targeted constitutive activation of β -catenin transcription factor (*Ctmb1*) results in GC tumours in 57% of mice by 7.5 mo. Conditional double knockout of the TGF β family members *MAD homolog 1 (Smad1)* and *Smad5* in GCs via the *Amhr2* promoter system resulted in GC tumour development in mice by 3 mo with complete penetrance (Pangas *et al.* 2008).

It is evident that deletion of tumour suppressor genes or transcription factors important for GC growth control leads to highly predictable tumour development, in a species inherently susceptible to SCSTs. Given the wealth of information obtained to date from the study of the mouse ovary as a model for human ovarian physiology, it is fair to speculate that these proteins could play a role at some point during GC tumour initiation or progression in human patients. At the level of genetic mutation, analysis of *Trp53*, *Fshr* and *Inha* have not revealed GC tumour susceptibility candidates in adult-onset human GC tumours (Watson *et al.* 1997, Fuller *et al.* 1998, Horny *et al.* 1999), although epigenetic mechanisms that may down-regulate their expression have not been reported. For human adult GC tumours, a specific, somatic mutation in the *FOXL2* gene is the strongest associative mutation reported to date, yet for juvenile-onset GC tumours, little to no genetic information is available. This research thesis has focused upon a spontaneous model for juvenile-onset GC tumour development in an inbred mouse strain, as a means to define a genetic locus that confers susceptibility to GC tumour initiation at

a pre-pubertal stage in the presence of normal endocrinological stimulation, and provide new insight to the pathways that drive juvenile-onset GC tumourigenesis.

1.3.1 The SWR/Bm Mouse Model of Juvenile GC Tumourigenesis

The SWR/Bm (SWR) inbred mouse strain and its related recombinant inbred and congenic derivatives are unique in their heritable and spontaneous GC tumour phenotype that affects $\leq 1\%$ to approximately 25% of the young female population, depending on strain background (Beamer *et al.* 1985). The GC tumours first arise during a restricted initiation window at 3 to 4 wk of age, as pre-neoplastic blood-filled follicles that are macroscopically visible on the ovarian surface (Tennent *et al.* 1990). Those females that progress through the pubertal transition unaffected remain tumour-free, retain fertility with average litter sizes, and age normally without the development of other primary tumours. The follicular lesions found at 3 to 4 wk are composed of degenerating oocytes surrounded by a large fluid- or erythrocyte-filled antrum lined by irregular masses of GCs and hypertrophied theca cells. Within 6 to 8 wk, the tumours progress to a highly vascularized, cystic or hemorrhagic mass homogenously comprised of GCs and enclosed within the ovarian bursa, with occasional luteinized or necrotic areas (Beamer *et al.* 1985, Tennent *et al.* 1990; Figure 1.6). The mouse GC tumours may be unilateral or bilateral, and their malignant potential has been demonstrated by tumour occurrence in both ovariectomized and intact transplant hosts that leads to death within 3 to 5 mo (Beamer *et al.* 1985). Furthermore, Tennent *et al.* (1990) found 42% of mice with GC tumours aged

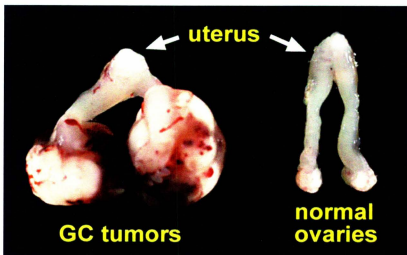


Figure 1.6 Bilateral GC tumours isolated from a genetically susceptible female mouse.

The tumours and uterus were removed at 8 wk. The normal ovaries and uterus from a littermate are shown for comparison.

6 to 9 mo had metastases in major abdominal and thoracic organs, particularly the renal lymph nodes, liver, and lungs. The mouse GC tumours secrete high levels of estrogens and inhibin, mimicking their human juvenile GC tumour counterparts (Beamer *et al.* 1988a, Gocze *et al.* 1997). Excessive estrogen output from the mouse GC tumours is reflected in significantly increased estrogen-responsive uterine weights and high percentages of cornified vaginal cells (Beamer *et al.* 1988a), as well as the suppression of the contralateral ovary, which ceases ovulation (Beamer *et al.* 1985). Mice with GC tumours have decreased levels of hypothalamic GnRH, pituitary FSH and LH, and serum FSH, progesterone, dihydrotestosterone (DHT) and T (Beamer 1986). This unique and heritable trait of early-onset GC tumorigenesis occurs at puberty, prior to the depletion of the ovarian reserve, and shows numerous parallels with the human juvenile condition; therefore, the SWR mouse is a promising spontaneous animal model for the identification of genes involved in the initiation of GC tumours in infants and young girls.

Spontaneous GC tumour appearance in SWR mice is a hormone-sensitive trait. Tumour grafting studies have determined that an intact HPG axis is required for GC tumour development, such that transfer of pre-pubertal, genetically susceptible ovaries to host mice that are hypogonadal and incapable of sex steroid production do not support GC tumour development (Beamer *et al.* 1993). In the intact SWR female mouse, tumour frequency is significantly increased with exogenous treatment of the functional LH analog human chorionic gonadotropin (hCG), as well as downstream androgens dehydroepiandrosterone (DHEA) and T synthesized by thecal cells in response to LH during the pubertal transition (Beamer *et al.* 1988a, Tennent *et al.* 1993, Dorward *et al.*

2007). In accordance with the lack of spontaneous GC tumour development outside the restricted susceptibility window, post-pubertal treatment with these hormones does not stimulate GC tumour initiation (Beamer *et al.* 1993). Furthermore, short-term exposure to E₂ before, but not after, the appearance of pre-neoplastic follicular lesions suppresses GC tumour incidence (Dorward *et al.* 2007), indicating that the window of tumour initiation overlaps with that of tumour prevention in the mouse model. This precise hormonal regulation suggests that the first pubertal LH wave and subsequent downstream androgenic signaling stimulates GC tumour initiation, and suppression of initiation by E₂ occurs due to the inhibition of LH release from the anterior pituitary.

Genetics

The trait of juvenile-type GC tumour appearance is polygenic in SWR mice, and multiple autosomal and X-linked loci influence GC tumour initiation (Table 1.2). To overcome the issue of low penetrance in the mouse model, initial efforts to identify these loci involved incredibly high numbers of animal examinations. Genomic loci that showed significant linkage to spontaneous GC tumour initiation were named *Granulosa cell tumour susceptibility (Gct)* loci, until such time that genes and alleles are identified. The GC tumour susceptibility genes function autonomously within the ovarian compartment, as ovaries obtained from genetically susceptible females develop GC tumours when transferred to endocrinologically normal, pre-pubertal female hosts that are genetically resistant to GC tumour development (Beamer *et al.* 1993). Despite the drastic

Table 1.2 Autosomal and X-linked loci associated with GC tumour susceptibility in SWR mice

Locus	Chr	Mapping Cross	Reference
		Partner Strains	
<i>Gct1</i>	4	SWR/SJL	Beamer <i>et al.</i> 1988b
		SWR/SJL	Beamer <i>et al.</i> 1998
		SWXJ-9/CAST	Dorward <i>et al.</i> 2005
<i>Gct2</i>	12	SWR/SJL	Beamer <i>et al.</i> 1998
<i>Gct3</i>	15	SWR/SJL	Beamer <i>et al.</i> 1998
<i>Gct4</i>	X	SWR/SJL	Beamer <i>et al.</i> 1998
		SWR/CAST	Dorward <i>et al.</i> 2003
<i>Gct5</i>	9	SWR/SJL	Beamer <i>et al.</i> 1998
<i>Gct6</i>	X	SWR/CAST	Dorward <i>et al.</i> 2003
<i>Gct7</i>	1	SWXJ-9/CAST	Dorward <i>et al.</i> 2005
<i>Gct8</i>	2	SWXJ-9/CAST	Dorward <i>et al.</i> 2005
<i>Gct9</i>	13	SWXJ-9/CAST	Dorward <i>et al.</i> 2005

effect observed in females, no discernable phenotypic consequence of the GC tumour susceptibility alleles in male SWR mice has been observed.

Although GC tumour susceptibility is a complex trait involving multiple hereditary loci, a significant body of genetic evidence supports the *Gct1* locus on distal Chr 4 as fundamental for spontaneous tumour initiation, with susceptibility alleles contributed by the SWR strain (*Gct1*^{SWR}). *Gct1* has been consistently associated with the spontaneous GC tumour phenotype in three independent mapping crosses. Beamer *et al.* (1988b) generated 14 recombinant inbred (RI) SWXJ strains (SWXJ-1 through 14) from SWR and the naturally GC tumour resistant inbred strain SJL/Bm (SJL), and found a significant association linking both spontaneous and androgen-induced GC tumour occurrence with SWR-derived distal Chr 4. A second mapping cross using (SWR x SJL)₂F₂ mice examined spontaneous GC tumour frequency, and confirmed the importance of the *Gct1* locus, placing it within the vicinity of the simple sequence length polymorphism (SSLP) deoxyribonucleic acid (DNA) marker *D4Mit232* with high significance (Beamer *et al.* 1998). Finally, to improve mapping resolution and for experimental replication of suggested autosomal determinants related to spontaneous tumour initiation, a third mapping cross between GC tumour susceptible SWXJ-9 mice and the GC tumour resistant Castaneus (CAST) mouse strain was performed using an N₂F₁ backcross strategy. The CAST strain is a common mapping partner in mouse mapping crosses, given its genomic divergence from more common laboratory mouse strains and the subsequent potential for higher genetic resolution (Petkov *et al.* 2004). The result of the N₂F₁ backcross study provided further evidence for linkage between

D4Mit232 and the spontaneous GC tumour phenotype (Dorward *et al.* 2005), with the susceptibility allele contributed by the SWR genome. These mapping crosses suggested associations between the GC tumour phenotype and numerous other autosomal susceptibility loci in addition to *Gct1*; however, a lack of consistent linkage of any other loci over multiple mapping crosses suggest that their influence is contingent upon strain background and potential epistatic interactions.

It was recognized early on that the androgenic stimulation of the pre-pubertal, genetically susceptible SWR mouse ovary could significantly increase the number of females with GC tumours (Beamer *et al.* 1988a). Inbred SWR female mice have a spontaneous GC tumour frequency of $\leq 1\%$, which increases to $\geq 20\%$ upon DHEA or T treatment at puberty (Figure 1.7; Beamer *et al.* 1993). Given that DHEA is an upstream metabolite of the androgenic steroids (Figure 1.8), Tennent *et al.* (1993) examined whether DHEA supplementation was simply a substitute for T administration. An interesting phenotypic segregation arose between the eight lines of the SWXJ RI strain set that maintained the *Gct1^{SW}* allele. GC tumour frequencies from four RI strains with low spontaneous tumour incidence were significantly increased with either DHEA or T exposure, whereas another group of four "DHEA-dependent RI strains" that were previously resistant to spontaneous GC tumour initiation only responded to DHEA, and not T, treatment. As a result, *Gct1^{SW}* is described as a DHEA-responsive locus, and DHEA stimulation has been used to further map the region.

In addition to *Gct1*, two other confirmed, independent loci, *Gct4* and *Gct6* on Chr X, are strong modifiers of GC tumour susceptibility, and were identified using a

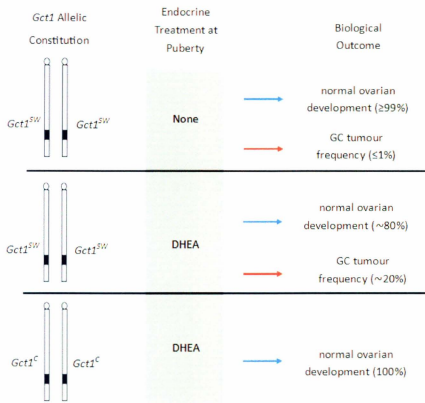


Figure 1.7 Impact of the allelic constitution at *Gct1* and the endocrine environment on GC tumour susceptibility in female mice

Mice with *Gct1^{SW}* alleles have a natural GC tumour frequency of $<1\%$, which increases to approximately 20% when given DHEA at puberty. Mice with *Gct1^C* are completely resistant to GC tumour development, even when given exogenous DHEA.

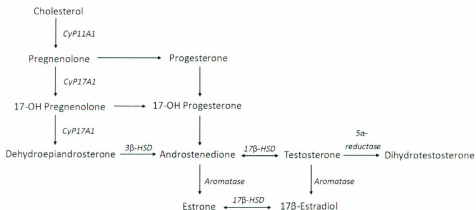


Figure 1.8 The steroid biosynthetic pathway for the conversion of substrate cholesterol to androgens and estrogens

DHEA is converted to androstenedione by 3β -HSD, which is converted to T in a reversible reaction catalyzed by the dehydrogenase/reductase enzyme 17β -HSD. 17β -HSD also catalyzes the reversible conversion of estrone to E_2 , which are derived from the androgens via aromatase activity. The synthesis of DHT from T is catalyzed by the enzyme 5α -reductase.

recombinant progeny test mapping strategy (Dorward *et al.* 2003). However, the capacity for *Gct4* and *Gct6* to support GC tumour initiation is dependent upon the presence of the *Gct1^{SW}* allele. Mapping of these two X-linked loci using SJL and CAST as mapping partners has been accelerated by the high GC tumour frequency and parent-of-origin effect associated with the paternally inherited SJL (*Gct4^J*) allele. To date, *Gct4* and *Gct6* have been mapped to a high resolution of 1.345 million base pairs (megabase; Mb) and 1.019 Mb, respectively (Dorward *et al.* unpublished), although at present the identities of *Gct4* and *Gct6* remain undefined. Given the role of androgens in GC tumour initiation, the *Androgen receptor (Ar)* gene has been considered and remains a primary candidate for *Gct4* identity; however, no nucleotide differences are evident in the protein coding region sequence of *Ar* in SWR and SJL mice compared to C57BL/6 (B6) and BALB/c reference sequences (Dorward *et al.* 2003). The strong paternal parent-of-origin effect associated with the X-linked loci suggests epigenetic regulation, and that allelic differences at the level of gene expression rather than protein sequence underlie their modifier activity.

The required contribution of SWR-derived susceptibility alleles at *Gct1* to support spontaneous and hormone-induced GC tumourigenesis, as well as its consistent identification from three independent mapping crosses, cements the *Gct1^{SW}* allele as the fundamental driver for this complex, developmentally restricted phenotype. No other inbred mouse strains contribute *Gct1* alleles that support GC tumour susceptibility even with androgen treatment, indicating that a genetic determinant unique to SWR contributes to tumour initiation, and the *Gct1^{SW}* allele should be identifiable by genetic comparison to

other strains (Beamer *et al.* 1988b). A comparison of the mouse chromosomal locations of genes associated with sporadic adult-type human GC tumour appearance (*FOXL2* (Chr 9), *STK11*(Chr 10)) or engineered mouse models of GC tumourigenesis (e.g. *Ctmb1*, *Inha*) do not overlap with the distal Chr 4 region (Tables 1.1 and 1.2), suggesting the *Gct1* gene is a unique entity impacting upon GC tumour susceptibility. However, this does not discount the possibility that the tumourigenic pathways initiated by *Gct1* may directly impact upon these reported pathways for GC tumourigenesis. Resolution of the identity of *Gct1*^{SW} in the mouse model will provide candidates for translation into the human condition of juvenile GC tumourigenesis.

Strategies to Positionally Clone Gct1: Preliminary Work

In the field of mouse genetics, a common strategy to resolve important genetic loci independently from other loci that underly polygenic traits is the creation of a congenic strain. Congenic strain development begins with an outcross between two inbred strains, followed by backcrossing to the inbred paternal strain for 10 or more generations, while maintaining heterozygosity at a selected locus (Silver 1995). This breeding pattern effectively results in a “swap” of the alleles at a particular locus from a donor strain into a recipient strain background, which after 10 generations of backcrossing is 99.8% homozygous (Figure 1.9; Flaherty 1981). The resulting congenic strain is maintained by brother-sister intercrossing. Preliminary work has been completed to isolate *Gct1* in a congenic strain, SWR.SJL-X.CAST-4-T (Line 4-T). Line 4-T is in

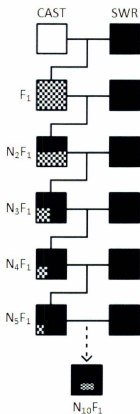


Figure 1.9 Isolating *GctI* in a congenic strain

A schematic representation of the relative contributions of donor (CAST) and recipient (SWR) alleles at sequential generations of backcrossing. *GctI^C* alleles are swapped with *GctI^{SW}* alleles into an SWR background which is 99.8% homozygous after 10 generations. Black: SWR alleles; white: CAST alleles; checkerboard pattern: heterozygous alleles. Adapted from Flaherty (1981).

fact a double congenic strain and maintains an SWR genome with the exception of two distinct genomic segments: the distal segment of Chr 4 and the middle portion of Chr X. The Chr 4 region harbours a homozygous segment of the GC tumour resistant CAST inbred strain genome, from DNA marker *D4Mit31* (106.7 Mb) to *D4Mit256* (154.3 Mb), for a total segment swap of approximately 47 Mb inclusive of the *D4Mit232* marker. To overcome low GC tumour penetrance in the mouse model, Line 4-T also carries the *Gct4*^f allele for increased GC tumour appearance. Line 4-T mice are resistant to GC tumour development both spontaneously and following pubertal exposure to either of the androgens DHEA or T, which confirms the swap of *Gct1*^C alleles for *Gct1*^{SW} alleles and thus makes Line 4-T a suitable congenic line for further mapping (unpublished data). Loss of the GC tumour phenotype in Line 4-T also confirms the requirement of *Gct1*^{SW} alleles for tumour appearance even in the presence of the GC tumour permissive *Gct4*^f alleles.

Following the development of Line 4-T, informative recombinant subcongenic lines were created by fragmenting the large region inclusive of *Gct1*, breeding to homozygosity, and testing for susceptibility to GC tumour initiation. Homozygous Line 4-T individuals were backcrossed to produce heterozygotes at *Gct1*, and subsequent backcrossing generated N₂F₁ mice with unique combinations of the CAST and SWR genomes across the *Gct1* locus via meiotic recombination. The 10 best representatives covering the *Gct1* locus were chosen for further intercrossing to produce homozygous individuals at *Gct1*, which formed a series of nested subcongenic strains (SWR.SJL-X.CAST-4-1 through 10; Figure 1.10). Nine of these lines were successfully created and

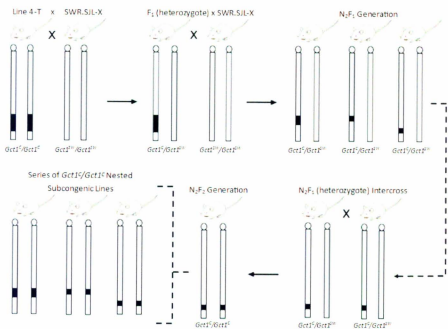


Figure 1.10 Creating subcongenic strains to map *Gct1*

An N_2F_1 backcross breeding scheme was utilized to generate unique combinations of the CAST and SWR genomes across the *Gct1* locus by meiotic recombination. Informative mice were chosen for further breeding to create a series of homozygous, nested subcongenic lines.

tested for GC tumour incidence following pubertal exposure to DHEA to increase trait penetrance, using a group size (n) of 50 animals. Six lines had the most informative combinations of the SWR and CAST genomes to resolve the *Gct1* locus and are shown in Figure 1.11. This first round of phenotypic mapping has been completed, and resulted in a refined *Gct1* interval of 6.48 Mb between markers *D4Mit13* (142.09 Mb) and *D4Mit49* (148.57 Mb), a region that contains approximately 300 pseudo-, protein coding, and non-coding RNA genes. The Line 4-T recombinant subcongenic lines that retain GC tumour resistance indicate that no other CAST genomic elements remain in the Line 4-T genomic segment that repress GC tumour susceptibility, and that the *Gct1* locus independently controls GC tumour initiation in congenic females. The successful development of the recombinant subcongenic lines also suggests an absence of chromosomal inversions within the *Gct1* interval, which would suppress recombination across the region and interfere with the congenic mapping strategy. Line 4-3 is homozygous for a smaller portion of the CAST genomic segment on Chr 4 than Line 4-T, from DNA marker *D4Mit31* (106.7 Mb) to *D4Mit362* (148.7 Mb), and retains resistance to both spontaneous and androgen-induced GC tumour incidence. A second round of phenotypic mapping has been initiated with Line 4-3 as the starting donor for recombination between *Gct1^C* and *Gct1^{SIF}* alleles. Line 4-3 will be used in the same way as Line 4-T to generate a series of nested subcongenic lines to improve mapping resolution at *Gct1*. This refined interval will be the focus of expression and sequence examination for the identification of a gene with shared identity with *Gct1*. A summary of the inbred, congenic and recombinant subcongenic lines including their alleles at *Gct1* and the X-linked loci *Gct4* and *Gct6* is shown in Table 1.3.

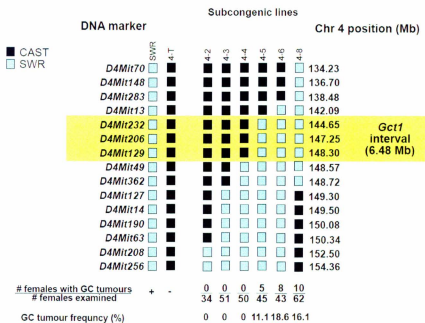


Figure 1.11 Chr 4 haplotypes of SWR and Line 4-T subcongenic mouse lines at *Gctf*

Females from the Line 4-T recombinant congenic lines 4-5, 4-6, and 4-8 have a significantly higher GC tumour incidence than Line 4-T and 4-2, 4-3, and 4-4 females. Thus lines 4-5, 4-6, and 4-8 carry the *Gctf*^{SWR} allele, whereas lines 4-2, 4-3, and 4-4 do not, and *Gctf* resides in the approximately 6.48 Mb interval between *D4Mit13* and *D4Mit129*. +: GC tumour susceptible; -: GC tumour resistant; black boxes: CAST alleles; blue boxes: SWR alleles; yellow rectangle: the *Gctf* interval.

Table 1.3 Descriptions of inbred and congenic mouse strains. Inbred, congenic and recombinant subcongenic mouse strains and their abbreviations, homozygous alleles at *Gct1* on Chr 4 and the *Gct4* and *Gct6* loci on Chr X, and spontaneous GC tumour frequencies. C: CAST; J: SJL; SW: SWR

Strain	Strain		<i>Gct1</i> Allele		<i>Gct4</i> Allele		<i>Gct6</i> Allele		Spontaneous GC Tumour Frequency	Reference
	Abbreviation	(Chr 4)	(Chr X)	(Chr X)	(Chr X)	(Chr X)	(Chr X)			
SWR/Bm	SWR	SW	SW	SW	SW	SW	SW	SW	<1%	Beamer <i>et al.</i> 1985
SJL/Bm	SJL	J	J	J	J	J	J	J	0%	Beamer <i>et al.</i> 1985
CAST/Ei	CAST	C	C	C	C	C	C	C	0%	Dorward <i>et al.</i> 2003
SWR.SJL-X5-CAST-4T	Line 4-T	C	C	J	J	S	S	S	0%	unpublished
SWR.SJL-X5-CAST-4-3	Line 4-3	C	C	J	J	S	S	S	0%	unpublished

1.4. Hypothesis and Research Objectives

Hypothesis:

A unique genetic determinant is present within the *Gct1* locus in SWR mice, which supports the initiation of ovarian GC tumours in an androgen-responsive and ovarian-autonomous manner during the mouse pubertal transition.

Research Objectives:

- 1) Completion of the phenotype assessment and fine mapping for the genomic boundaries of six recombinant subcongenic lines derived from Line 4-3, to reduce the *Gct1* candidate gene interval
- 2) Qualitative assessment of the genes in the refined *Gct1* interval for expression in the ovary
- 3) Evaluation of prioritized candidates for shared *Gct1* identity, based on known biological roles and the qualitative assessment, by quantitative expression and sequencing analyses

2. Materials and Methods

2.1 Animal Husbandry

Animal Housing

All mice were maintained in a facility operated by Animal Care Services of Memorial University of Newfoundland in accordance with the guidelines of the Canadian Council on Animal Care. Mice were housed under a 12:12 h light/dark cycle and provided with Laboratory Autoclavable Rodent Diet 5010 food (27.5% protein, 13.5% fat, 59% carbohydrate; PMI Nutrition International, Richmond, IN) and water *ad libitum*. Animals were weaned at 20-23 d of age and housed in groups of two to five animals per cage in 11"L x 7"W x 5"H rodent cages containing Bed-O-Cobs[®] corn-cob bedding material (The Andersons, Maumee, OH). All animal procedures were approved by the Institutional Animal Care Committee of Memorial University of Newfoundland.

Mouse Strains

Line 4-3 was used in the generation of new recombinant subcongenic lines as it contained the smallest defined *Gct1* interval at the start of the second round of phenotypic mapping. The lines genotyped and brought to homozygosity before phenotyping. SWR and Line 4-T were used for all serum, candidate gene sequencing, and gene expression analyses. Genotyping assay standards were: SWR, Line 4-T, and (SWR.SJL-X5 x Line 4-3) first filial generation (F_1) hybrid.

Surgical Capsule Implantation

The Line 4-3 recombinant subcongenic mice were treated with DHEA to increase trait penetrance to facilitate phenotypic mapping, and SWR and Line 4-T mice were treated with DHEA or a control treatment for the quantitative expression analysis. Mice were anaesthetized with isoflurane (2-chloro-2-(difluoromethoxy)-1,1,1-trifluoro-ethane) (Baxter Corporation, Mississauga, ON) and subcutaneously implanted with a capsule via a small dorsal incision at 3 wk of age. Capsules were composed of 10 mm long Silastic tubing (1.98 mm inner diameter; Dow Corning, Midland, MI) filled with approximately 150 mg of 99.5% pure powdered DHEA (5-androstenolone-3 β -ol-17-one; Catalogue ID A8500-000, Steraloids Inc., Newport, RI) and were sealed at each end with a 3 mm glass bead (Fisher Scientific, Fair Lawn, NJ). Control capsules were empty. Incisions were closed using a 9 mm AutoClip[®] stainless steel wound clip (MikRon Precision Inc., Gardena, CA). Mice were subcutaneously injected with 0.1 mL 0.5 ng/mL (5 mg/kg) Rimadyl[®] (carprofen; Pfizer Animal Health, Kirkland, QC) analgesic postoperatively. Wound clips were removed from Line 4-3 recombinant subcongenic mice approximately 1 wk after surgery. Illustrations of the phenotypic mapping and quantitative expression analysis treatment paradigms are shown in Figures 2.1 and 2.2, respectively.

2.2 Phenotypic Mapping

Animal Examination and Statistical Analysis

Mice were euthanized with CO₂ gas at 8 wk of age, and GC tumour development

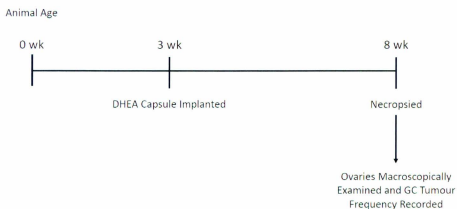


Figure 2.1 Phenotypic mapping paradigm for GC tumour susceptibility versus resistance

Line 4-3 recombinant subcongenic mice were subcutaneously implanted with a DHEA capsule at 3 wk of age. After 5 wk of treatment (at 8 wk of age), mice with present and intact DHEA capsules were necropsied and their ovaries were macroscopically examined for the presence of GC tumours. Tumour frequency was recorded in those mice with present and intact DHEA capsules.

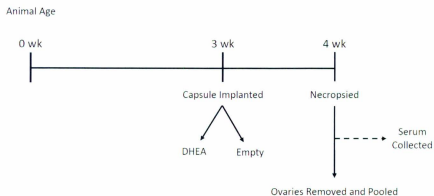


Figure 2.2 Sample collection paradigm for quantitative gene expression in the ovary and serum analysis

SWR and Line 4-T mice were subcutaneously implanted with a DHEA or control capsule at 3 wk of age. After 1 wk of treatment (at 4 wk of age), mice were necropsied and whole ovaries from mice with present and intact DHEA capsules were collected and pooled. Serum samples were collected at the time of necropsy.

was assessed by macroscopic examination of the ovaries in mice with present and intact DHEA capsules. Mice with palpable GC tumour masses were necropsied earlier than 8 wk. The minimum sample size of $n = 50$ individual animals per recombinant subcongenic line was determined through power calculations (Type I error probability, $\alpha = 0.05$, Type II error probability, $\beta = 0.20$), based on an expected GC tumour frequency of approximately 20% in SWR mice supplemented with DHEA at puberty, and 0% in mice with CAST alleles at *Gct1*. GC tumour frequencies were compared by chi-square test ($P = 0.05$) using GraphPad Prism version 5.00 for Windows (GraphPad Software, San Diego, California, USA, www.graphpad.com).

Genotypic Mapping

Genotyping markers used were SSLPs and single nucleotide polymorphisms (SNPs) empirically determined to be polymorphic between the SWR and CAST genomes. SSLPs and their primer sequences were annotated in the Mouse Genome Database (MGD; Blake *et al.* 2011; www.informatics.jax.org), or identified and designed in-house (Appendix A). SNPs were annotated in the National Center for Biotechnology Information (NCBI) Single Nucleotide Polymorphism Database (dbSNP) Build 132 (Sherry *et al.* 2001; www.ncbi.nlm.nih.gov/projects/SNP), or identified during preliminary candidate gene sequencing. Because the SWR strain has not been re-sequenced, annotated SNPs were chosen on the basis of differences between CAST alleles and the alleles of other common inbred strains, particularly Swiss-derived strains

which are phylogenetically related to SWR (Petkov *et al.* 2004). SSLP markers were confirmed from tail DNA and assessed for allele size by horizontal agarose gel electrophoresis, whereas SNP markers were amplified from kidney DNA and assessed for nucleotide changes by cycle sequencing. Newly recombinant Line 4-3 subcongenic individuals and their initial homozygous progeny were tested against the panel of SSLP and SNP markers to establish Chr 4 haplotype patterns. SNPs were identified in at least two individuals from each Line 4-3 recombinant subcongenic line. Primer sequences for annotated SSLP genotyping markers were obtained from MGD; all other genotyping primer sequences were designed using Primer3 version 0.4.0 (Rozen and Skaletsky 2000; www.frodo.wi.mit.edu/primer3). Genotyping marker primer sequences, SSLP allele sizes for CAST and SWR, and their locations on Chr 4 are shown in Table 2.1.

2.2.1 Genotyping by Simple Sequence Length Polymorphisms

Tail Tip Biopsy and DNA Extraction

Approximately 2 mm of tissue was removed from the tail tip using scissors upon necropsy or before mice reached 4 wk of age. Tail samples were placed in a 1.5 mL microcentrifuge tube with 500 μ L of 50 mM sodium hydroxide (BDH Inc., Toronto, ON). The tubes were placed on a heat block for 10 min at 95 $^{\circ}$ C, after which 50 μ L of tris-HCl pH 8.0 (Sigma-Aldrich Inc., St. Louis, MO; Fisher Scientific, Fair Lawn, NJ) was added. The samples were centrifuged at 10,000 x g for 30 s, and 500 μ L of supernatant was transferred to a 1.5 mL microcentrifuge tube. The DNA samples were

Table 2.1 SSLP and SNP genotyping markers. Primer sequences and location on Chr 4 are shown (Ensembl release 61, NCBI m37). SSLP sizes were determined from horizontal agarose gel electrophoresis. Genotyping using SNP markers was based on multiple bp substitutions at each marker and can be found in the results' text. C: CAST; n/a: not applicable; S: SWR

Marker Symbol	Forward Sequence (5'→3')	Reverse Sequence (5'→3')	Amplified Region of Chr 4 (bp)	Assay Type	Relative SSLP Allele Size
<i>D4Mit13</i>	GCTGGTAGCTGGCTTTTCTC	CAGATGTCCTACTGCTTGG	142,094,205–142,094,293	SSLP	C < S
<i>D4Mit126</i>	TGCACTTTTGAGATTGCCAG	GTCTTCCCTCTCCCTCCC	142,152,658–142,152,805	SSLP	C > S
<i>D4sjh19</i>	GTGGGGAGCATGCTCTTAAA	TGGGAGTGTGTAGCAGAGGA	142,633,317–142,633,544	SSLP	C > S
<i>D4Mit160</i>	ACTATGCTAAACCAACAATCTCCC	CCGAGAAACCTAATCTTGATGA	144,040,010–144,040,205	SSLP	C > S
<i>D4sjh10</i>	GCAGAAATGGCACAGGAGAT	CCCACATTTGAAACCACTC	144,208,822–144,209,061	SSLP	C > S
<i>D4sjh9</i>	GGACTGGCTCTGAGGAACAA	GCCAAGCAGCTTCTCTTAG	144,635,848–144,636,084	SSLP	C < S
<i>D4Mit232</i>	GCGTCACCACACTGCTCTT	ACTCAGAGTCCCCTGGCC	144,647,559–144,647,676	SSLP	C > S
<i>D4Mit233</i>	TGGTCATGTGTGCCATGC	ACTTCATGTAGCCAGGTGGG	144,814,847–144,815,021	SSLP	C > S
<i>D4Mit285</i>	CTTTAGGTAGAACTTCTCCGTTTT	GTGGCAGTAAACTTATTCAACC	146,815,380–146,815,479	SSLP	C > S
<i>D4Mit206</i>	TGAAGGCTGAGTTAATACCTAGC	TCATCAACTAAGTGACAAGGAAGG	147,251,451–147,251,598	SSLP	C < S
<i>Nppb</i>	GAAGACACCAGTGCACAAGC	AATCCCCATCTTCCATAG	147,360,003–147,360,359	SNP	n/a
<i>D4sjh11</i>	CCACCAGGTCTGGATAGCAT	GCCAGGAAGGCTAGCATAAA	147,540,887–147,541,118	SSLP	C < S
<i>D4sjh12</i>	TTTGGAGACCAAAGATGAGACA	CTTTTCTGGCCTCTGACCTG	147,643,331–147,643,561	SSLP	C < S
<i>D4sjh13</i>	TCTGGTTTCTATGCGTGTGC	CGGGATCCATATGGTAGTGG	148,093,433–148,093,658	SSLP	C > S
<i>D4Mit129</i>	GTAATAACACAACCATAGAGACCTGC	TGCTGCCTACTTGTGTTTTG	148,297,268–148,297,396	SSLP	C > S
<i>D4Mit49</i>	TTGCCTAGCATACTGCATG	GCTGGGTTTGTGGCTCAG	148,572,905–148,573,054	SSLP	C > S

stored at -20 °C until assayed.

Polymerase Chain Reaction

SSLP genotyping markers were amplified by PCR using a MasterTaq Kit (5 PRIME Inc., Gaithersburg, MD) from genomic DNA extracted from Line 4-3 recombinant subeogenic mice tail samples, and from SWR, Line 4-T and (SWR.SJL-X5 x Line 4-3) F₁ genotyping standards. The following reagents were combined in a 0.2 mL PCR tube (Bio-Rad Laboratories, Hercules CA): 7.3 µL of distilled water, 1 µL of 5X TaqMaster PCR Enhancer heated to 65 °C, 1 µL of 10X Reaction Buffer, 0.2 µL of 10 mM deoxynucleotide triphosphates (dNTPs) (Invitrogen, Carlsbad, CA), 0.22 µL of 10 µM forward and reverse primers (Integrated DNA Technologies, Coralville, IA), 0.05 µL of Taq DNA polymerase, and 1 µL of DNA template. A negative control was included with each PCR with distilled water in place of DNA template. The tubes were placed in a Veriti™ 96-Well Thermal Cycler (Applied Biosystems Inc., Foster City, CA) where PCR was performed using the following profile: 97 °C for 30 s; 39 cycles of 94 °C for 15 s, 55 °C for 30 s, and 72 °C for 30 s; 72 °C for 10 min. The PCR products were stored at 4 °C until gel electrophoresis.

Gel Electrophoresis

SSLP genotyping PCR products were separated by horizontal electrophoresis

through a 4% agarose gel. PCR products (9.99 μ L) were combined with 3 μ L of gel loading buffer (Bromophenol Blue, Sodium Salt; EMD Millipore, Billerica, MA) in a 0.2 mL PCR tube and mixed by pipetting. The gels were comprised of 8 g of MetaPhor[®] agarose (Lonza, Rockland, ME), 20 mL of 10X tris-borate ethylenediaminetetraacetic acid (EDTA) buffer (TBE; 0.89 M tris, 0.89 M boric acid [Fisher Scientific, Fair Lawn, NJ], 0.02 M EDTA [Sigma-Aldrich Inc., St. Louis, MO]) and 180 mL of distilled water. The gel mixture was boiled using a microwave, and after cooling was poured into a gel electrophoresis chamber taped at both ends and containing loading well combs. After the gel solidified the combs were removed and the PCR product/loading buffer solution or 10 μ L of 100 base pair (bp) DNA ladder marker (Bio Basic Inc., Markham, ON) were pipetted into the wells. The gels were electrophoresed for 3 h at 120 V, after which they were post-stained with 10 mg/mL ethidium bromide (Sigma-Aldrich Inc., St. Louis, MO) for approximately 30 min. The SSLP PCR products were visualized using a U:Genius GelVue UV transilluminator (302 nm; Syngene, Frederick, MD) and scored for allele size differences between SWR, CAST and F₁ DNA standards.

2.2.2 Genotyping by Single Nucleotide Polymorphisms

Kidney DNA Extraction

DNA was extracted from single whole kidneys homogenized on ice in 6 mL of isotonic high pH (Iso-Hi-pH) buffer (0.14 M sodium chloride [BDH Inc., Toronto, ON], 0.01 M tris pH 8.4, 1.5 mM magnesium chloride [Sigma-Aldrich, St. Louis, MO]) with

0.1% Igepal CA-630 (Sigma-Aldrich, St. Louis, MO) using a Dounce homogenizer. Lysates were transferred to a 15 mL centrifuge tube (Corning Incorporated, Corning, NY) and centrifuged at 800 x g for 5 min at 4 °C. Supernatants were discarded and nuclear pellets resuspended in 6 mL of Iso-Hi-pH Buffer with 0.1% NP-40. A 300 µL aliquot of 20% sodium dodecyl sulfate (Sigma-Aldrich, St. Louis, MO) and 150 µL of 10 mg/mL Proteinase K (Sigma-Aldrich, St. Louis, MO) were added to the tubes, which were immediately and repeatedly inverted and placed in a water bath at 37 °C for 3 h with periodic inversions. Following incubation, 2 mL of 6 M sodium chloride was added to the tubes, which were mixed by vigorous inversion and centrifuged at 2,000 x g for 15 min at room temperature (RT). The supernatant was transferred to a 50 mL centrifuge tube (Corning Incorporated, Corning, NY) with a wide-bore transfer pipette and the DNA was precipitated by overlaying two volumes of anhydrous 95% ethanol (Commercial Alcohols, Brampton, ON). DNA was spooled on a glass rod, soaked in 70% ethanol (Commercial Alcohols, Brampton, ON) for 10 min, and air dried overnight. The dried DNA was resuspended in 600 µL of tris-EDTA (TE; 10 mM tris pH 8.0, 1 mM EDTA pH 8.0) and mixed on a rotator overnight. The DNA stock solutions were diluted 1:9 DNA to distilled water and stored at -20 °C.

Polymerase Chain Reaction

SNP genotyping markers were amplified by PCR using an Accuprime™ Kit (Invitrogen, Carlsbad, CA) from genomic DNA extracted from SWR, Line 4-T, and Line

4-3 recombinant subcongenic line mouse kidneys. The following reagents were combined in a 0.2 mL PCR tube: 22.5 μ L of Accuprime™ Pfx Supermix, 0.25 μ L of 10 μ M forward and reverse primers, and 2 μ L of DNA template. A negative control was included with each PCR with distilled water in place of DNA template. The tubes were placed in a Veriti™ 96-Well Thermal Cycler where PCR was performed using the following profile: 95 °C for 5 min; 35 cycles of 95 °C for 15 s, 55 °C for 30 s, and 68 °C for 45 s; 72 °C for 10 min. The PCR products were stored at 4 °C until gel electrophoresis.

Gel Electrophoresis

Successful amplification of SNP genotyping marker amplicons was confirmed by electrophoresis through a 1.5% agarose gel. PCR products (5 μ L) were combined with 3 μ L gel loading buffer in a 0.2 mL PCR tube and mixed by pipetting. The gels were comprised of 0.75 g of agarose (Sigma-Aldrich, St. Louis, MO), 5 mL of 10X TBE and 45 mL of distilled water. The gels were cast, loaded and PCR products visualized as per the protocol for SSCP genotyping markers (section 2.2.1.3). The gels were electrophoresed for 30 min at 120 V.

PCR Product Purification

PCR products were purified using a QIAquick® PCR Purification Kit (Catalogue

Number 28106; Qiagen Inc., Mississauga, ON) as per the manufacturer's standard protocol. Briefly, five volumes of binding buffer to one volume of PCR product were combined with 10 μ L sodium acetate (J.T. Baker Chemical Co., Phillipsburg, NJ) and transferred to a 2 mL filter column in a collection tube. After centrifugation, the flow-through was discarded and 750 μ L of elution buffer was added to the filter column. After two sequential centrifugations, the filter column was transferred to a 1.5 mL microcentrifuge tube and 30 μ L of distilled water was pipetted directly onto the filter membrane. The tubes were centrifuged after a 1 min incubation at RT, and the purified PCR products were stored at -20 °C.

Cycle Sequencing

All cycle sequencing reactions were carried out at the Genomics and Proteomics Facility, Core Research and Equipment and Instrument Training Network, Memorial University of Newfoundland, using a BigDye[®] Terminator v3.1 Cycle Sequencing Kit (Applied Biosystems Inc., Foster City, CA). The following reagents were combined in a 0.2 mL PCR tube and made up to a volume of 17.5 μ L with distilled water: 2 μ L of 5X Sequencing Buffer, 0.5 μ L of Ready Reaction Mix, 2 μ L of either 1.6 pmol/ μ L forward or reverse primer and 10-40 ng purified PCR product template. A control reaction was included with each sequencing run and consisted of 2 μ L of 5X Sequencing Buffer, 0.5 μ L of Ready Reaction Mix, 2 μ L of -21 M13 Control Primer, 2 μ L of pGEM[®]-3Zf(+) template, and 13.5 μ L of distilled water. The tubes were placed in an GeneAmp[®] PCR

System 9700 Thermal Cycler (Applied Biosystems Inc., Foster City, CA) and PCR was performed using the following profile: 25 cycles of 96 °C for 10 s, 50 °C for 5 s, and 60 °C for 4 min; and a 4 °C hold. The PCR products were stored at 4 °C until purification, when they were combined with 5 µL of 125 mM EDTA and 65 µL of 95% ethanol (Commercial Alcohols, Brampton, ON). The tubes were briefly vortexed and centrifuged, covered in foil and stored at 4°C overnight. The tubes were centrifuged at 3,000 x g for 30 min at RT, and the supernatants were discarded by quickly inverting the tubes. The tubes were centrifuged at 200 x g for 25-30 s, after which 150 µL of 70% ethanol was added. The tubes were vortexed briefly and centrifuged at 3,000 x g for 15 min. The supernatants were discarded and the tubes were air-dried for 10-15 min. The purified PCR products were resuspended in 20 µL of Hi-Di™ Formamide (Applied Biosystems Inc., Foster City, CA) and briefly vortexed and centrifuged. The samples were then loaded into a cassette and placed in a 3130 or 3730 Genetic Analyzer (Applied Biosystems Inc., Foster City, CA).

Sequence Analysis

Sequences were analyzed using Sequencher® version 4.10.1 (Gene Codes Corporation). Experimental sequences were aligned to the B6 reference genome, downloaded from Ensembl Mouse Genome Browser release 61 (NCBI m37; February 2011; Flicek *et al.* 2011; www.ensembl.org).

2.3 Serum Analysis

Serum Collection

Whole-blood was collected between 9:00 am and 11:00 am to ensure consistency in cycling hormone levels. Mice were decapitated using scissors and approximately 1 mL of trunk blood was collected in a 1.5 mL microcentrifuge tube. The blood samples were left on ice for 2 h to permit clotting, after which they were centrifuged at 15,000 x g for 10 min. The clear upper serum phase was transferred in 100 μ L aliquots to a 0.6 mL microcentrifuge tube (Fisher Scientific, Fair Lawn, NJ) and stored at -20 °C.

Enzyme-linked Immunosorbent Assay

Seven samples from each of the following groups were assayed for serum DHEA levels: SWR control, SWR DHEA-treated, Line 4-T DHEA-treated; and three samples from the Line 4-T control group. Samples were packaged in dry ice and express shipped to the University of Virginia Center for Research in Reproduction Ligand Assay & Analysis Core Laboratory where an enzyme-linked immunosorbent assay (ELISA) for serum DHEA was conducted using a DRG DHEA ELISA Kit (ALPCO Diagnostics, Salem, NH). Control samples were undiluted and DHEA-treated samples were diluted 1/10 to be within the reportable assay range of 0.37 to 3.70 ng/mL. Serum DHEA levels were assayed in duplicate when the serum volume permitted and averaged. Group DHEA levels were expressed as mean \pm standard error of the mean. Serum DHEA was

analyzed using a Student's unpaired t-test ($P < 0.05$) using GraphPad Prism.

2.4 Gene Expression Analyses

Tissue Collection

Mice were euthanized by exposure to CO₂ gas between 3-4 wk of age for the qualitative gene analysis and 1 wk post DHEA implantation (4 wk of age) for the quantitative gene analysis. The tissues were dissected using scissors and tweezers cleaned with an Ambion® RNaseZap® wipe (Applied Biosystems Inc., Foster City, CA), and were placed in a dish of 1X Dulbecco's phosphate-buffered saline (Invitrogen, Carlsbad, CA). The tissues were blotted on a kim wipe, placed in a nuclease-free 2.0 mL cryogenic vial (Corning Incorporated, Corning, NY), and flash frozen in liquid nitrogen. The tissues were stored at -80 °C.

RNA Extraction from Mouse Ovaries

Total ribonucleic acid (RNA) was extracted from whole mouse ovaries using an Ambion® RNAqueous®-4PCR Kit (Catalogue Number AM1914; Applied Biosystems Inc., Foster City, CA) with a number of protocol changes to optimize RNA concentration. Pools of at least six ovaries from three individual mice were placed in nuclease-free 1.5 mL microcentrifuge tubes with 150 µL of Lysis/Binding Solution, and homogenized using a plastic pestle cleaned with an Ambion® RNaseZap® wipe. A 150 µL aliquot of

64% ethanol was added to the lysate, which was mixed by pipetting, applied to a filter column in a collection tube, and centrifuged at 15,000 x g for 1 min. A 700 μ L aliquot of Wash Solution #1 was added to the filter column, followed by two aliquots of 500 μ L of Wash Solution #2/3. The tubes were centrifuged at 15,000 x g for 1 min after the addition of each reagent, followed by a final 30 s centrifugation at 15,000 x g. The flow-through was discarded after each centrifugation. The filter column was transferred to a new collection tube and aliquots of 60 and 40 μ L of Elution Solution heated to 75°C were pipetted onto the center of the filter, with 30 s centrifugations at 15,000 x g after the addition of each aliquot. The eluate was combined with 10 μ L of 10X DNase I Buffer and 1 μ L of DNase I in a nuclease-free 0.2 mL PCR tube, which was placed in a Veriti™ 96-Well Thermal Cycler where they were incubated for 30 min at 37 °C. Following the incubation, 11.1 μ L of DNase Inactivation Reagent was added to the tubes, which were then incubated at RT for 2 min and centrifuged at 10,000 x g for 1 min. The supernatant was transferred to a nuclease-free 1.5 mL microcentrifuge tube, and 12.2 μ L of 5 M Ammonium Acetate, 2.69 μ L of Linear Acrylamide, and 343 μ L of anhydrous ethanol (Bio Basic Inc., Markham, ON) was added. The tubes were vigorously inverted and placed at -20 °C for 1 h, after which they were centrifuged at 15,000 x g for 15 min. The supernatant was removed and the RNA pellets were resuspended in 20 μ L of Elution Solution heated to 75 °C. The RNA samples were stored at -80 °C until assayed for RNA integrity.

RNA Extraction from Other Tissues

Total RNA was extracted from liver, brain, and testes of SWR and Line 4-T littermate males, and GC tumour tissue from Line 4-3 recombinant subcongenic GC tumour susceptible females used for phenotypic mapping, using TRIzol[®] Reagent (Invitrogen, Carlsbad, CA). Samples were placed in a nuclease-free 1.5 mL microcentrifuge tube with 400 μ L of TRIzol[®] Reagent and homogenized on ice using a nuclease-free plastic pestle. A second aliquot of 400 μ L of TRIzol[®] Reagent was added to the tubes, and the lysate was transferred to a Qias shredder[™] (Qiagen Inc., Mississauga, ON) filter column in a collection tube. The Qias shredder[™] was centrifuged at 15,000 x g for 2 min at RT, and the supernatant was transferred to a nuclease-free 1.5 mL microcentrifuge tube and centrifuged at 15,000 x g for 5 min at 4 °C. The supernatant was transferred to a nuclease-free 1.5 mL microcentrifuge tube, and was incubated at RT for 5 min. A 200 μ L aliquot of chloroform (Fisher Scientific, Fair Lawn, NJ) was added to the tubes, which were vigorously inverted for 15 s and incubated at RT for 3 min. The tubes were centrifuged at 15,000 x g for 15 min at 4 °C to separate the aqueous and organic phases. The clear upper aqueous phase was transferred in 100 μ L aliquots to a nuclease-free 1.5 mL microcentrifuge tube. A 500 μ L aliquot of isopropanol (BDH Inc., Toronto, ON) was added to the solution, which was mixed by pipetting. The tubes were centrifuged at 15,000 x g for 10 min at 4 °C to pellet the RNA, and the supernatant was removed. The RNA pellet was resuspended with two sequential aliquots of 800 μ L of 75% ethanol, after which the tubes were centrifuged at 15,000 x g for 5 min at 4 °C and the supernatant was removed. The RNA pellets were resuspended in 25-50 μ L of

nuclease-free water (Applied Biosystems Inc., Foster City, CA) depending on the size of the pellet, and the tubes were gently agitated to aid in solubilization of the pellet. The RNA samples were stored at -80 °C until assayed for RNA integrity.

RNA samples from liver, brain, testes and GC tumour tissues obtained using the TRIzol[®] Reagent method were purified and concentrated using an RNeasy[®] MinElute[®] Cleanup Kit and RNase-Free DNase Set (Catalogue Numbers 72404 and 79254; Qiagen Inc., Mississauga, ON) as per the manufacturer's standard protocol. Briefly, 30-40 µg of RNA was combined in a nuclease-free 1.5 mL microcentrifuge tube with 10 µL of Buffer RDD and 2.5 µL of DNase I stock solution, and made up to a 100 µL volume with nuclease-free water. The solution was left to incubate for 10 min at RT, after which 350 µL of Buffer RLT and 250 µL of anhydrous ethanol (Bio Basic Inc., Markham, ON) was added. The sample was centrifuged at 15,000 x g for 15 s in a filter column in a collection tube. The filter column was placed in a new collection tube, and 500 µL of Buffer RPE was added and the tubes were centrifuged at 15,000 x g for 15 s. A 500 µL aliquot of 80% ethanol (Commercial Alcohols, Brampton, ON) was added to the filter column, and the tubes were centrifuged at 15,000 x g for 2 min. The filter column was transferred to a new collection tube, and the tubes were centrifuged at 15,000 x g for 5 min with the lid of the filter column open. The filter column was transferred to a nuclease-free 1.5 mL microcentrifuge tube, and 14 µL of nuclease-free water was pipetted directly onto the center of the filter membrane. The tubes were centrifuged at 15,000 x g for 1 min. All centrifugations were conducted at RT. The concentrated RNA samples were stored at -80 °C.

RNA Electrophoresis and Spectrophotometry

The integrity of all RNA samples was assessed by horizontal electrophoresis through a 1% agarose gel. Nuclease-free water (7 μ L), 2 μ L of gel loading buffer and 1 μ L of RNA were combined in a nuclease-free 0.2 mL PCR tube and mixed by pipetting. The gels were comprised of 0.5 g of agarose (Sigma-Aldrich Inc., St. Louis, MO), 5 mL of 10X TBE and 45 mL of distilled water. The gels were cast, loaded and PCR products visualized as per the protocol for SSCP genotyping markers (section 2.2.1.3). The gels were electrophoresed for 30 min at 100 V. Intact RNA was indicated by two distinct bands representing 28S and 18S rRNA subunits, whereas a smear on the gel indicated degraded RNA. RNA samples obtained using the TRIzol[®] Reagent extraction method were assessed for integrity before and after purification and concentration.

The RNA samples were assessed for concentration and purity using a NanoDrop 1000 Spectrophotometer (Thermo Fisher Scientific, Wilmington, DE). A 1 μ L sample of RNA was analyzed for absorbency at 260 nm. RNA samples obtained using the TRIzol[®] Reagent extraction method were assessed for concentration and purity before and after purification and concentration. Identical samples of intact RNA from the same sample pool that were found to be of similar concentration and purity by spectrophotometry were combined and assessed as a single sample.

cDNA Synthesis by Reverse Transcriptase PCR

Complementary DNA (cDNA) was synthesized using an Ambion[®] RETROscript[®] Kit (Catalogue Number AM1710; Applied Biosystems Inc., Foster City, CA) via a two-step reverse transcriptase polymerase chain reaction as per the manufacturer's standard protocol. Briefly, a 2 µg sample of purified and concentrated total RNA was combined with 2 µL of Random Decamers and made up to a 12 µL volume using nuclease-free water. The tubes were heated in a thermal cycler for 3 min at 75 °C, after which the following reagents were added to each tube: 2 µL of 10X Reverse Transcriptase Buffer, 4 µL of dNTP mix, 1 µL of RNase Inhibitor, and 1 µL of MMLV-RT. The tubes were heated in a thermal cycler for 1 h at 44 °C followed by a 10 min incubation at 92 °C, after which they were stored at -20 °C. The cDNA samples were assessed for concentration and purity by spectrophotometry as per the protocol for RNA samples (section 2.4.4), with identical samples of similar concentration and purity combined and assessed as a single sample. Prior to gene expression analyses, cDNA samples were tested for integrity by amplification of a 154 bp mouse beta-actin (*Actb*) gene amplicon as per the protocol for SSLP genotyping markers (section 2.2.1), and electrophoresed through a 1.5% agarose gel as per the protocol for SNP genotyping markers (section 2.2.2.3) (forward primer: 5'-GGC TGT ATT CCC CTC CAT CG-3'; reverse primer: 5'-CCA GTT GGT AAC AAT GCC ATG T-3'; Harvard PrimerBank ID: 6671509a1; Wang and Seed 2003; Spandidos *et al.* 2008; Spandidos *et al.* 2010; <http://pga.mgh.harvard.edu/primerbank>).

Primer Design

Primers used for expression analyses were designed using PerlPrimer version 1.1.19 for Windows (Marshall 2004; <http://perlprimer.sourceforge.net>) or retrieved from Harvard PrimerBank (Appendix B). Primers were designed to maximize the number of unique transcripts represented, and primers spanning exon-exon boundaries were preferred to prevent the amplification of unspliced transcripts from un-transcribed DNA, or contaminating DNA. All primer pairs were analyzed for gene target specificity using the NCBI Primer Basic Local Alignment Search Tool (BLAST; Altschul *et al.* 1990; www.ncbi.nlm.nih.gov/tools/primer-blast) program. Forward and reverse primer pairs had melting temperatures within 1°C and produced amplicons between 82 and 124 base pairs in length. Primer sequences, their amplicon lengths, and the number of unique transcripts amplified by each primer pair are shown in Table 2.2.

2.4.1 Qualitative Gene Expression Analysis

Qualitative expression of protein coding transcripts was assessed in 3-4 wk old SWR or Line 4-T whole pooled mouse ovaries by end-point PCR. Primers were amplified from cDNA by PCR as per the protocol for SSLP genotyping markers (section 2.2.1) using 1 μ L 10 μ M primers, and PCR products were electrophoresed through a 1.5% agarose gel as per the protocol for SNP genotyping markers (section 2.2.2) using 40% (w/v) sucrose (Fisher Scientific, Fair Lawn, NJ) gel loading buffer. Positive

Table 2.2 Qualitative expression analysis primers. Primer sequences used to amplify amplicons from protein coding transcripts within *Gcl1*, their amplicon sizes and the number of unique transcripts amplified. * indicates primers downloaded from the Harvard PrimerBank (Appendix B).

Gene	Forward Sequence (5'→3')	Reverse Sequence (5'→3')	Amplicon (bp)	Transcripts
Gm436*	TGCTGCTCTTAATGATTGCCTG	ACCTCCAAAACATATCTCCACAGA	109	1/1
Gm13178*	AACCTATGGGGTAGATCCCTCT	GAAGTATGGCTTGACTGACCAAA	104	1/1
Gm438	GAAGAACTCTAATGTGGCGG	CATGGTAAGTATCTCGCCTG	107	1/1
Dhrs3*	CGGGAGTCAGTCCATCAC	GCCCCAGAGAACAAATCTTTC	100	5/5
Vps13d	TCATACTGCCTCAAATACAGC	CAGGTCTCCTTCAATCATCTC	101	1/1
Vps13d*	CTGGAGAGGGAGCGTAACAAA	ACGATTCTCGTGACACTGATG	107	3/3
Tnfrsf1b*	GCCCAGGTTGTCTTGACACC	CACAGCACATCTGAGCCTTCC	94	1/1
Tnfrsf8*	ACTACGTCAATGAAGACGGGA	TGACACTCACAGATTCGAGGAG	106	1/1
Gm13225	GTAATACACCACAGGGTCTG	ATGTACAGTCTCCTCTGAGC	101	3/3
Gm13242	GATCAGAGGTCTCCATATGCT	CTGGATCCTTTGTGAGAGTG	100	3/3
Gm13212	ATCAAGGAATCCACATGCAG	GTTCACTCCAGTATTGTTTCGT	109	2/3

amplification was confirmed by the presence of a single band matching the predicted amplicon size, and the 154 bp *Actb* amplicon was included with each PCR as a positive control. Primer pairs that failed to produce a band in ovary cDNA were tested against testes, liver, and/or brain tissue cDNA, as necessary. Primer pairs that failed in all tissues were redesigned using the protocol above (section 2.4).

2.4.2 Quantitative Gene Expression Analysis

Experimental Groups for Quantitative Comparison

Quantitative real-time PCR (qPCR) was conducted to assay for differences in mouse tumour necrosis factor receptor superfamily, member 1b (*Tnfrsf1b*) messenger RNA (mRNA) expression (Ensembl gene ID: ENSMUSG00000028599, transcript ID: ENSMUST00000030336) between 4 wk of age whole pooled mouse ovaries in two experimental comparisons: 1) DHEA-treated SWR and Line 4-T, and 2) DHEA-treated and untreated (control) SWR (Figure 2.3). Three ovary pools were assessed from each group. *Tnfrsf1b* gene expression was normalized to the endogenous housekeeping mouse *Actb* gene in all quantitative gene expression analyses.

Determination of Primer Efficiency

Primer efficiency (E) was calculated as follows, using the slope of the standard



Figure 2.3 Quantitative *Tnfrsf1b* expression analysis paradigm

qPCR was conducted to assay for differences in *Tnfrsf1b* mRNA expression between 4 wk of age whole pooled mouse ovaries in two experimental comparisons: 1) SWR and Line 4-T treated with DHEA, and 2) DHEA-treated and untreated (control) SWR. Three ovary pools were assessed from each group.

curve generated by plotting threshold cycle (C_T) versus template concentration for the *Tnfrsf1b* and *Actb* primer pairs:

$$E = 10^{[-1/slope]}$$

Five ¼ serial dilutions of cDNA were prepared by combining approximately 1.5 µg/µL cDNA with distilled water in a 0.6 mL microcentrifuge tube. Duplicates of each cDNA dilution were pipetted into the wells of a MicroAmp® Optical 96-Well Reaction Plate (Applied Biosystems Inc., Foster City, CA) with 12.5 µL of Power SYBR® Green PCR Master Mix (Applied Biosystems Inc., Foster City, CA) and 3 µL of 0.583 µM forward and reverse primers. Each reaction plate included two non-template control reactions per primer pair/cDNA sample as a negative control. The reaction plates were covered with a MicroAmp® Optical Adhesive Film (Applied Biosystems Inc., Foster City, CA) and centrifuged at 670 x g for 2 min, after which they were placed in an ABI PRISM® 7000 Sequence Detection System (Applied Biosystems Inc., Foster City, CA) where qPCR was performed using the following profile: 95 °C for 10 min; 40 cycles of 95 °C for 15 s and 60 °C for 1 min. Data was analyzed using ABI PRISM® 7000 Sequence Detection System Software version 1.2.3 (Applied Biosystems Inc., Foster City, CA). A primer efficiency between 85% and 100% was considered to be acceptable.

Quantitative Real-time PCR

Based on the standard curve generated during primer efficiency testing, cDNA

samples used for the qPCR analysis were diluted to a 1/16 concentration by combining 2.69 μL of approximately 1.5 $\mu\text{g}/\mu\text{L}$ cDNA with 40.31 μL of distilled water in a 0.6 mL microcentrifuge tube. The dilutions were briefly vortexed and centrifuged, and a 6.5 μL aliquot of each cDNA dilution was combined with 12.5 μL of *Power SYBR[®] Green PCR Master Mix* and 3 μL of 0.583 μM forward and reverse primers in the wells of a *MicroAmp[®] Optical 96-Well Reaction Plate*. Each reaction was assayed in triplicate in three independent experiments. qPCR was conducted as per the protocol for primer efficiency determination.

Statistical Analysis

Triplicate Ct measurements were averaged for each gene; outliers were excluded, in which case means were determined using two replicate values. Fold changes in gene expression were calculated according to Pfaffl (2001) using the equation:

$$\text{ratio} = \frac{(E_{\text{target}})^{\Delta\text{Ct}_{\text{target}}(\text{control} - \text{sample})}}{(E_{\text{ref}})^{\Delta\text{Ct}_{\text{ref}}(\text{control} - \text{sample})}}$$

where E_{target} is the primer efficiency of the *Tnfrsf1b* primer pair and E_{ref} is the primer efficiency of the *Actb* primer pair. Fold changes calculated from each reaction plate were expressed as mean \pm standard error of the mean, relative to Line 4-T (comparison 1) or DHEA-treated SWR (comparison 2) samples, and were analyzed by two-way analysis of variance with Tukey's post test using GraphPad Prism.

2.5 Candidate Gene Sequencing

The *Tnfrsf1b* gene was amplified from genomic (exon 1 and 10) or complimentary (exons 2-9) DNA using nine primer pairs with overlapping amplicons. Primer sequences and their amplicon lengths and are shown in Table 2.3. Primers were amplified by PCR and products were electrophoresed, purified, and sequenced as per the protocol for SNP genotyping markers (section 2.2.2). *Tnfrsf1b* was sequenced from four individuals from both SWR and Line 4-T, and all primer pairs except for those amplifying exon 10-D were also sequenced from three B6 individuals. A c.1148T>C mutation in *Tnfrsf1b* cDNA found in SWR resulting in an amino acid change was amplified from genomic DNA (forward primer: 5'- AGC AGC ACC TGT TGA CCA -3'; reverse primer: 5'- GCC AGC TAT CTG TCC AGA GC -3') as per the protocol above.

Table 2.3 *Tnfrsf1b* sequencing primers. Primer sequences used to amplify overlapping exon segments of the *Tnfrsf1b* gene, their nucleotide ranges and exons amplified, amplicon lengths, and type of template input required. Nucleotide ranges are relative to *Tnfrsf1b* cDNA bp 1. cDNA: complementary DNA; gDNA: genomic DNA.

Exons Amplified	Nucleotide Ranges	Forward Sequence (5'→3')	Reverse Sequence (5'→3')	Amplicon (bp)	Template Input
Exon 1	-39–190	CTGGTCTGCCCTAGCTCCT	CAGTAGCTGGAATGGGCACT	249	gDNA
Exons 2-5	100–641	GTCTTCGAAGTGCAGCTGTG	CTGCATCTGTGCTTGCATTT	571	cDNA
Exons 6-9	575–1226	GGACGTTCTCTGACACCACA	GCTGCTACAGACGTTCCACGA	671	cDNA
Exon 10	1135–1902	TGTCCTCCAAGATCCCCAGAC	GGGCTTGGAGAGGGTACTTC	787	gDNA
Exon 10	1867–2556	CACAGAGGCCCTTCAGGTTA	TAGGCTCCTCTGCCAAGTTC	709	gDNA
Exon 10	2471–3217	GGAAGGAAAGGGTTCAGGAG	TGAAGGAGGGAGATTCTGGA	766	gDNA
Exon 10	3165–3354	GCAGGGAACAATTTGAGTGC	ATGAGAGCCCTGCCTCAGTA	209	gDNA
Exon 10	3226–3429	TCCCTCCTTCAGTGTGTGTG	AACCTGAGCACTCCATAGGC	223	gDNA
Exon 10	3379 – +43	CCCAGAGCTTGACATTTTC	GATGCAGCCAGACTGGGTAT	500	gDNA

3. Results

3.1 Phenotypic Mapping of *Gct1*

3.1.1 Development of the Line 4-3 Recombinant Subcongenic Lines

Six informative SWR.SJL-X.CAST-4 recombinant subcongenic lines (hereafter referred to as Lines 4-11 through 4-16) with unique recombinations of the *Gct1*^{SW} and *Gct1*^C alleles across the *Gct1* locus were successfully derived from Line 4-3 and tested for GC tumour incidence. Females homozygous for the new congenic portions around *Gct1* were exposed to DHEA at puberty to increase trait penetrance with a desired cohort of n = 50 females per line, with an 8 wk endpoint for GC tumour assessment. The haplotype patterns of SWR, Line 4-3, and Lines 4-11 through 4-16 for annotated (*D4Mit*) and in-house designed (*D4sjh*) polymorphic DNA markers in the *Gct1* interval are shown in Figure 3.1. GC tumour frequencies, indicated as the number of females with GC tumours versus the total number of females examined, are reported below the locus haplotype for each line.

The GC tumour phenotype observed in Lines 4-11 through 4-16 was similar to that reported in the literature, i.e. lines that did not develop GC tumours were completely resistant to GC initiation up to 8 wk, and those lines that were GC tumour susceptible developed large unilateral or bilateral tumours within 8 wk at the expected frequency of approximately 20%. Females from Lines 4-11, 4-13, and 4-15 had a significantly higher GC tumour incidence (27.3%, 18.4%, and 17.6%, respectively) than Line 4-3, 4-12, 4-14,

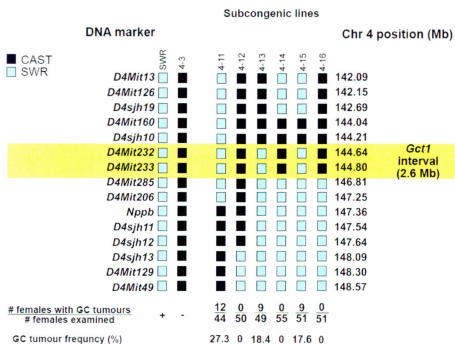


Figure 3.1 Chr 4 haplotypes of SWR, Line 4-3, and the SWR.SJL-X.CAST-4 recombinant subcongenic mouse lines at *Gct1*

Females from SWR and the subcongenic lines 4-11, 4-13, and 4-15 have significantly increased GC tumour incidence than Line 4-3 and lines 4-12, 4-14, and 4-16 ($P < 0.0026$). The GC tumour susceptible strains share common regions of SWR genetic background between markers *D4sjh10* and *D4Mit285*, for a minimal genetic segment containing *Gct1* of approximately 2.6 Mb. +: GC tumour susceptible; -: GC tumour resistant; black boxes: CAST alleles; blue boxes: SWR alleles; yellow rectangle: the *Gct1* interval.

and 4-16 females, which were completely GC tumour resistant (0%; $P < 0.0026$). GC tumour frequencies between the three susceptible lines were not statistically different. This indicates that the Line 4-3 recombinant subcongenic Lines 4-11, 4-13, and 4-15 carry the *Gct1*^{SW} allele, whereas Lines 4-12, 4-14, and 4-16 retain the *Gct1*^C tumour resistance allele. The phenotype-driven mapping process indicated that *Gct1*^{SW} resides in the region between *D4sjh10* and *D4Mit285*, an approximately 2.6 Mb interval.

3.1.2 Refining the Genetic Boundaries of *Gct1*

Subcongenic Lines 4-13 and 4-15 defined the proximal boundary for *Gct1*, whereas Lines 4-14 and 4-16 defined the distal boundary (Figure 3.1). To achieve greater resolution of the *Gct1* interval and exclude potential candidate genes, it was desirable to achieve greater mapping resolution at these boundaries.

A lack of annotated, informative SSLP markers or predicted SSLPs around which primers could be designed within the 2.6 Mb interval necessitated the identification of other polymorphisms between the CAST genome and the as yet un-sequenced strain SWR. SNP genotyping markers were pursued for several genes: *Natriuretic peptide type B* (*Nppb*; Appendix A), *Tnfrsf1b*, and *Dehydrogenase/reductase (SDR family) member 3* (*Dhrs3*). SNP-based genotyping markers were designed to amplify a single product with one or more predicted single bp differences between SWR and CAST, or were designed around annotated SNPs for which the CAST allele is known and different from all other strains (Table 3.1).

Eleven SNPs were identified within the three markers designed to amplify

Table 3.1 SSLP and SNP genotyping markers. Primer sequences and location on Chr 4 are shown (Ensembl release 61, NCBI m37). Entries in bold were empirically derived in-house. C: CAST; n/a: not applicable; S: SWR

Marker Symbol	Forward Sequence (5'→3')	Reverse Sequence (5'→3')	Amplified Region of Chr 4 (bp)	Assay Type	Relative SSLP Allele Size
<i>D4Mit13</i>	GCTGGTAGCTGGCTTTTCTC	CAGATGTTCTACTGCTTGG	142,094,205–142,094,293	SSLP	C < S
<i>D4Mit126</i>	TGCACTTTGGAGATTGCCAG	GTCTTCCCTCTCCCTCCC	142,152,658–142,152,805	SSLP	C > S
<i>D4sjh19</i>	GTGGGGAGCATGTCCTAAA	TGGGAGTGTGTAGCAGAGGA	142,633,317–142,633,544	SSLP	C > S
<i>D4Mit160</i>	ACTATGCTAAACCAACAATCTCCC	CCGAGAAACCTAATCTTGATGA	144,040,010–144,040,205	SSLP	C > S
<i>D4sjh10</i>	GCAGAAATGGCACAGGAGAT	CCCACATTTGAAACCACCTC	144,208,822–144,209,061	SSLP	C > S
<i>Dhrs3</i>	ACATCTGGTTGTTGGGAGACGGAAA	AGCCAGAGATGCTTAGGCTGTGT	144,517,967–144,518,288	SNP	n/a
<i>D4sjh9</i>	GGACTGGCTCTGAGGAACAA	GCCAAGCAGCTTCTCTTAG	144,635,848–144,636,084	SSLP	C < S
<i>D4Mit232</i>	GGCTCACACACTGCTCTT	ACTCAGAGTCCCCTGGCC	144,647,559–144,647,676	SSLP	C > S
<i>D4Mit233</i>	TGGTCATGTGTGCCATGC	ACTTCATGTAGCCAGGTGGG	144,814,847–144,815,021	SSLP	C > S
<i>Tnfrsf1b</i>	CACAGAGGCCCTTCAGGTTA	TAGGCTCCTCTGCCAAGTTC	144,804,628–144,805,298	SNP	n/a
<i>D4kns1</i>	TTTACAGAGAGAAAACCCGGGCACT	ACACCCAAGTTGCGCAAGAATCTG	145,720,468–145,720,843	SNP	n/a
<i>D4Mit285</i>	CTTTAGGTAGAACTTCTCCGTTTT	GTGGCAGTGAACCTATTCAACC	146,815,380–146,815,479	SSLP	C > S
<i>D4Mit206</i>	TGAAGGCCTGAGTTAATACCTAGC	TCATCAACTAAGTGACAAGGAAGG	147,251,451–147,251,598	SSLP	C < S
<i>Npb</i>	GAAGACACCAGTGCACAAGC	AATCCCCATCCTCCATAG	147,360,003–147,360,359	SNP	n/a
<i>D4sjh11</i>	CCACCAGGCTGGATAGCAT	GCCAGGAAGGTAGCATATAA	147,540,887–147,541,118	SSLP	C < S
<i>D4sjh12</i>	TTTGAGACCAAAGATGAGACA	CTTTTCTGGCCTCTGACCTG	147,643,331–147,643,561	SSLP	C < S
<i>D4sjh13</i>	TCTGGTTTCTATGCGTGTGC	CGGGATCCATATGGTAGTGG	148,093,433–148,093,658	SSLP	C > S
<i>D4Mit129</i>	GTAATACACAACCATAGACACCTGC	TGCCTGCCTACTGTGTTTTG	148,297,268–148,297,396	SSLP	C > S
<i>D4Mit49</i>	TTGCCTAGCATACCTGCATG	GCTGGGTTTGTGGCTCAG	148,572,905–148,573,054	SSLP	C > S

segments in and around candidate genes in SWR and Line 4-T, which were later assessed in individuals from the informative Line 4-3 recombinant subcongenic lines. These included three SNPs within *Nppb*, six SNPs within *Tnfrsf1b*, and two SNPs slightly upstream of *Dhrs3* (Table 3.2). All three SNPs amplified by the *Nppb* marker and two of the SNPs amplified by the *Tnfrsf1b* marker were novel; all others were annotated in dbSNP Build 132. Although *Nppb* sequencing was informative for mapping purposes, it was excluded as a candidate gene based on the haplotype patterns of Lines 4-11, 4-14, 4-16. *Tnfrsf1b* and *Dhrs3* were located within the 2.6 Mb *Gct1* interval and were sequenced for mapping and/or candidacy as GC tumour susceptibility genes. The identification of polymorphisms between CAST and SWR alleles within *Tnfrsf1b* and 62 and 145 bp downstream of the 3' untranslated region (UTR) of *Dhrs3* allowed for genotype assignment of the subcongenic lines as well as inclusion of these genes within the candidate *Gct1* interval.

Annotated SNP genotyping markers from dbSNP Build 132 were empirically tested for polymorphic base changes between CAST and SWR; only one marker, *D4kns1*, amplified a single product that was polymorphic between CAST and SWR and could be reliably assessed in all recombinant subcongenic lines. Twenty previously unreported SNPs were identified within the 376 bp *D4kns1* amplicon designed to amplify *rs27631336*, a G→T substitution at bp position 232 of the amplicon at genomic position 145,720,699 that lies within the pseudogene *Gm13241* (Table 3.3). The expected *rs27631336* bp substitution was not present in Line 4-T or recombinant subcongenic mice inferred to be carrying the CAST allele. In addition to the 20 novel SNPs, the annotated SNP *rs49752369* was also identified in the *D4kns1* amplicon. Two SNPs at bp positions

Table 3.2 Annotated and novel SNPs identified within gene candidates. Genes, geneic and genomic locations, alleles and dbSNP ID numbers, if applicable, are shown. (+): forward strand; (-): reverse strand; +: prior to gene cDNA bp 1

Associated Gene (strand)	Genic Location (bp)	Genomic Location (bp)	CAST Allele	SWR Allele	dbSNP ID
Dhrs3 (+)	+62	144,518,174	C	T	rs32447066
	+145	144,518,257	G	A	rs33013120
Tnfrsf1b (-)	2387	144,804,797	T	G	novel
	2348	144,804,836	G	A	rs32429059
	2325	144,804,859	C	T	rs27627703
	2050	144,805,134	T	C	novel
	1994	144,805,190	G	A	rs47203705
	1966	144,805,218	G	A	rs27627701
Nppb (+)	149	147,360,045	T	G	novel
	161	147,360,056	C	T	novel
	267	147,360,163	T	C	rs32950646

Table 3.3 Annotated and novel SNPs identified within the fragment amplified by***D4kns1***. SNP locations, alleles and dbSNP ID numbers, if applicable are shown. *

indicates SNPs used for genotyping

Position in Amplicon (bp)	Genomic Position (bp)	B6 Allele	CAST Allele	SWR Allele	dbSNP ID
39	145,720,506	T	C	C	novel
58	145,720,525	A	T	T	novel
74	145,720,541	C	T	T	novel
77	145,720,544	C	A	A	novel
88	145,720,555	A	G	G	novel
99	145,720,566	T	C	C	novel
109	145,720,576	T	G	G	novel
117	145,720,584	A	G	G	rs49752369
148	145,720,615	G	A	A	novel
174	145,720,641	A	C	C	novel
185	145,720,652	T	C	C	novel
186	145,720,653	T	G	G	novel
218	145,720,685	C	T	T	novel
228*	145,720,695	C	T	C	novel
264*	145,720,731	C	T	C	novel
288	145,720,755	G	A	A	novel
290	145,720,757	T	C	C	novel
294	145,720,761	C	T	T	novel
301	145,720,768	G	C	C	novel
304	145,720,771	T	C	C	novel
330	145,720,797	C	T	T	novel

228 and 264 of the amplicon were polymorphic between CAST and SWR and were used for genotyping. The addition of *D4kns1* to the Chr 4 haplotype map resulted in a refined *Gct1* interval of 1.51 Mb (Figure 3.2).

3.2 The Refined *Gct1* Interval

3.2.1. *In silico* Data

The 1.51 Mb *Gct1* interval contains 43 unique genetic determinants, including 15 protein coding genes, four processed transcripts, four non-coding RNA genes, and 20 pseudogenes (Figure 3.3; Ensembl Mouse Genome Browser release 61; NCBI m37 February 2011). The majority of the genetic entities in *Gct1* are located at the distal end of the interval, which is particularly pseudogene-rich and contains repetitive genetic elements. Table 3.4 summarizes the features of the 23 genes which we hypothesize will include a genetic determinant that is causative for GC tumorigenesis.

Only four of the 15 protein coding genes – *Dhrs3*, *Vps13D*, *Tnfrsf1b*, and *Tnfrsf8* – have been described in the literature with defined or speculated roles in human or mouse. Tissue specific gene expression levels have been examined for these four genes by microarray in both species; Table 3.5 shows the relative expression data for these genes between the male and female mouse gonads, based on the Gene Expression Atlas initiative (Su *et al.* 2004) accessed through the BioGPS web portal (Wu *et al.* 2009; www.biogps.gnf.org). All four genes show detectable expression in the testis and ovary in both species; however, *Dhrs3* and *Tnfrsf1b* show greater abundance in the female

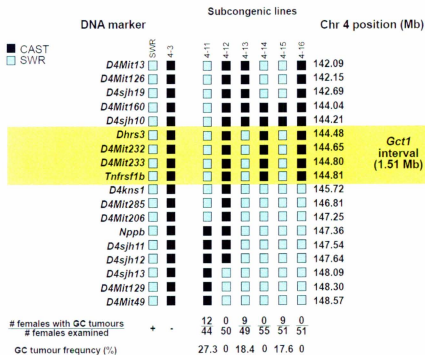


Figure 3.2 Chr 4 haplotypes of SWR, Line 4-3, and the SWR.SJL-X.CAST-4 recombinant subcongenic mouse lines at the refined *Gct1* interval.

The GC tumour susceptible strains share common regions of SWR genetic background between markers *D4sjh10* and *D4kns1*, for a minimal genetic segment containing *Gct1* of approximately 1.51 Mb. +: GC tumour susceptible; -: GC tumour resistant; black boxes: CAST alleles; blue boxes: SWR alleles; yellow rectangle: the *Gct1* interval.

Table 3.4 Summary of the genetic determinants within the 1.51 Mb *GctI* interval. ncRNA: non-coding RNA; ND: not determined; NA: none available; +: forward; -: reverse

Gene	Description	Gene Ontology	Location on Chr 4 (bp)	Strand	Gene type	Unique Transcripts
<i>Gm13177</i>	predicted gene 13177	ND	144,203,610	+	protein coding	1
<i>Gm436</i>	predicted gene 436	ND	144,259,840	-	protein coding	1
<i>Gm13178</i>	predicted gene 13178	ND	144,293,094	-	protein coding	1
<i>U1.125</i>	U1 spliceosomal RNA	ND	144,355,530	-	small nuclear ncRNA	1
<i>Gm438</i>	predicted gene 438	ND	144,367,107	-	protein coding	1
<i>Dhrs3</i>	dehydrogenase/reductase (SDR family) member 3	oxidoreductase activity	144,482,730	+	protein coding	8
<i>Vps13d</i>	vacuolar protein sorting 13 D (yeast)	ND	144,562,526	-	protein coding	1
<i>Vps13d</i>	vacuolar protein sorting 13 D (yeast)	ND	144,562,529	-	protein coding	10
<i>Tnfrsf1b</i>	tumour necrosis factor receptor superfamily member 1b	TNF receptor	144,803,366	-	protein coding	2
<i>Tnfrsf8</i>	tumour necrosis factor receptor superfamily member 8	TNF receptor	144,857,040	-	protein coding	2
<i>Gm13227</i>	predicted gene 13227	ND	145,000,148	+	processed transcript	2
<i>Vmn2r-ps14</i>	vomeronasal 2, receptor, pseudogene 14	ND	145,054,107	+	processed transcript	3
<i>Gm13225</i>	predicted gene 13225	ND	145,100,662	+	protein coding	4
<i>Gm13242</i>	predicted gene 13242	ND	145,104,787	+	protein coding	3
<i>Gm13212</i>	predicted gene 13212	ND	145,175,069	+	protein coding	3
<i>AL627304.1</i>	NA	ND	145,191,866	-	long ncRNA	1
<i>Gm13236</i>	predicted gene 13236	ND	145,352,832	+	processed transcript	1
<i>AL929465.1</i>	NA	ND	145,454,975	+	micro RNA	1
<i>Gm13235</i>	predicted gene 13235	ND	145,458,697	+	protein coding	2
<i>2610036A22Rik</i>	RIKEN cDNA <i>2610036A22</i>	ND	145,439,879	-	protein coding	2
<i>1700095A21Rik</i>	RIKEN cDNA <i>1700095A21</i>	ND	145,651,166	+	processed transcript	1
<i>Gm13247</i>	predicted gene 13247	ND	145,658,647	-	protein coding	2
<i>AL627077.1</i>	NA	ND	145,686,275	+	long ncRNA	1

Table 3.5 Relative gene expression in the mouse gonad. Expression levels were determined by microarray (Sue *et al.* 2004) and were accessed through the BioGPS web portal (Wu *et al.* 2009). *Dhrs3* and *Tnfrsf1b* are highly expressed in the mouse ovary compared to testis.

Gene	Ovary	Testis	Relative Expression (ovary/testis)
<i>Dhrs3</i>	969.90	40.67	23.85
<i>Vps13d</i>	5.97	4.60	1.29
<i>Tnfrsf1b</i>	112.62	13.11	8.59
<i>Tnfrsf8</i>	4.36	4.49	0.97

versus male gonad in mice.

3.2.2 Qualitative Gene Expression Analysis

To empirically determine the expression of the *Gct1* gene candidates in the young ovary of tumour susceptible and tumour resistant mice, the design of gene-specific primers was attempted to capture unique amplicons representing as many transcripts as possible.

Of the 23 entities, only 11 were successfully amplified by end-point PCR. Three genes at the distal end of *Gct1* were not pursued as their repetitive sequences prevented their specific amplification. *Gm13177* is interrupted by the SSLP marker *D4sjh10* at the proximal boundary of the *Gct1* interval, and therefore was given low priority and was not assessed. Furthermore, the four processed transcripts and four non-coding RNA genes were assigned low priority for assessment. Although it is recognized that non-coding RNA genes can have a large impact on gene expression and disease susceptibility, they were given a lower priority for analysis until the protein coding genes were definitively excluded for shared identity with *Gct1*.

Primers were initially tested for the amplification of a single band in SWR testis cDNA. Those primer pairs that failed were tested in liver and brain cDNA as necessary to determine if the primer pairs were functional. Primer pairs that failed in all tissues were redesigned, whereas those that were successful in amplifying a single amplicon of the desired length were tested in two pools each of ovary cDNA from 4 wk old Line 4-T

and SWR mice. As shown in Table 3.6, all 11 of the genes that were assessed showed positive expression in testes and the four ovary cDNA pools after 39 cycles of PCR. Based on qualitative expression analysis, there was no reason to exclude these genes as potential candidates for shared identity with *Gct1*.

Qualitative assessment of the *Gct1* gene transcripts served as a confirmation of primer specificity prior to quantitative analysis by qPCR. In addition to the testes, Line 4-T, and SWR ovary pools, the *Tnfrsf1b* protein coding transcript was found to be expressed in SWR liver, brain, and GC tumour tissue. Based on its biological role as a mediator of TNF α function in the mouse ovary, *Tnfrsf1b* was prioritized as a candidate for *Gct1* identity and therefore for subsequent quantitative and sequence analyses.

3.2.3 Quantitative Gene Expression Analysis

The quantitative analysis paradigm was dependent upon 1 wk of DHEA stimulation from subcutaneous capsules. As this had not been previously measured in SWR mice, and to ensure that the capsules were having the desired effect on circulating DHEA levels, serum DHEA was measured by ELISA. As shown in Table 3.7, there was no significant difference between serum DHEA levels in SWR (6.51 ± 2.43 ng/mL) and Line 4-T (30.93 ± 37.59 ng/mL) mice after 1 wk of DHEA treatment, although the DHEA-treated Line 4-T group showed a high degree of variability in serum DHEA levels. Serum DHEA levels in all seven samples in the SWR control group were less than 0.37 ng/mL and therefore below the reportable range of the assay. The fourth group

Table 3.6 Qualitative expression of the *Get1* transcripts within the 1.51 Mb interval.
 ND: not determined; ✓: positive expression

Gene	Gene Type	Qualitative Transcript Expression		
		Testes	CAST Ovary	SWR Ovary
<i>Gm13177</i>	known protein coding	ND	ND	ND
<i>Gm436</i>	known protein coding	✓	✓	✓
<i>Gm13178</i>	known protein coding	✓	✓	✓
<i>U1.125</i>	novel small nuclear RNA	ND	ND	ND
<i>Gm438</i>	known protein coding	✓	✓	✓
<i>Dhrs3</i>	known protein coding	✓	✓	✓
<i>Vps13d</i>	known protein coding	✓	✓	✓
<i>Vps13d</i>	known protein coding	✓	✓	✓
<i>Tnfrsf1b</i>	known protein coding	✓	✓	✓
<i>Tnfrsf8</i>	known protein coding	✓	✓	✓
<i>Gm13227</i>	novel processed transcript	ND	ND	ND
<i>Vmn2r-ps14</i>	known processed transcript	ND	ND	ND
<i>Gm13225</i>	known protein coding	✓	✓	✓
<i>Gm13242</i>	known protein coding	✓	✓	✓
<i>Gm13212</i>	known protein coding	✓	✓	✓
<i>AL627304.1</i>	known long non-coding RNA	ND	ND	ND
<i>Gm13236</i>	novel processed transcript	ND	ND	ND
<i>AL929465.1</i>	novel micro RNA	ND	ND	ND
<i>Gm13235</i>	known protein coding	ND	ND	ND
<i>2610036A22Rik</i>	known protein coding	ND	ND	ND
<i>1700095A21Rik</i>	novel processed transcript	ND	ND	ND
<i>Gm13247</i>	known protein coding	ND	ND	ND
<i>AL627077.1</i>	known long non-coding RNA	ND	ND	ND

Table 3.7 Serum DHEA levels in SWR and Line 4-T mice treated with DHEA or empty capsules. Serums were taken 1 wk following capsule implantation.

	SWR	Line 4-T
DHEA Capsule	6.51 ± 2.43 ng/mL (n = 6)	30.93 ± 37.59 ng/mL (n = 7)
Empty Capsule	< 0.37 ng/mL (n = 7)	—

(Line 4-T control, n = 3), which was not incorporated into the quantitative gene expression analysis, could not be compared, as two values were outside either end of the assay's reportable range. The only sample from this group with a serum DHEA level that fell within the reportable range of the assay was 1.446 ng/mL.

Tnfrsf1b mRNA expression was compared between ovary pools from DHEA-treated SWR and Line 4-T mice. As shown in Figure 3.4A, no significant difference in *Tnfrsf1b* mRNA expression was detected over three repeated experiments comparing triplicates of three sets of ovary pools. Figure 3.4B shows the comparison of *Tnfrsf1b* mRNA expression between ovary pools from DHEA-treated SWR and SWR control mice who received an empty capsule. Again, no significant difference in *Tnfrsf1b* mRNA expression was detected over three repeated experiments comparing triplicates of three sets of ovary pools.

3.2.4 *Tnfrsf1b* Sequencing

The *Tnfrsf1b* cDNA was sequenced from SWR, Line 4-T, and B6 mice. Nucleotide and amino acid sequence alignments for the three sequenced strains are shown in Appendix C and Figure 3.5, respectively. As shown in Table 3.8, 12 SNPs and two dinucleotide deletions were identified in SWR compared to Line 4-T and the published and/or sequenced B6 reference. All 14 polymorphisms were found in exons 9 and 10, which span the distal coding and 3' UTR regions of the *Tnfrsf1b* cDNA. The 12 SNPs were base pair substitutions, five of which were in the coding region and resulted in

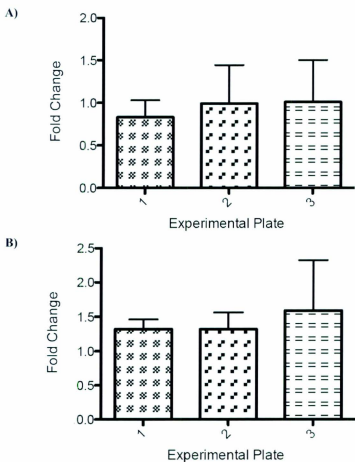


Figure 3.4 Fold change in *Tnfrsf1b* mRNA relative to *Actb*

No significant difference in *Tnfrsf1b* mRNA expression was detected over three repeated experiments comparing triplicates of A) DHEA-treated Line 4-T ovaries relative to DHEA-treated SWR ovaries, or B) DHEA-treated SWR ovaries relative to control-treated SWR ovaries.

```

CAST  MAPAALWVALVFELQLWATGHTVPAQVVLTTPYKPEPGYECQISQEYYDRKAQMCCAACPP
SWR   MAPAALWVALVFELQLWATGHTVPAQVVLTTPYKPEPGYECQISQEYYDRKAQMCCAACPP
B6    MAPAALWVALVFELQLWATGHTVPAQVVLTTPYKPEPGYECQISQEYYDRKAQMCCAACPP
*****

CAST  GQYVKHFNCNKTSDTVCADCEASMYTQVWNQFRTCLSCSSSCTDQVETRACKQKQNRVCA
SWR   GQYVKHFNCNKTSDTVCADCEASMYTQVWNQFRTCLSCSSSCTDQVETRACKQKQNRVCA
B6    GQYVKHFNCNKTSDTVCADCEASMYTQVWNQFRTCLSCSSSCTDQVEIRACTKQKQNRVCA
*****

4-T   CEAGRYCALKTHSGSCRQCMRLSKCGPGFGVASSRAPNGNVLCRACAPGTFSDTTSSTDV
SWR   CEAGRYCALKTHSGSCRQCMRLSKCGPGFGVASSRAPNGNVLCRACAPGTFSDTTSSTDV
B6    CEAGRYCALKTHSGSCRQCMRLSKCGPGFGVASSRAPNGNVLCRACAPGTFSDTTSSTDV
*****

4-T   CRPHRRCISILAI PGNASTDAVCAPESPTLSAI PRTLYVVSQPEPTRSQPLDQEPGSPQTPS
SWR   CRPHRRCISILAI PGNASTDAVCAPESPTLSAI PRTLYVVSQPEPTRSQPLDQEPGSPQTPS
B6    CRPHRRCISILAI PGNASTDAVCAPESPTLSAI PRTLYVVSQPEPTRSQPLDQEPGSPQTPS
*****

4-T   ILTSLGSTPIIEQSTKGGISLPIGLIVGVTSLGLLMLGLVNCFILVQRKKKPSCLQRDAK
SWR   ILTSLGSTPIIEQSTKGGISLPIGLIVGVTSLGLLMLGLVNCFILVQRKKKPSCLQRDAK
B6    ILTSLGSTPIIEQSTKGGISLPIGLIVGVTSLGLLMLGLVNCIILVQRKKKPSCLQRDAK
*****

4-T   VPHVPDEKSDAVGLEQQHLLTTAPSSSSSSLESSASAGDRRAPPGGHPQARVMAEAQGS
SWR   VPHVPDEKSDAVGLEQQHLLTTAPSSSSSSLESSASAGDRRAPPGGHPQARVMAEAQGS
B6    VPHVPDEKSDAVGLEQQHLLTTAPSSSSSSLESSASAGDRRAPPGGHPQARVMAEAQGS
*****

4-T   QEARASSRISDSHSGSHGTHVNVTCIVNVCSSSDHSSQCSSQASATVGDPAKPSASPDK
SWR   QEARASSRISDSHSGSHGTHVNVTCIVNVCSSSDHSSQCSSQASATVGDPAKPSASPDK
B6    QEARASSRISDSHSGSHGTHVNVTCIVNVCSSSDHSSQCSSQASATVGDPAKPSASPDK
*****

4-T   EQVFPFSQECCPSQSPYETTETLQSHKPLPLGVPDMGMKPSQAGWFDQIAVKVA
SWR   EQVFPFSQECCPSQSPYETTETLQSHKPLPLGVPDMGMKPSQAGWFDQIAVKVA
B6    EQVFPFSQECCPSQSPCETTETLQSHKPLPLGVPDMGMKPSQAGWFDQIAVKVA
*****

```

Figure 3.5 Alignment of the SWR, Line 4-T, and B6 Tnfrsf1b amino acid sequences

The single amino acid change in SWR compared to Line 4-T and B6 (p.Phe360Ser) is

highlighted. (*) identity; (:) conservative change; () radical change.

Table 3.8 Nucleotide changes in SWR *Tnfrsf1b* cDNA versus B6 and Line 4-T.Nucleotide ranges are relative to *Tnfrsf1b* cDNA bp 1

Exon	Gene Region	Nucleotide Number	Polymorphism Type	Base(s) Changed or Deleted	Amino Acid Substitution	dbSNP ID
9	Coding	1035	Substitution	C→T	None	rs27627669
9	Coding	1089	Substitution	C→T	None	rs51045832
9	Coding	1148	Substitution	T→C	F→S	rs27627670
9	Coding	1161	Substitution	T→C	None	rs27627671
10	Coding	1431	Substitution	G→A	None	rs27627694
10	3' UTR	1994	Substitution	G→A	-	rs47203705
10	3' UTR	2325	Substitution	C→T	-	rs27627703
10	3' UTR	2348	Substitution	G→A	-	rs32429059
10	3' UTR	2802	Substitution	C→T	-	rs48956371
10	3' UTR	2803	Substitution	T→G	-	rs47232340
10	3' UTR	3094	Substitution	C→T	-	rs48070559
10	3' UTR	3099	Substitution	C→T	-	rs48011026
10	3' UTR	3279-3280	Deletion	CC	-	Novel
10	3' UTR	3288-3289	Deletion	CA	-	Novel

four silent mutations and a single missense mutation, phenylalanine to serine at amino acid 360 (p.Phe360Ser). Originally identified in cDNA, the p.Phe360Ser variant was confirmed in genomic DNA by PCR and sequencing. All 12 SNPs identified in the SWR *Tnfrsf1b* cDNA sequence, including that which resulted in p.Phe360Ser, are known variants in other mouse strains annotated in dbSNP Build 132, and therefore not unique to the SWR strain. The two dinucleotide deletions in the SWR *Tnfrsf1b* cDNA were present in the 3' UTR are novel, although this region is conserved only between mice and human with low sequence identity.

4. Discussion

Overview

GC tumours of the SCST class can affect women at either end of the reproductive spectrum, and based on age of onset and histology, are divided into adult and juvenile subtypes. Despite the association between *FOXL2* and adult GC tumours in humans, as well as the observation that the engineered alteration of a number of critical genes results in exceptionally high frequency SCST phenotypes in mice, no genes conferring innate susceptibility to juvenile-onset GC tumours in humans or mice have been identified. GC tumourigenesis in the SWR mouse recapitulates inherent susceptibility to early-onset GC tumours at a frequency of $\geq 1\%$; genetic investigation of this trait has identified *Gct1* on distal mouse Chr 4 as a fundamental locus for GC tumour initiation.

The *Gct1* locus shows the strongest and most consistent association with the GC tumour phenotype for this polygenic trait, which is characterized by a restricted window of susceptibility and endocrinological sensitivity that coincides with the mouse's pubertal transition. The use of androgens as a method to increase trait penetrance has facilitated the genetic mapping of *Gct1*, and reinforces the extent of steroid hormone influence upon the mechanism of GC tumour initiation in the complex biology of the mammalian ovary. The objective of this thesis was to positionally clone the *Gct1* locus, using a subcongenic mapping strategy to produce a shortlist of candidate genes for prioritized qualitative, quantitative and sequence-based assessments, to resolve the genetic determinant that shares identity with *Gct1*.

4.1 *Gct1* Resides Within a 1.51 Mb Interval

The phenotypic mapping strategy using Line 4-3 as a starting strain for the generation of recombinant subcongenic lines successfully refined the *Gct1* interval from 6.48 Mb to 1.51 Mb, a region between the markers *D4shj10* and *D4kns1*. This region of mouse Chr 4 contains a total of 23 protein coding genes, processed transcripts, and non-coding RNA genes, as well as 20 annotated pseudogenes. The refinement of *Gct1* was aided by the empirical identification of novel SSLP- and SNP-based genotyping DNA markers that are polymorphic between the SWR and CAST strains, as the published DNA marker resources had been exhausted. The identification of polymorphisms within *Gct1* gene candidates was essential for mapping purposes and the exclusion of genes from the interval. It should be noted that until *Gct1* is identified and validated, all DNA polymorphisms unique to the SWR strain within the mapped *Gct1* interval will be under consideration as causative of the trait; however, we have applied a selection scheme for assessment of potential candidates, with known genes given the highest priority.

Successful reduction of the *Gct1* interval during the second round of phenotypic mapping eliminated a number of genes previously considered as candidates for shared identity with *Gct1*, including *Nppb* and *5,10-methylenetetrahydrofolate reductase* (*Mthfr*). Further refinement of the distal end of *Gct1* has been impeded by a high degree of repetitive DNA sequence, which has prevented the development of accurate and specific genotyping markers. Should this hurdle be overcome, a more exact boundary genotyping information of subcongenic lines already phenotyped, and may reduce the 1.51 Mb interval further.

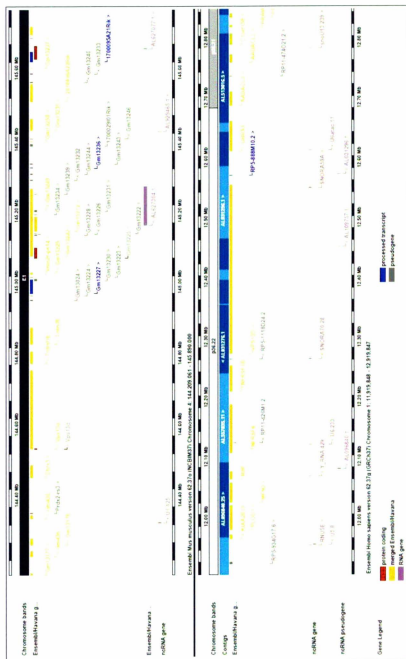
4.2 Prioritizing *Gct1* Candidates: Qualitative Expression Analysis

In an attempt to prioritize candidate genes within the 1.51 Mb *Gct1* interval for further investigation, a qualitative assessment of the determinants within the pubertal SWR and CAST ovary was conducted to achieve two goals: 1) to confirm expression in the mouse ovary at the pubertal stage and, 2) to investigate differential gene expression between the tumour-sensitive and tumour-resistant strains with the hypothesis that the *Gct1* candidate gene may have a severe regulatory mutation that eliminated transcript production or increased transcript turnover. Though not excluded from potential *Gct1* candidacy, processed transcripts and non-coding RNA genes were not included in this initial screen, as they were prioritized below protein coding transcripts contained within the interval. The repetitive nature of the distal end of *Gct1* also prevented the assessment of three protein coding genes due to lack of primer specificity. Further pursuit of these three genes awaits refinement of the distal interval boundary by genotyping, to firmly determine if they are mapped in or out of the *Gct1* locus. A fourth protein coding gene was not assessed as it is interrupted by the proximal marker delineating *Gct1*. All 11 protein coding determinants assessed (*Gm436*, *Gm13178*, *Gm438*, *Dhrs3*, *Vps13d*, *Vps13d*, *Tnfrsf1b*, *Tnfrsf8*, *Gm13225*, *Gm13242*, and *Gm13212*) showed positive expression in ovary cDNA from both strains, and thus no gene candidates were excluded by this strategy.

4.3 The *Gct1* Interval in Mouse and Human

Gct1 is orthologous to human Chr 1p36.22, a region that has been implicated in a number of disorders through genome wide association and cytogenetic studies (Figure 4.1). Kreisel *et al.* (2011) identified copy number alterations at Chr 1p36.22 in a subset of diffuse large B-cell lymphomas, an aggressive form of non-Hodgkin's lymphoma. Human Chr 1p36.22 has also been identified as a region frequently lost in human hepatocellular carcinoma (Nishimura *et al.* 2006), and is a susceptibility locus for hepatocellular carcinoma in patients with hepatitis B virus infection (Zhang *et al.* 2010, Casper *et al.* 2011). Deletions at human Chr 1p36.22 are also frequent in infiltrating ductal carcinoma of the breast (Hawthorn *et al.* 2010), as well as pre-menopausal breast cancers (Varma *et al.* 2005). Loss of heterozygosity at the Chr 1p36.2 region has been speculated to be involved in neuroblastoma (Mora *et al.* 2000), and multiple putative tumour suppressor genes within the region, but outside *Gct1*, have been identified (Geli *et al.* 2010, Munirajan *et al.* 2008, Schlisio *et al.* 2008, Liu *et al.* 2011, Krona *et al.* 2004, Chen *et al.* 2003). In addition to the association between Chr 1p36.22 and neoplastic conditions, deletion or duplication of the region has also been found in cases of congenital abnormalities including dysmorphic facial features and cardiomyopathy, and achalasia (esophageal deformity), respectively (Keppler-Noreuil *et al.* 1995, Chen *et al.* 2006). The identification of *Gct1* will permit a cross examination of the role this GC tumour susceptibility gene might play in other disease conditions associated with Chr 1p36.22 in the future.

Figure 4.1 Ensembl screenshot of the mouse *Gctf* interval and the orthologous human region Chr 1p36.22



Only four well-annotated genes within the *Gct1* interval are conserved between mouse and human based on our current knowledge: *Dhrs3*, *Vps13d*, *Tnfrsf1b*, and *Tnfrsf8* (Figure 4.1). Given our hypothesis that mouse GC tumour susceptibility candidates will provide translational information for juvenile-onset GC tumours in young patients, these genes have been given top priority for further investigation. A comparison of fully differentiated tissue-specific expression patterns is available for these four candidates based on the Gene Expression Atlas initiative (Su *et al.* 2004) accessed through the BioGPS web portal (Wu *et al.* 2009; www.biogps.gnf.org). Relative gene expression levels determined by microarray analysis for mouse versus human, and female versus male gonad, are listed in Table 4.1. We have included the male gonad information based on the evidence that male mice of the GC tumour susceptible SWR strain do not develop SCST tumours at any age, and we speculate that the *Gct1* candidate gene either has ovary-specific functions and/or ovary-restricted expression patterns. In summary, the four genes show evidence for expression in both mouse and human ovary (in agreement with our qualitative assessment), with expression ratios that are comparable in the human ovary and testis, but 2 genes show greater expression in the mouse ovary relative to the testis: *Dhrs3* (23.85 fold) and *Tnfrsf1b* (8.59 fold). Since it is our goal to identify the mechanism of GC tumourigenesis in the mouse, these genes were of significant interest, given their reported biological functions, and this suggestive expression pattern.

Vps13d

Vps13d is a large and complex mouse gene with multiple isoforms that has not

Table 4.1 Relative gene expression in human and mouse gonads. Expression levels were determined by microarray (Sue *et al.* 2004) and were accessed through the BioGPS web portal (Wu *et al.* 2009). *Dhrs3* and *Tnfrsf1b* are highly expressed in the mouse ovary compared to testis, whereas expression of all four genes is relatively equal between human gonads.

Gene	Species	Ovary	Testis	Relative Expression (ovary/testis)
<i>Dhrs3</i>	Mouse	969.90	40.67	23.85
	Human	34.0	48.40	0.70
<i>Vps13d</i>	Mouse	5.97	4.60	1.29
	Human	9.65	19.65	0.49
<i>Tnfrsf1b</i>	Mouse	112.62	13.11	8.59
	Human	7.55	6.75	1.12
<i>Tnfrsf8</i>	Mouse	4.36	4.49	0.97
	Human	2.60	4.0	0.65

been assigned a function. In humans, the *VPS13D* gene encodes a protein belonging to the vacuolar-protein-sorting 13 (VPS13) gene family. In yeast, these proteins are involved in the trafficking of membrane proteins between the trans-Golgi network and the pre-vacuolar compartment. Velayos-Baeza *et al.* (2004) described the four genes in the human VPS13 gene family (*VPS13A* through *D*). Mutations in the *VPS13A* gene have been associated with choreo-acanthocytosis (OMIM 200150), a rare, progressive neurodegenerative disorder that presents between the third and fifth decades of life (Rampoldi *et al.* 2001, Ueno *et al.* 2001). *VPS13B* has been found to be mutated in patients with Cohen syndrome (OMIM 216550), a rare, non-progressive psychomotor retardation disorder characterized by microcephaly, retinal dystrophy, and distinctive facial features (Kolehmainen *et al.* 2003). Velayos-Baeza *et al.* (2004) determined through *in silico* analyses that the VPS13D protein may have two putative domains: a ubiquitin-associated domain (UBA), which may be involved in conferring protein target specificity in the ubiquitination pathway (Hofmann and Bucher 1996), and a ricin-B-lectin domain, which is present in many carbohydrate-recognition proteins and can bind simple sugars (Hazes 1996). Despite a lack of a functional analysis of VPS13D, Velayos-Baeza *et al.* (2004) hypothesized that if these putative domains are indeed present, VPS13D may be involved in the trafficking of ubiquitin-tagged proteins and/or carbohydrates. The potential ontology of *Vps13d* does not immediately highlight it as the most likely candidate for *Get1*, although it cannot be ruled out until more is known of its function.

Tnfrsf8

Tnfrsf8 is a member of the TNF-receptor superfamily expressed mainly in activated cells of the immune system (Berro *et al.* 2004). Downstream signaling from *Tnfrsf8* is mainly transduced through the mitogen-activated protein kinase (MAPK) and nuclear factor kappa B (NF- κ B) pathways (Duckett *et al.* 1997, Horie *et al.* 1998). *Tnfrsf8* signaling can have proliferative and survival or anti-proliferative and apoptotic effects depending on the cellular and stimulatory context (Mir *et al.* 2000, Gruss *et al.* 1994). Serum *Tnfrsf8* levels have been found to be increased in patients with autoimmune diseases and those infected with hepatitis B, hepatitis C, Epstein-Barr, and HIV (reviewed by Oflazoglu *et al.* 2009). Furthermore, *Tnfrsf8* expression is up-regulated in hematological malignancies, including Hodgkin's and non-Hodgkin's lymphomas (Kaudewitz *et al.* 1986, Granados and Hwang 2004, Stein *et al.* 2000). The role of *Tnfrsf8* in cell proliferation, survival, and apoptosis, as well as its increased expression in blood cancers, enhances its standing as an interesting candidate for *Gct1*. Although the action of *Gct1* is confined to the ovary, the exact cellular compartment has not been determined, and it is possible that a molecular factor circulating in the blood or lymph of the ovary may influence growing follicles and disrupt their normal progression, resulting in malignancy. The limited expression pattern of *Tnfrsf8* on cells of the immune system therefore cannot exclude it from the list of gene candidates.

Dhrs3

The human *DHRS3* gene encodes a short-chain dehydrogenase/reductase (SDR). Other members of the SDR family catalyze the oxidation/reduction of steroid hormones, and include 17 β -HSD, which catalyzes the reversible conversion of androstenedione to T and estrone to E₂ (Figure 1.8). *DHRS3* is induced by RA (Cerignoli *et al.* 2002), and reduces all-*trans*-retinol, a storage form of vitamin A, in a process necessary for photoreception (Haeseleer *et al.* 1998). *DHRS3* expression has been found to be up-regulated in papillary thyroid carcinomas, although it is negatively correlated with subsequent lymph node metastasis (Oler *et al.* 2008). Finally, *Dhrs3* was found to be a downstream target of bone morphogenic protein 2 (BMP2), a TGF β family member expressed in GCs of antral follicles that up-regulates FSH receptor and aromatase expression, and which may be involved in the prevention of premature follicle luteinization (Bächner *et al.* 1998, Shi *et al.* 2011). Furthermore, BMP2 expression has been associated with poor prognosis in epithelial ovarian cancer (Le Page *et al.* 2009, Ma *et al.* 2010). The knowledge that *DHRS3* belongs to an enzymatic family that catalyzes steroid hormone conversion, that it is induced by RA, the initiator of oocyte meiosis, and that it has been associated with epithelial ovarian cancer progression, elevates the mouse *Dhrs3* gene in the prioritized ranking of *Gct1* candidate genes.

Tnfrsf1b

Tnfrsf1b, a member of the TNF-receptor superfamily, is a type I transmembrane receptor that binds tumour necrosis factor alpha (TNF α). The *Tnfrsf1b* protein consists of a cysteine-rich extracellular domain that is similar to the extracellular domain of

Tnfrsf1a, the other receptor for TNF α . Binding of the receptors to their ligand shows a 3/3 stoichiometry, in which a complex of three TNF α molecules bind three receptors (Banner *et al.* 1993). The subsequent conformational change in the receptors' cytoplasmic tails results in signal transduction (Chan *et al.* 2000). Tnfrsf1a and Tnfrsf1b differ in their cytoplasmic domains, which relates to their different modes of action. Tnfrsf1b contains a short, C-terminal intracellular region that is involved in binding TNF receptor associated factor 2 (TRAF2). TRAF2 binding triggers the recruitment of cellular inhibitor of apoptosis 1 (c-IAP1) and c-IAP2, which leads to Jun N-terminal kinase (JNK) and NF- κ B activation, resulting in cell survival and proliferation. On the other hand, Tnfrsf1a activates the caspase cascade, resulting in cell death through apoptosis (reviewed by Carpentier *et al.* 2004).

TNF α potentially regulates a number of processes in the mammalian ovary, including that of germ cell cyst breakdown and follicle formation, oocyte death, gonadotropin-induced steroidogenesis, and GC proliferation or apoptosis depending on the follicular context (Morrison and Marcinkiewicz 2002, Son *et al.* 2004, Terranova 1997, Kaipia *et al.* 1996, Sasson *et al.* 2002, Abdo *et al.* 2003). When signaling through Tnfrsf1b, TNF α may also regulate initial follicle recruitment, as *Tnfrsf1b* null mice had increased growing follicle cohorts compared to controls (Greenfeld *et al.* 2007). In humans, the p.M196R TNFRSF1B variant has been associated with hyperandrogenism and polycystic ovary syndrome in women (Peral *et al.* 2002). An established role for *Tnfrsf1b* in the ovary and its activation of pathways resulting in proliferation and cell survival strengthens its standing as the best potential candidate for *Gct1*.

4.4 Summary

The SWR mouse model for GC tumorigenesis is a unique and realistic model for genetically complex and stochastic cancer risk in general, and more specifically, a recognized model for juvenile GC tumours in pediatric patients. Pursuit of GC tumour susceptibility genes in the mouse will provide specific candidates for further investigation in juvenile GC tumour cases, to elucidate a genetic etiology for this unique ovarian tumour class. A phenotype-driven mapping strategy using congenic lines to isolate the fundamental *Gct1* locus has successfully resolved the genetic interval to 1.51 Mb, using DHEA stimulation at puberty to increase trait penetrance for the purpose of mapping. The refined interval in the mouse is still relatively gene-rich, with 43 entities currently annotated, although 20 are repetitive pseudogenes that have hindered resolution of the distal interval boundary. Of 23 total genes, 11 protein-coding genes underwent qualitative gene expression assessment in the pubertal mouse ovary, and showed positive evidence for expression that was similar between GC tumour-susceptible and resistant females, essentially eliminating none from the search for *Gct1*. Our prioritization strategy for the remaining gene candidates focused on the known genes that were also present in the homologous human interval on Chr 1p36.22: *Dhrs3*, *Vps13d*, *Tnfrsf8*, *Tnfrsf1b*. Functional information for *Tnfrsf1b* made it a very interesting and probable candidate for *Gct1*. Sequencing of the coding region did not reveal variations that were unique to the SWR strain, although two dinucleotide deletions in the 3' UTR regions of the SWR transcript could potentially impact transcript stability. DHEA treatment of tumour susceptible or resistant ovaries did not alter *Tnfrsf1b* gene expression, and so did

not shed light on DHEA responsiveness, or *Tnfrsf1b* candidacy. The low phenotypic penetrance of GC tumours in the SWR mouse model, and the lack of an overt phenotype in male SWR mice, suggests a subtle mutation unique to this strain may interfere with a normal ovarian process, leading to tumorigenesis in only a small fraction of mice. Strategies to resolve *Gct1* identity will incorporate additional genotype refinement, but also fine-phenotype analysis, for consideration of which ovarian cellular compartment *Gct1* may act through or influence to initiate GC tumour formation. Close examination of pre-neoplastic follicular lesions by immunohistochemistry for the protein-coding candidate genes identified will complement the strategies already employed for *Gct1* identification.

4.5 Future Directions

- 1) To improve mapping resolution and exclude potential gene candidates, refining the *Gct1* interval using the six phenotyped, congenic sublines is the greatest priority
- 2) Sequencing of the coding and regulatory regions of *Dhrs3* and a quantitative expression analysis similar to that performed for *Tnfrsf1b*, to determine if the SWR *Dhrs3*cDNA possesses a unique variant or is differentially expressed in the SWR ovary

- 3) Protein expression patterns in early pre-neoplastic follicles by immunohistochemistry, to reveal information about cell-specific protein expression for the four known protein coding genes homologous between mouse and human, in the presence or absence of DHEA

5. References

- Abdo M, Hisheh S, Dharmarajan A. 2003. Role of tumor necrosis factor-alpha and the modulating effect of the caspases in rat corpus luteum apoptosis. *Biol Reprod* 68(4):1241-8.
- Al-Agha OM, Huwait HF, Chow C, Yang W, Senz J, Kalloger SE, Huntsman DG, Young RH, Gilks CB. 2011. FOXL2 is a sensitive and specific marker for sex cord-stromal tumors of the ovary. *Am J Surg Pathol* 35(4):484-94.
- Altschul SF, Gish W, Miller W, Myers EW, Lipman DJ. 1990. Basic local alignment search tool. *J Mol Biol* 215(3):403-10.
- Bächner D, Ahrens M, Schroder D, Hoffmann A, Lauber J, Betat N, Steinert P, Flohe L, Gross G. 1998. Bmp-2 downstream targets in mesenchymal development identified by subtractive cloning from recombinant mesenchymal progenitors (C3H10T1/2). *Dev Dyn* 213(4):398-411.
- Baker TG. 1963. A quantitative and cytological study of germ cells in human ovaries. *Proc R Soc Lond B Biol S* 158:417-33.
- Banner DW, D'Arcy A, Janes W, Gentz R, Schoenfeld HJ, Broger C, Loetscher H, Lesslauer W. 1993. Crystal structure of the soluble human 55 kd TNF receptor-human TNF beta complex: Implications for TNF receptor activation. *Cell* 73(3):431-45.
- Bast RC, Hennessy B, Gordon BM. 2009. The biology of ovarian cancer: New opportunities for translation. *Nat Rev Cancer* 9(6):415-28.
- Beamer WG. 1986. Gonadotropin, steroid, and thyroid hormone milieu of young SWR mice bearing spontaneous granulosa cell tumors. *J Natl Cancer Inst* 77(5):1117-23.
- Beamer WG, Shultz KL, Tennent BJ. 1988. Induction of ovarian granulosa cell tumors in SWXJ-9 mice with dehydroepiandrosterone. *Cancer Res* 48(10):2788-92.
- Beamer WG, Hoppe PC, Whitten WK. 1985. Spontaneous malignant granulosa cell tumors in ovaries of young SWR mice. *Cancer Res* 45(11):5575-81.
- Beamer WG, Shultz KL, Tennent BJ, Shultz LD. 1993. Granulosa cell tumorigenesis in genetically hypogonadal-immunodeficient mice grafted with ovaries from tumor-susceptible donors. *Cancer Res* 53(16):3741-6.
- Beamer WG, Shultz KL, Tennent BJ, Nadeau JH, Churchill GA, Eicher EM. 1998. Multigenic and imprinting control of ovarian granulosa cell tumorigenesis in mice. *Cancer Res* 58(16):3694-9.
- Beamer WG, Tennent BJ, Shultz KL, Nadeau JH, Shultz LD, Skow LC. 1988. Gene for ovarian granulosa cell tumor susceptibility, gct, in SWXJ recombinant inbred strains of mice revealed by dehydroepiandrosterone. *Cancer Res* 48(18):5092-5.
- Bedell MA, Brannan CI, Evans EP, Copeland NG, Jenkins NA, Donovan PJ. 1995. DNA rearrangements located over 100 kb 5' of the steel (sl)-coding region in steel-panda and steel-contrasted mice deregulate sl expression and cause female sterility by disrupting ovarian follicle development. *Genes* 9(4):455-70.
- Berro AI, Perry GA, Agrawal DK. 2004. Increased expression and activation of CD30 induce apoptosis in human blood eosinophils. *J Immunol* 173(3):2174-83.

- Bertolino P, Tong W, Galendo D, Wang Z, Zhang C. 2003. Heterozygous Men1 mutant mice develop a range of endocrine tumors mimicking multiple endocrine neoplasia type 1. *Mol Endocrinol* 17(9):1880-92.
- Bielschowsky M and D'Ath EF. 1973. Spontaneous granulosa cell tumours in mice of strains NZC-B1, NZO-B1, NZY-B1 and NZB-B1. *Pathology* 5(4):303-10.
- Björkholm E, and Silfverswärd C. 1981. Prognostic factors in granulosa-cell tumors. *Gynecol Oncol* 11(3):261-74.
- Blake JA, Bult CJ, Kadin JA, Richardson JE, Eppig JT, Mouse Genome Database Group. 2011. The mouse genome database (MGD): Premier model organism resource for mammalian genomics and genetics. *Nucleic Acids Res* 39(Database issue):D842-8.
- Boerboom D, Paquet M, Hsieh M, Liu J, Jamin SP, Behringer RR, Sirois J, Taketo MM, Richards JS. 2005. Misregulated Wnt/beta-catenin signaling leads to ovarian granulosa cell tumor development. *Cancer Res* 65(20):9206-15.
- Bowles J, and Koopman P. 2007. Retinoic acid, meiosis and germ cell fate in mammals. *Development* 134(19):3401-11.
- Bowles J, Knight D, Smith C, Wilhelm D, Richman J, Mamiya S. 2006. Retinoid signaling determines germ cell fate in mice. *Science* 312(5773):596-600.
- Breslow NE, Day NE, Tomatis L, Turusov VS. 1974. Associations between tumor types in a large-scale carcinogenesis study of CF-1 mice. *J Natl Cancer Inst* 52(1):233-9.
- Canadian Cancer Society's Steering Committee on Cancer Statistics. 2011. Canadian cancer statistics 2011. Toronto, ON: Canadian Cancer Society.
- Carpentier I, Coornaert B, Beyaert R. 2004. Function and regulation of tumor necrosis factor receptor type 2. *Curr Med Chem* 11(16):2205-12.
- Casagrande JT, Louie EW, Pike MC, Roy S, Ross RK, Henderson BE. 1979. "Incessant ovulation" and ovarian cancer. *Lancet* 2(8135):170-3.
- Casper M, Grunhage F, Lammert F. 2011. Cancer risk in chronic hepatitis B: Do genome-wide association studies hit the mark? *Hepatology* 53(4):1390-2.
- Cerignoli F, Guo X, Cardinali B, Rinaldi C, Casaletto J, Frati L, Serepanti I, Gudas LJ, Gulino A, Thiele CJ, et al. 2002. retSDR1, a short-chain retinol dehydrogenase/reductase, is retinoic acid-inducible and frequently deleted in human neuroblastoma cell lines. *Cancer Res* 62(4):1196-204.
- Chan FK, Chun HJ, Zheng L, Siegel RM, Bui KL, Lenardo MJ. 2000. A domain in TNF receptors that mediates ligand-independent receptor assembly and signaling. *Science* 288(5475):2351-4.
- Chen CP, Lin SP, Lee CC, Town DD, Wang W. 2006. Partial trisomy 1p (1p36.22-->pter) and partial monosomy 9p (9p22.2-->pter) associated with achalasia, flexion deformity of the fingers and epilepsy in a girl. *Genet Couns* 17(3):301-6.
- Chen YY, Takita J, Chen YZ, Yang HW, Hanada R, Yamamoto K, Hayashi Y. 2003. Genomic structure and mutational analysis of the human KIF1B α gene located at 1p36.2 in neuroblastoma. *Int J Oncol* 23(3):737-44.
- Choi Y, Yuan D, Rajkovic A. 2008. Germ cell-specific transcriptional regulator sohlh2 is essential for early mouse folliculogenesis and oocyte-specific gene expression. *Biol Reprod* 79(6):1176-82.

- Colombo N, Parma G, Zanagnolo V, Insinga A. 2007. Management of ovarian stromal cell tumors. *J Clin Oncol* 25(20):2944-51.
- Crum CP. 1999. The female genital tract. In: Robbins' pathologic basis of disease. Cotran RS, Kumar V, Collins T, editors. 6th ed. Philadelphia: W.B. Saunders Company.
- Danilovich N, Roy I, Sairam MR. 2001. Ovarian pathology and high incidence of sex cord tumors in follitropin receptor knockout (FORKO) mice. *Endocrinology* 142(8):3673-84.
- Dickie MM. 1954. The use of F1 hybrid and backcross generations to reveal new and/or uncommon tumor types. *J Natl Cancer Inst* 15(3):791-9.
- Dong J, Albertini DF, Nishimori K, Kumar TR, Lu N, Matzuk MM. 1996. Growth differentiation factor-9 is required during early ovarian folliculogenesis. *Nature* 383(6600):531-5.
- Dorward AM, Shultz KL, Beamer WG. 2007. LH analog and dietary isoflavones support ovarian granulosa cell tumor development in a spontaneous mouse model. *Endocr Relat Cancer* 14(2):369-79.
- Dorward AM, Shultz KL, Ackert-Bicknell CL, Eicher EM, Beamer WG. 2003. High-resolution genetic map of X-linked juvenile-type granulosa cell tumor susceptibility genes in mouse. *Cancer Res* 63(23):8197-202.
- Dorward AM, Shultz KL, Horton LG, Li R, Churchill GA, Beamer WG. 2005. Distal chr 4 harbors a genetic locus (Gct1) fundamental for spontaneous ovarian granulosa cell tumorigenesis in a mouse model. *Cancer Res* 65(4):1259-64.
- Dozois RR, Kempers RD, Dahlin DC, Bartholomeew JG. 1970. Ovarian tumors associated with the peutz-jeghers syndrome. *Ann Surg* 172(2):233-8.
- Duckett CS, Gedrich RW, Gilfillan MC, Thompson CB. 1997. Induction of nuclear factor kappaB by the CD30 receptor is mediated by TRAF1 and TRAF2. *Mol Cell Biol* 17(3):1535-42.
- Elvin JA, Yan C, Wang P, Nishimori K, Matzuk MM. 1999. Molecular characterization of the follicle defects in the growth differentiation factor 9-deficient ovary. *Mol Endocrinol* 13(6):1018-34.
- Eppig JJ, Wigglesworth K, Pendola FL. 2002. The mammalian oocyte orchestrates the rate of ovarian follicular development. *Proc Natl Acad Sci USA* 99(5):2890-4.
- Everett NB. 1943. Observational and experimental evidences relating to the origin and differentiation of the definitive germ cells in mice. *J Exp Zool* 92(1):49-91.
- Farini D, Sala GL, Tedesco M, Felici MD. 2007. Chemoattractant action and molecular signaling pathways of kit ligand on mouse primordial germ cells. *Dev Biol* 306(2):572-83.
- Fathalla MF. 1971. Incessant ovulation--a factor in ovarian neoplasia? *Lancet* 2(7716):163.
- Fauser BC and van Heusden AM. 1997. Manipulation of human ovarian function: Physiological concepts and clinical consequences. *Endocr Rev* 18(1):71-106.
- Flaherty L. 1981. Congenic strains. In: The mouse in biomedical research. Foster HL, Small JD, Fox JG, editors. New York: Academic Press. 215-222 p.

- Flicek P, Amode MR, Barrell D, Beal K, Brent S, Chen Y, Clapham P, Coates G, Fairley S, Fitzgerald S, et al. 2011. Ensembl 2011. *Nucleic Acids Res* 39(Database issue):D800-6.
- Frith CH, Zuna RE, Morgan K. 1981. A morphologic classification and incidence of spontaneous ovarian neoplasms in three strains of mice. *J Natl Cancer Inst* 67(3):693-702.
- Fuller PJ, Verity K, Shen Y, Mammers P, Jobling T, Burger HG. 1998. No evidence of a role for mutations or polymorphisms of the follicle-stimulating hormone receptor in ovarian granulosa cell tumors. *J Clin Endocrinol Metab* 83(1):274-9.
- Gardner RL, and Rossant J. 1979. Investigation of the fate of 4-5 day post-coitum mouse inner cell mass cells by blastocyst injection. *J Embryol Exp Morphol* 52:141-52.
- Geary CP. 1984. Carcinogen-induced granulosa cell tumours in NZC/B1 mice. *Pathology* 16(2):131-5.
- Geetha P and Nair MK. 2010. Granulosa cell tumours of the ovary. *Aust N Z J Obstet Gynaecol* 50(3):216-20.
- Geli J, Kiss N, Kogner P, Larsson C. 2010. Suppression of RIZ in biologically unfavourable neuroblastomas. *Int J Oncol* 37(5):1323-30.
- Goeze PM, Beamer WG, de Jong FH, Freeman DA. 1997. Hormone synthesis and responsiveness of spontaneous granulosa cell tumors in (SWR x SWXJ-9) F1 mice. *Gynecol Oncol* 65(1):143-8.
- Granados S and Hwang ST. 2004. Roles for CD30 in the biology and treatment of CD30 lymphoproliferative diseases. *J Invest Dermatol* 122(6):1345-7.
- Greenacre CB. 2004. Spontaneous tumors of small mammals. *Vet Clin North Am Exot Anim Pract* 7(3):627,51, vi.
- Greenfield CR, Roby KF, Pepling ME, Babus JK, Terranova PF, Flaws JA. 2007. Tumor necrosis factor (TNF) receptor type 2 is an important mediator of TNF alpha function in the mouse ovary. *Biol Reprod* 76(2):224-31.
- Gross HJ, Boiani N, Williams DE, Armitage RJ, Smith CA, Goodwin RG. 1994. Pleiotropic effects of the CD30 ligand on CD30-expressing cells and lymphoma cell lines. *Blood* 83(8):2045-56.
- Hacker A, Capel B, Goodfellow P, Lovell-Badge R. 1995. Expression of *sry*, the mouse sex determining gene. *Development* 121(6):1603-14.
- Haeseleer F, Huang J, Lebiada L, Saari JC, Palezewski K. 1998. Molecular characterization of a novel short-chain dehydrogenase/reductase that reduces all-trans-retinal. *J Biol Chem* 273(34):21790-9.
- Halperin D, Visscher DW, Wallis T, Lawrence WD. 1995. Evaluation of chromosome 12 copy number in ovarian granulosa cell tumors using interphase cytogenetics. *Int J Gynecol Pathol* 14(4):319-23.
- Hao J, Yamamoto M, Timothy ER, Karen MC, Bray SD, Robert EH. 2008. *Sohlh2* knockout mice are male-sterile because of degeneration of differentiating type A spermatogonia. *Stem Cells* 26(6):1587-97.
- Hawthorn L, Luce J, Stein L, Rothschild J. 2010. Integration of transcript expression, copy number and LOH analysis of infiltrating ductal carcinoma of the breast. *BMC Cancer* 10:460.

- Hazes B. 1996. The (QxW)₃ domain: A flexible lectin scaffold. *Protein Sci* 5(8):1490-501.
- Hemminki A, Markie D, Tomlinson I, Avizienyte E, Roth S, Loukola A. 1998. A serine/threonine kinase gene defective in peutz-jeghers syndrome. *Nature* 391(6663):184-7.
- Hirshfield AN. 1991. Development of follicles in the mammalian ovary. *Int Rev Cytol* 124:43-101.
- Hofmann K and Bucher P. 1996. The UBA domain: A sequence motif present in multiple enzyme classes of the ubiquitination pathway. *Trends Biochem Sci* 21(5):172-3.
- Horie R, Aizawa S, Nagai M, Ito K, Higashihara M, Ishida T, Inoue J, Watanabe T. 1998. A novel domain in the CD30 cytoplasmic tail mediates NFkappaB activation. *Int Immunol* 10(2):203-10.
- Horny HP, Marx L, Krober S, Luttes J, Kaiserling E, Dietl J. 1999. Granulosa cell tumor of the ovary. immunohistochemical evidence of low proliferative activity and virtual absence of mutation of the p53 tumor-suppressor gene. *Gynecol Obstet Invest* 47(2):133-8.
- Houghtaling S, Granville L, Akkari Y, Torimaru Y, Olson S, Finegold M. 2005. Heterozygosity for p53 (Trp53^{-/-}) accelerates epithelial tumor formation in fanconi anemia complementation group D2 (Fancd2) knockout mice. *Cancer Res* 65(1):85-91.
- Huang EJ, Manova K, Packer AI, Sanchez S, Bachvarova RF, Besmer P. 1993. The murine steel panda mutation affects kit ligand expression and growth of early ovarian follicles. *Dev Biol* 157(1):100-9.
- Jemal A, Siegel R, Ward E, Hao Y, Xu J, Murray T, Thun MJ. 2008. Cancer statistics, 2008. *CA Cancer J Clin* 58(2):71-96.
- Jeske YW, Bowles J, Greenfield A, Koopman P. 1995. Expression of a linear sry transcript in the mouse genital ridge. *Nat Genet* 10(4):480-2.
- Johnson J, Canning J, Kaneko T, James KP, Jonathan LT. 2004. Germline stem cells and follicular renewal in the postnatal mammalian ovary. *Nature* 428(6979):145-50.
- Juneja SC, Barr KJ, Enders GC, Kidder GM. 1999. Defects in the germ line and gonads of mice lacking connexin43. *Biol Reprod* 60(5):1263-70.
- Kaipia A, Chun SY, Eisenhauer K, Hsueh AJ. 1996. Tumor necrosis factor-alpha and its second messenger, ceramide, stimulate apoptosis in cultured ovarian follicles. *Endocrinology* 137(11):4864-70.
- Kato N, Romero M, Catusas L, Prat J. 2004. The STK11/LKB1 peutz-jegher gene is not involved in the pathogenesis of sporadic sex cord-stromal tumors, although loss of heterozygosity at 19p13.3 indicates other gene alteration in these tumors. *Hum Pathol* 35(9):1101-4.
- Kaudewitz P, Stein H, Burg G, Mason DY, Braun-Falco O. 1986. Atypical cells in lymphomatoid papulosis express the hodgkin cell-associated antigen ki-1. *J Invest Dermatol* 86(4):350-4.
- Kauff ND, Satagopan JM, Robson ME, Scheuer L, Hensley M, Hudis CA, Ellis NA, Boyd J, Borgen PI, Barakat RR, et al. 2002. Risk-reducing salpingo-oophorectomy in women with a BRCA1 or BRCA2 mutation. *N Engl J Med* 346(21):1609-15.

- Kaufman MH. 1991. Histochemical identification of primordial germ cells and differentiation of the gonads in homozygous tetraploid mouse embryos. *J Anat* 179:169-81.
- Kepler-Noreuil KM, Carroll AJ, Finley WH, Rutledge SL. 1995. Chromosome 1p terminal deletion: Report of new findings and confirmation of two characteristic phenotypes. *J Med Genet* 32(8):619-22.
- Keri RA, Lozada KL, Abdul-Karim FW, Nadeau JH, Nilson JH. 2000. Luteinizing hormone induction of ovarian tumors: Oligogenic differences between mouse strains dictates tumor disposition. *Proc Natl Acad Sci USA* 97(1):383-7.
- Köbel M, Kalloger SE, Huntsman DG, Santos JL, Swenerton KD, Seidman JD, Gilks CB, Cheryl Brown Ovarian Cancer Outcomes Unit of the British Columbia Cancer Agency, Vancouver BC. 2010. Differences in tumor type in low-stage versus high-stage ovarian carcinomas. *Int J Gynecol Pathol* 29(3):203-11.
- Kolehmainen J, Black GC, Saarinen A, Chandler K, Clayton-Smith J, Traskelin AL, Perveen R, Kivitić-Kallio S, Norio R, Warburg M, et al. 2003. Cohen syndrome is caused by mutations in a novel gene, COH1, encoding a transmembrane protein with a presumed role in vesicle-mediated sorting and intracellular protein transport. *Am J Hum Genet* 72(6):1359-69.
- Koonings PP, Campbell K, Mishell DR, Grimes DA. 1989. Relative frequency of primary ovarian neoplasms: A 10-year review. *Obstet Gynecol* 74(6):921-6.
- Koopman P, Gubbay J, Vivian N, Goodfellow P, Lovell-Badge R. 1991. Male development of chromosomally female mice transgenic for *sry*. *Nature* 351(6322):117-21.
- Koubova J, Douglas BM, Zhou Q, Capel B, Michael DG, David CP. 2006. Retinoic acid regulates sex-specific timing of meiotic initiation in mice. *Proc Natl Acad Sci USA* 103(8):2474-9.
- Kreisel F, Kulkarni S, Kerns RT, Hassan A, Deshmukh H, Nagarajan R, Frater JL, Cashen A. 2011. High resolution array comparative genomic hybridization identifies copy number alterations in diffuse large B-cell lymphoma that predict response to immuno-chemotherapy. *Cancer Genet* 204(3):129-37.
- Krona C, Ejeskar K, Caren H, Abel F, Sjöberg RM, Martinsson T. 2004. A novel 1p36.2 located gene, APITD1, with tumour-suppressive properties and a putative p53-binding domain, shows low expression in neuroblastoma tumours. *Br J Cancer* 91(6):1119-30.
- Kurilo LF. 1981. Oogenesis in antenatal development in man. *Hum Genet* 57(1):86-92.
- Kurman RJ, and le-Ming Shih. 2010. The origin and pathogenesis of epithelial ovarian cancer: A proposed unifying theory. *Am J Surg Pathol* 34(3):433-43.
- Kuroda H, Terada N, Nakayama H, Matsumoto K, Kitamura Y. 1988. Infertility due to growth arrest of ovarian follicles in Sl/Sl mice. *Dev Biol* 126(1):71-9.
- Lawson KA, and W JH. 1994. Clonal analysis of the origin of primordial germ cells in the mouse. *Ciba found Symp* 182:68,84; discussion 84-91.
- Le Page C, Puiffie ML, Meunier L, Zietarska M, de Ladurantaye M, Tonin PN, Provencher D, Mes-Masson AM. 2009. BMP-2 signaling in ovarian cancer and its association with poor prognosis. *J Ovarian Res* 2:4.

- Lindgren V, Waggoner S, Rotmensch J. 1996. Monosomy 22 in two ovarian granulosa cell tumors. *Cancer Genet Cytogenet* 89(2):93-7.
- Liu Z, Yang X, Li Z, McMahon C, Sizer C, Barenboim-Stapleton L, Bliskovsky V, Mock B, Ried T, London WB, et al. 2011. CASZ1, a candidate tumor-suppressor gene, suppresses neuroblastoma tumor growth through reprogramming gene expression. *Cell Death Differ* Epub.
- Ma Y, Ma L, Guo Q, Zhang S. 2010. Expression of bone morphogenetic protein-2 and its receptors in epithelial ovarian cancer and their influence on the prognosis of ovarian cancer patients. *J Exp Clin Cancer Res* 29(1):85-90.
- Maatouk DM, DiNapoli L, Alvers A, Keith LP, Makoto MT, Capel B. 2008. Stabilization of beta-catenin in XY gonads causes male-to-female sex-reversal. *Hum Mol Genet* 17(19):2949-55.
- Marshall OJ. 2004. PerlPrimer: Cross-platform, graphical primer design for standard, bisulphite and real-time PCR. *Bioinformatics* 20(15):2471-2.
- Matias-Guiu X, Pons C, Prat J. 1998. Mullerian inhibiting substance, alpha-inhibin, and CD99 expression in sex cord-stromal tumors and endometrioid ovarian carcinomas resembling sex cord-stromal tumors. *Hum Pathol* 29(8):840-5.
- Matzuk MM, Finegold MJ, Su JG, Hsueh AJ, Bradley A. 1992. Alpha-inhibin is a tumour-suppressor gene with gonadal specificity in mice. *Nature* 360(6402):313-9.
- McCluggage WG and Maxwell P. 2001. Immunohistochemical staining for calretinin is useful in the diagnosis of ovarian sex cord-stromal tumours. *Histopathology* 38(5):403-8.
- Mintz B and Russell ES. 1957. Gene-induced embryological modifications of primordial germ cells in the mouse. *J Exp Zool* 134(2):207-37.
- Mir SS, Richter BW, Duckett CS. 2000. Differential effects of CD30 activation in anaplastic large cell lymphoma and hodgkin disease cells. *Blood* 96(13):4307-12.
- Mora J, Cheung NK, Kushner BH, LaQuaglia MP, Kramer K, Fazzari M, Heller G, Chen L, Gerald WL. 2000. Clinical categories of neuroblastoma are associated with different patterns of loss of heterozygosity on chromosome arm 1p. *J Mol Diagn* 2(1):37-46.
- Morrison LJ and Marcinkiewicz JL. 2002. Tumor necrosis factor alpha enhances oocyte/follicle apoptosis in the neonatal rat ovary. *Biol Reprod* 66(2):450-7.
- Munirajan AK, Ando K, Mukai A, Takahashi M, Suenaga Y, Ohira M, Koda T, Hirota T, Ozaki T, Nakagawara A. 2008. KIF1Bbeta functions as a haploinsufficient tumor suppressor gene mapped to chromosome 1p36.2 by inducing apoptotic cell death. *J Biol Chem* 283(36):24426-34.
- Nishimura T, Nishida N, Komeda T, Fukuda Y, Imai Y, Yamaoka Y, Nakao K. 2006. Genome-wide semiquantitative microsatellite analysis of human hepatocellular carcinoma: Discrete mapping of smallest region of overlap of recurrent chromosomal gains and losses. *Cancer Genet Cytogenet* 167(1):57-65.
- Nomellini RS, Micheletti ARM, Adad SJ, Murta EFC. 2007. Androgenic juvenile granulosa cell tumor of the ovary with cystic presentation: A case report. *Eur J Gynaecol Oncol* 28(3):236-8.

- Oflazoglu E, Grewal IS, Gerber H. 2009. Targeting CD30/CD30L in oncology and autoimmune and inflammatory diseases. *Adv Exp Med Biol* 647:174-85.
- Oler G, Camacho CP, Hojaij FC, Michaluart P, Jr, Riggins GJ, Cerutti JM. 2008. Gene expression profiling of papillary thyroid carcinoma identifies transcripts correlated with BRAF mutational status and lymph node metastasis. *Clin Cancer Res* 14(15):4735-42.
- Pangas SA, Li X, Umans L, Zwijsen A, Huylebroeck D, Gutierrez C, Wang D, Martin JF, Jamin SP, Behringer RR, et al. 2008. Conditional deletion of Smad1 and Smad5 in somatic cells of male and female gonads leads to metastatic tumor development in mice. *Mol Cell Biol* 28(1):248-57.
- Pangas SA, Choi Y, Daniel JB, Zhao Y, Westphal H, Martin MM. 2006. Oogenesis requires germ cell-specific transcriptional regulators Sohlh1 and Lhx8. *Proc Natl Acad Sci USA* 103(21):8090-5.
- Pectasides D, Pectasides E, Kassanos D. 2008. Germ cell tumors of the ovary. *Cancer Treat Rev* 34(5):427-41.
- Pepling ME and Spradling AC. 2001. Mouse ovarian germ cell cysts undergo programmed breakdown to form primordial follicles. *Dev Biol* 234(2):339-51.
- Peral B, San Millan JL, Castello R, Moghetti P, Escobar-Morreale HF. 2002. Comment: The methionine 196 arginine polymorphism in exon 6 of the TNF receptor 2 gene (TNFRSF1B) is associated with the polycystic ovary syndrome and hyperandrogenism. *J Clin Endocrinol Metab* 87(8):3977-83.
- Petkov PM, Ding Y, Cassell MA, Zhang W, Wagner G, Sargent EE, Asquith S, Crew V, Johnson KA, Robinson P, et al. 2004. An efficient SNP system for mouse genome scanning and elucidating strain relationships. *Genome Res* 14(9):1806-11.
- Pfaffl MW. 2001. A new mathematical model for relative quantification in real-time RT-PCR. *Nucleic Acids Res* 29(9):e45.
- Purdie DM, Christopher JB, Siskind V, Penelope MW, Adèle CG. 2003. Ovulation and risk of epithelial ovarian cancer. *Int J Cancer* 104(2):228-32.
- Rahman NA, Kananen Rilianawati K, Paukku T, Mikola M, Markkula M, Hamalainen T, Huhtaniemi IT. 1998. Transgenic mouse models for gonadal tumorigenesis. *Mol Cell Endocrinol* 145(1-2):167-74.
- Rajkovic A, Stephanie AP, Ballow D, Suzumori N, Martin MM. 2004. NOBOX deficiency disrupts early folliculogenesis and oocyte-specific gene expression. *Science* 305(5687):1157-9.
- Rampoldi L, Dobson-Stone C, Rubio JP, Danek A, Chalmers RM, Wood NW, Verellen C, Ferrer X, Malandrini A, Fabrizi GM, et al. 2001. A conserved sorting-associated protein is mutant in chorea-acanthocytosis. *Nat Genet* 28(2):119-20.
- Risma KA, Clay CM, Nett TM, Wagner T, Yun J, Nilson JH. 1995. Targeted overexpression of luteinizing hormone in transgenic mice leads to infertility, polycystic ovaries, and ovarian tumors. *Proc Natl Acad Sci USA* 92(5):1322-6.
- Rozen S and Skaletsky H. 2000. Primer3 on the WWW for general users and for biologist programmers. *Methods Mol Biol* 132:365-86.
- Ruby JR, Dyer RF, Skalko RG. 1969. The occurrence of intercellular bridges during oogenesis in the mouse. *J Morphol* 127(3):307-39.

- Saga Y. 2008. Mouse germ cell development during embryogenesis. *Curr Opin Genet Dev* 18(4):337-41.
- Sasson R, Winder N, Kees S, Amsterdam A. 2002. Induction of apoptosis in granulosa cells by TNF alpha and its attenuation by glucocorticoids involve modulation of bel-2. *Biochem Biophys Res Commun* 294(1):51-9.
- Schlisio S, Kenchappa RS, Vredeveld LC, George RE, Stewart R, Greulich H, Shahriari K, Nguyen NV, Pigny P, Dahia PL, et al. 2008. The kinesin KIF1Bbeta acts downstream from EglN3 to induce apoptosis and is a potential 1p36 tumor suppressor. *Genes Dev* 22(7):884-93.
- Schmidt D, Catherine EO, Anlag K, Fehsenfeld S, Gredsted L, Treier A. 2004. The murine winged-helix transcription factor Foxl2 is required for granulosa cell differentiation and ovary maintenance. *Development* 131(4):933-42.
- Schofield DE and Fletcher JA. 1992. Trisomy 12 in pediatric granulosa-stromal cell tumors. demonstration by a modified method of fluorescence in situ hybridization on paraffin-embedded material. *Am J Pathol* 141(6):1265-9.
- Scully RE, Young RH, Clement PB. 1998. Tumors of the ovary, maldeveloped gonads, fallopian tube, and broad ligament. 3rd ed. Washington DC: Armed Forces Institute of Pathology.
- Sekido R, Bar I, Narváez V, Penny G, Lovell-Badge R. 2004. SOX9 is up-regulated by the transient expression of SRY specifically in sertoli cell precursors. *Dev Biol* 274(2):271-9.
- Shah SP, Kobel M, Senz J, Morin RD, Clarke BA, Wiegand KC, Leung G, Zayed A, Mehl E, Kalloger SE, et al. 2009. Mutation of FOXL2 in granulosa-cell tumors of the ovary. *N Engl J Med* 360(26):2719-29.
- Shashi V, Golden WL, von Kap C, Andersen WA, Gaffey MJ. 1994. Interphase fluorescence in situ hybridization for trisomy 12 on archival ovarian sex cord-stromal tumors. *Gynecol Oncol* 55(3):349-54.
- Sherry ST, Ward MH, Kholodov M, Baker J, Phan L, Smigielski EM, Sirotkin K. 2001. dbSNP: The NCBI database of genetic variation. *Nucleic Acids Res* 29(1):308-11.
- Shi J, Yoshino O, Osuga Y, Koga K, Hirota Y, Nose E, Nishii O, Yano T, Taketani Y. 2011. Bone morphogenetic protein-2 (BMP-2) increases gene expression of FSH receptor and aromatase and decreases gene expression of LH receptor and StAR in human granulosa cells. *Am J Reprod Immunol* 65(4):421-7.
- Silver LM. 1995. Mouse genetics: Concepts and applications. New York: Oxford University Press.
- Silverman LA and Gitelman SE. 1996. Immunoreactive inhibin, müllerian inhibitory substance, and activin as biochemical markers for juvenile granulosa cell tumors. *J Pediatr* 129(6):918-21.
- Simon AM, Goodenough DA, Li E, Paul DL. 1997. Female infertility in mice lacking connexin 37. *Nature* 385(6616):525-9.
- Sinclair AH, Berta P, Palmer MS, Hawkins JR, Griffiths BL, Smith MJ. 1990. A gene from the human sex-determining region encodes a protein with homology to a conserved DNA-binding motif. *Nature* 346(6281):240-4.

- Sivasankaran S, Itam P, Ayensu-Coker L, Sanchez J, Egler RA, Anderson ML, Brandt ML, Dietrich JE. 2009. Juvenile granulosa cell ovarian tumor: A case report and review of literature. *J Pediatr Adolesc Gynecol* 22(5):e114-7.
- Son DS, Arai KY, Roby KF, Terranova PF. 2004. Tumor necrosis factor alpha (TNF) increases granulosa cell proliferation: Dependence on c-jun and TNF receptor type 1. *Endocrinology* 145(3):1218-26.
- Spandidos A, Wang X, Wang H, Seed B. 2010. PrimerBank: A resource of human and mouse PCR primer pairs for gene expression detection and quantification. *Nucleic Acids Res* 38(Database issue):D792-9.
- Spandidos A, Wang X, Wang H, Dragnev S, Thurber T, Seed B. 2008. A comprehensive collection of experimentally validated primers for polymerase chain reaction quantitation of murine transcript abundance. *BMC Genomics* 9:633.
- Stein H, Foss HD, Durkop H, Marafioti T, Delsol G, Pulford K, Pileri S, Falini B. 2000. CD30(+) anaplastic large cell lymphoma: A review of its histopathologic, genetic, and clinical features. *Blood* 96(12):3681-95.
- Su AI, Wiltshire T, Batalov S, Lapp H, Ching KA, Block D, Zhang J, Soden R, Hayakawa M, Kreiman G, et al. 2004. A gene atlas of the mouse and human protein-coding transcriptomes. *Proc Natl Acad Sci U S A* 101(16):6062-7.
- Tavassoli FA, Mooney E, Gersell DJ, McCluggage WG, Konishi I, Fujii S, Kiyokawa T, Schwartz P, Kubik-Huch RA, Roth LM. 2003. Sex cord-stromal tumours. In: Pathology and genetics of tumours of the breast and female genital organs. Tavassoli FA and Devilee P, editors. Lyon: IARC.
- Tennent BJ, Shultz KL, Beamer WG. 1993. Genetic susceptibility for C19 androgen induction of ovarian granulosa cell tumorigenesis in SWXJ strains of mice. *Cancer Res* 53(5):1059-63.
- Tennent BJ, Shultz KL, Sundberg JP, Beamer WG. 1990. Ovarian granulosa cell tumorigenesis in SWR-derived F1 hybrid mice: Preneoplastic follicular abnormality and malignant disease progression. *Am J Obstet Gynecol* 163(2):625-34.
- Terranova PF. 1997. Potential roles of tumor necrosis factor-alpha in follicular development, ovulation, and the life span of the corpus luteum. *Domest Anim Endocrinol* 14(1):1-15.
- Thayer KA and Foster PM. 2007. Workgroup report: National toxicology program workshop on hormonally induced reproductive tumors - relevance of rodent bioassays. *Environ Health Perspect* 115(9):1351-6.
- Tilly JL. 2001. Commuting the death sentence: How oocytes strive to survive. *Nature Reviews Molecular Cell Biology* 2(11):838-48.
- Uda M, Ottolenghi C, Crisponi L, Jose EG, Deiana M, Kimber W. 2004. Foxl2 disruption causes mouse ovarian failure by pervasive blockage of follicle development. *Hum Mol Genet* 13(11):1171-81.
- Ueno S, Maruki Y, Nakamura M, Tomemori Y, Kamae K, Tanabe H, Yamashita Y, Matsuda S, Kaneko S, Sano A. 2001. The gene encoding a newly discovered protein, chorein, is mutated in chorea-acanthocytosis. *Nat Genet* 28(2):121-2.

- Uhlenhaut NH, Jakob S, Anlag K, Eisenberger T, Sekido R, Kress J, Treier AC, Klugmann C, Klasen C, Holter NI, et al. 2009. Somatic sex reprogramming of adult ovaries to testes by FOXL2 ablation. *Cell* 139(6):1130-42.
- van Wagenen G, Simpson ME. 1965. Embryology of the ovary and testis: Homo sapiens and macaca mulatta. New Haven, CT: Yale University Press.
- Varma G, Varma R, Huang H, Pryschechava A, Groth J, Fleming D, Nowak NJ, McQuaid D, Conroy J, Mahoney M, et al. 2005. Array comparative genomic hybridisation (aCGH) analysis of premenopausal breast cancers from a nuclear fallout area and matched cases from western new york. *Br J Cancer* 93(6):699-708.
- Velayos-Baeza A, Vettori A, Copley RR, Dobson-Stone C, Monaco AP. 2004. Analysis of the human VPS13 gene family. *Genomics* 84(3):536-49.
- Wang X and Seed B. 2003. A PCR primer bank for quantitative gene expression analysis. *Nucleic Acids Res* 31(24):e154.
- Watson RH, Roy WJ Jr, Davis M, Hitchcock A, Campbell IG. 1997. Loss of heterozygosity at the alpha-inhibin locus on chromosome 2q is not a feature of human granulosa cell tumors. *Gynecol Oncol* 65(3):387-90.
- Wu C, Orozco C, Boyer J, Leglise M, Goodale J, Batalov S, Hodge CL, Haase J, Janes J, Huss JW 3rd, et al. 2009. BioGPS: An extensible and customizable portal for querying and organizing gene annotation resources. *Genome Biol* 10(11):R130.
- Young RH. 2005. Sex cord-stromal tumors of the ovary and testis: Their similarities and differences with consideration of selected problems. *Mod Pathol* 18 Suppl 2:S81-98.
- Young RH, Dickersin GR, Scully RE. 1984. Juvenile granulosa cell tumor of the ovary. A clinicopathological analysis of 125 cases. *Am J Surg Pathol* 8(8):575-96.
- Zhang H, Zhai Y, Hu Z, Wu C, Qian J, Jia W, Ma F, Huang W, Yu L, Yue W, et al. 2010. Genome-wide association study identifies 1p36.22 as a new susceptibility locus for hepatocellular carcinoma in chronic hepatitis B virus carriers. *Nat Genet* 42(9):755-8.

Appendix A

Contributions

- Sarah Halfyard, a research assistant in the Dorward laboratory, identified, designed, and tested novel SSLP genotyping markers (*D4sjh10*, *D4sjh11*, *D4sjh12*, *D4sjh13* and *D4sjh19*), and conducted sequencing of *Nppb*, for the purposes of phenotypic mapping at *Gct1*. Ms. Halfyard conducted the majority of subline generation ($n = 6$) and genotyping until December 2009, when the project transitioned into my hands. Overall, I was responsible for the majority of the capsule implantation surgeries and phenotype analysis, fine mapping of the *Gct1* interval, and candidate gene testing.
- Katie Macdonald, an MSc student in the Dorward laboratory, collected serum samples from SWR and Line 4-T mice for the serum DHEA analysis.

Appendix B

Copyright Permission



PERMISSION LICENSE - PRINT REPLICATION

Request ID/Invoice Number: KR44835

Date: June 17, 2011

To: Kerri Smith
5357, Health Sciences Centre
300 Prince Philip Drive
St. John's NL
A1B 3V6 NL
CANADA
"Licensee"

McGraw-Hill Material

Author: Mescher, Anthony
Title: Junqueira's Basic Histology, 12/e © 2010
ISBN: 0071604316
Description of material: Figures 22.2, pg. 390 and 22.3, pg. 391 (ONLY)

Fee: WAIVED [DISSERTATION]

Licensee Work:

Author: Kerri Smith
Title: Positional cloning of the Gc1d granulosa cell tumour susceptibility locus in SWR inbred mice [DISSERTATION]
Publisher: Memorial University of Newfoundland
Publication Date: 2011
Print Run: 2
Distribution Territory: Canada
Languages: English

Permission for the use described above is granted under the following conditions:

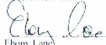
1. The permission fee is waived.
2. No adaptations, deletions, or changes will be made in the material without the prior written consent of The McGraw-Hill Companies.

Request ID/Invoice Number: KR44835

-
3. This permission is non-exclusive, non-transferable, and limited to the use specified herein. The McGraw-Hill Companies expressly reserves all rights in this material.
 4. A credit line must be printed on the first page in which the material appears. This credit must include the author, title, copyright date, and publisher, and indicate that the material is reproduced with permission of The McGraw-Hill Companies.
 5. This permission does not allow the use of any material, including but not limited to photographs, charts, and other illustrations, which appears in a McGraw-Hill Companies' work copyrighted in or credited to the name of any person or entity other than The McGraw-Hill Companies. Should you desire permission to use such material, you must seek permission directly from the owner of that material, and if you use such material you agree to indemnify The McGraw-Hill Companies against any claim from the owners of that material.

Please sign both copies and return one to the McGraw-Hill Permissions Department, 2 Penn Plaza, 10th Floor, New York, NY 10121.

For McGraw-Hill:


Ebony Lane _____
Permissions Department
McGraw-Hill Education

For Licensee:

Name _____

Title _____

Request ID Invoice Number: K1R44835

Appendix C

Harvard PrimerBank IDs for primer sequences used in the qualitative gene expression analysis

Gene	Harvard PrimerBank ID
<i>Gm436</i>	147905892b2
<i>Gm13178</i>	148222100b3
<i>Dhrs3</i>	14290432a3
<i>Vps13d</i>	189491888b2
<i>Tnfrsf1b</i>	6755827a2
<i>Tnfrsf8</i>	6678385a2

Appendix D

Alignment of the SWR, Line 4-T (4-T), and B6 *Tuf3flb* cDNA nucleotide sequences. Bp differences in SWR compared to Line 4-T and B6 are highlighted.

*: identities; -: deletion; gaps: nucleotide changes.

```
4-T AGTCACCAGCTAGAGCGCAGCTGAGGCACTAGAGCTCCAGGCACAAGGGCGGGAGCCACC
SWR AGTCACCAGCTAGAGCGCAGCTGAGGCACTAGAGCTCCAGGCACAAGGGCGGGAGCCACC
B6  AGTCACCAGCTAGAGCGCAGCTGAGGCACTAGAGCTCCAGGCACAAGGGCGGGAGCCACC
*****

4-T GCTGCCCCATATGGCGCCCGCCGCTCTGGGTGCGCTGGTCTTCGAACTGCAGCTGTGG
SWR GCTGCCCCATATGGCGCCCGCCGCTCTGGGTGCGCTGGTCTTCGAACTGCAGCTGTGG
B6  GCTGCCCCATATGGCGCCCGCCGCTCTGGGTGCGCTGGTCTTCGAACTGCAGCTGTGG
*****

4-T GCCACCGGGCACACAGTGCCCGCCAGGTTGTCTTGACACCCCTACAAACCGGAACCTGGG
SWR GCCACCGGGCACACAGTGCCCGCCAGGTTGTCTTGACACCCCTACAAACCGGAACCTGGG
B6  GCCACCGGGCACACAGTGCCCGCCAGGTTGTCTTGACACCCCTACAAACCGGAACCTGGG
*****

4-T TACGAGTGCCAGATCTCACAGGAATACTATGACAGGAAGGCTCAGATGTGCTGTGCTAAG
SWR TACGAGTGCCAGATCTCACAGGAATACTATGACAGGAAGGCTCAGATGTGCTGTGCTAAG
B6  TACGAGTGCCAGATCTCACAGGAATACTATGACAGGAAGGCTCAGATGTGCTGTGCTAAG
*****

4-T TGTCTCCTGGCCAATATGTGAAACATTTCTGCAACAAGACCTCGGACACCGTGTGTGCG
SWR TGTCTCCTGGCCAATATGTGAAACATTTCTGCAACAAGACCTCGGACACCGTGTGTGCG
B6  TGTCTCCTGGCCAATATGTGAAACATTTCTGCAACAAGACCTCGGACACCGTGTGTGCG
*****

4-T GACTGTGAGGCAAGCATGTATACCCAGGCTGGAACCAAGTTTCGTACATGTTTGAGCTGC
SWR GACTGTGAGGCAAGCATGTATACCCAGGCTGGAACCAAGTTTCGTACATGTTTGAGCTGC
B6  GACTGTGAGGCAAGCATGTATACCCAGGCTGGAACCAAGTTTCGTACATGTTTGAGCTGC
*****

4-T AGTTCTTCCTGTAGCACTGACCAGGTGGAGACCCGCGCTGCACTAAACAGCAGAACC GA
SWR AGTTCTTCCTGTAGCACTGACCAGGTGGAGACCCGCGCTGCACTAAACAGCAGAACC GA
B6  AGTTCTTCCTGTAGCACTGACCAGGTGGAGATCCGCGCTGCACTAAACAGCAGAACC GA
*****
```

```

4-T GTGTGTGCTTGCGAAGCTGGCAGGTA CTGCGCCTTGAAAACCCATTCTGGCAGCTGTCCA
SWR GTGTGTGCTTGCGAAGCTGGCAGGTA CTGCGCCTTGAAAACCCATTCTGGCAGCTGTCCA
B6 GTGTGTGCTTGCGAAGCTGGCAGGTA CTGCGCCTTGAAAACCCATTCTGGCAGCTGTCCA
*****

4-T CAGTGCATGAGGCTGAGCAAGTGC GGGCCCTGGCTTCGGAGTGGCCAGTTCAAGAGCCCCA
SWR CAGTGCATGAGGCTGAGCAAGTGC GGGCCCTGGCTTCGGAGTGGCCAGTTCAAGAGCCCCA
B6 CAGTGCATGAGGCTGAGCAAGTGC GGGCCCTGGCTTCGGAGTGGCCAGTTCAAGAGCCCCA
*****

4-T AATGGAAATGTGCTATGCAAGGCC TGTGCCCCAGGGACATTCCTGACACCACATCATCC
SWR AATGGAAATGTGCTATGCAAGGCC TGTGCCCCAGGGACATTCCTGACACCACATCATCC
B6 AATGGAAATGTGCTATGCAAGGCC TGTGCCCCAGGGACATTCCTGACACCACATCATCC
*****

4-T ACAGATGTGTGCAGGCCCCACCGCA TCTGTAGCATCCTGGCTATTCGCCGAAATGCAAGC
SWR ACAGATGTGTGCAGGCCCCACCGCA TCTGTAGCATCCTGGCTATTCGCCGAAATGCAAGC
B6 ACTGATGTGTGCAGGCCCCACCGCA TCTGTAGCATCCTGGCTATTCGCCGAAATGCAAGC
** *****

4-T ACAGATGCAGTCTGTGCGCCCGAGT CCCCCAACTCTAAGTGCCATCCCAAGGACACTCTAC
SWR ACAGATGCAGTCTGTGCGCCCGAGT CCCCCAACTCTAAGTGCCATCCCAAGGACACTCTAC
B6 ACAGATGCAGTCTGTGCGCCCGAGT CCCCCAACTCTAAGTGCCATCCCAAGGACACTCTAC
*****

4-T GTATCTCAGCCAGAGCCCCACAAGAT CCCCACCCCTGGATCAAGAGCCAGGGCCAGCCAA
SWR GTATCTCAGCCAGAGCCCCACAAGAT CCCCACCCCTGGATCAAGAGCCAGGGCCAGCCAA
B6 GTATCTCAGCCAGAGCCCCACAAGAT CCCCACCCCTGGATCAAGAGCCAGGGCCAGCCAA
*****

4-T ACTCCAAGCATCCTTACATCGTTGGG TTCAACCCCCATTATTGAACAAAGTACCAAGGGT
SWR ACTCCAAGCATCCTTACATCGTTGGG TTCAACCCCCATTATTGAACAAAGTACCAAGGGT
B6 ACTCCAAGCATCCTTACATCGTTGGG TTCAACCCCCATTATTGAACAAAGTACCAAGGGT
*****

4-T GGCATCTCTCTTCCAATTGGTCTGAT TGTTGGAGTGACATCACTGGGTCTGCTGATGTTA
SWR GGCATCTCTCTTCCAATTGGTCTGAT TGTTGGAGTGACATCACTGGGTCTGCTGATGTTA
B6 GGCATCTCTCTTCCAATTGGTCTGAT TGTTGGAGTGACATCACTGGGTCTGCTGATGTTA
*****

4-T GGACTGGTGAAGTCTTATCCTGGTGC AGAGGAAAAAGAAGCCCTCCTGCCTACAAAAGA
SWR GGACTGGTGAAGTCTTATCCTGGTGC AGAGGAAAAAGAAGCCCTCCTGCCTACAAAAGA
B6 GGACTGGTGAAGTCTTATCCTGGTGC AGAGGAAAAAGAAGCCCTCCTGCCTACAAAAGA
*****

4-T GATGCCAAGGTGCCTCATGTGCCTGAT GAGAAATCCCAGGATGCAGTAGGCCTTGAGCAG
SWR GATGCCAAGGTGCCTCATGTGCCTGAT GAGAAATCCCAGGATGCAGTAGGCCTTGAGCAG
B6 GATGCCAAGGTGCCTCATGTGCCTGAT GAGAAATCCCAGGATGCAGTAGGCCTTGAGCAG
*****

```

4-T CAGCACCTGTTGAC CACAGCACCCAGTTC CAGCAGCAGCTCCCTAGAGAGCTCAGCCAGC
 SWR CAGCACCTGTTGACTACAGCACCCAGTTC CAGCAGCAGCTCCCTAGAGAGCTCAGCCAGC
 B6 CAGCACCTGTTGAC CACAGCACCCAGTTC CAGCAGCAGCTCCCTAGAGAGCTCAGCCAGC

4-T GCTGGGGACCGAAGGGCGCCCCCTGGGGGCCATCCCCAAGCAAGAGTCATGGCGGAGGCC
 SWR GCTGGGGATCGAAGGGCGCCCCCTGGGGGCCATCCCCAAGCAAGAGTCATGGCGGAGGCC
 B6 GCTGGGGACCGAAGGGCGCCCCCTGGGGGCCATCCCCAAGCAAGAGTCATGGCGGAGGCC

4-T CAAGGGTTCAGGAGGCCCGTGCCAGCTCCAGGATTCAGATTCCTCCACGGGAAGCCAC
 SWR CAAGGGTTCAGGAGGCCCGTGCCAGCTCCAGGATTCAGATTCCTCCACGGGAAGCCAC
 B6 CAAGGGTTCAGGAGGCCCGTGCCAGCTCCAGGATTCAGATTCCTCCACGGGAAGCCAC

4-T GGGACCCACGTCAACGTCACTGCATCGTGAACGTCTGTAGCAGCTCTGACCCACAGCTCT
 SWR GGGACCCACGTCAACGTCACTGCATCGTGAACGTCTGTAGCAGCTCTGACCCACAGCTCT
 B6 GGGACCCACGTCAACGTCACTGCATCGTGAACGTCTGTAGCAGCTCTGACCCACAGTTC

4-T CAGTGCTCTTCCCAAGCCAGCGCCACGGTGGGAGACCCAGATGCCAAGCCCTCAGCGTCC
 SWR CAGTGCTCTTCCCAAGCCAGCGCCACGGTGGGAGACCCAGATGCCAAGCCCTCAGCGTCC
 B6 CAGTGCTCTTCCCAAGCCAGCGCCACAGTGGGAGACCCAGATGCCAAGCCCTCAGCGTCC

4-T CCAAAGGATGAGCAGGTCCCTTCTCTCAGGAGGAGTGTCGGTCTCAGTCCCCTGATGAG
 SWR CCAAAGGATGAGCAGGTCCCTTCTCTCAGGAGGAGTGTCGGTCTCAGTCCCCTGATGAG
 B6 CCAAAGGATGAGCAGGTCCCTTCTCTCAGGAGGAGTGTCGGTCTCAGTCCCCTGATGAG

4-T ACTACAGAGACTGCAGAGCCATGAGAAGCCCTTGCCCCCTGGGTGCCC GATATGGGC
 SWR ACTACAGAGACTGCAGAGCCATGAGAAGCCCTTGCCCCCTGGGTGCCC GATATGGGC
 B6 ACTACAGAGACTGCAGAGCCATGAGAAGCCCTTGCCCCCTGGGTGCCC GATATGGGC

4-T ATGAAGCCAGCCAAGCTGGCTGGTTTGATCAGATTGCAGTCAAAGTGGCCTGACCCCTG
 SWR ATGAAGCCAGCCAAGCTGGCTGGTTTGATCAGATTGCAGTCAAAGTGGCCTGACCCCTG
 B6 ATGAAGCCAGCCAAGCTGGCTGGTTTGATCAGATTGCAGTCAAAGTGGCCTGACCCCTG

4-T ACAGGGGTAACACCCTGCAAAGTGACCCCGAGACCCTGAACCCATGGAACCTTCATGACT
 SWR ACAGGGGTAACACCCTGCAAAGTGACCCCGAGACCCTGAACCCATGGAACCTTCATGACT
 B6 ACAGGGGTAACACCCTGCAAAGGGACCCCGAGACCCTGAACCCATGGAACCTTCATGACT

4-T TTTGCTGGATCCATTTCCCTTAGTGGCTTCCAGAGCCCCAGTTGCAGGTCAAAGTGAAGGC
 SWR TTTGCTGGATCCATTTCCCTTAGTGGCTTCCAGAGCCCCAGTTGCAGGTCAAAGTGAAGGC
 B6 TTTGCTGGATCCATTTCCCTTAGTGGCTTCCAGAGCCCCAGTTGCAGGTCAAAGTGAAGGC

4-T TGAGGCAGCTAGAGTGGTCAAAAACTGCCATGGTGTGTTTTATGGGGGCAGTCCCAGGAAGT
 SWR TGAGGCAGCTAGAGTGGTCAAAAACTGCCATGGTGTGTTTTATGGGGGCAGTCCCAGGAAGT
 B6 TGAGACAGCTAGAGTGGTCAAAAACTGCCATGGTGTGTTTTATGGGGGCAGTCCCAGGAAGT

4-T TGTGCTCTTCCATGACCCCTCTGGATCTCCTGGGCTCTTGCCTGATTCTTGCTTCTGAG
 SWR TGTGCTCTTCCATGACCCCTCTGGATCTCCTGGGCTCTTGCCTGATTCTTGCTTCTGAG
 B6 TGTGCTCTTCCATGACCCCTCTGGATCTCCTGGGCTCTTGCCTGATTCTTGCTTCTGAG

4-T AGGCCCCAGTATCTTTTCCTTCTAAGGAGCTAACATCCTCTTCCATGAATAGCACAGCTC
 SWR AGGCCCCAGTATCTTTTCCTTCTAAGGAGCTAACATCCTCTTCCATGAATAGCACAGCTC
 B6 AGGCCCCAGTATTTTCCTTCTAAGGAGCTAACATCCTCTTCCATGAATAGCACAGCTC

4-T TTCAGCCTGAATGCTGACACTGCAGGGCGGTCCAGCAAGTAGGAGCAAGTGGTGGCCTG
 SWR TTCAGCCTGAATGCTGACACTGCAGGGCGGTCCAGCAAGTAGGAGCAAGTGGTGGCCTG
 B6 TTCAGCCTGAATGCTGACACTGCAGGGCGGTCCAGCAAGTAGGAGCAAGTGGTGGCCTG

4-T GTAAGGCACAGAGGCCCTTCAGGTTAGTGCTAAACTCTTAGGAAGTACCCTCTCCAAGCC
 SWR GTAAGGCACAGAGGCCCTTCAGGTTAGTGCTAAACTCTTAGGAAGTACCCTCTCCAAGCC
 B6 GTAGGGCACAGAGGCCCTTCAGGTTAGTGCTAAACTCTTAGGAAGTACCCTCTCCAAGCC

4-T CACCGAAATTCCTTTTGATGCAAGAATCAGAGGCCCATCAGGCAGGGTTGCTCTGTATA
 SWR CACCGAAATTCCTTTTGATGCAAGAATCAGAGGCCCATCAGGCAGAGTTGCTCTGTATA
 B6 CACCGAAATTCCTTTTGATGCAAGAATCAGAGGCCCATCAGGCAGAGTTGCTCTGTATA

4-T GGATGGTAGGGCTTAAGTCAAGTGGTCCAGTGTGCTTTTAGCATGCCCCTGGGTTTGATCC
 SWR GGATGGTAGGGCTTAAGTCAAGTGGTCCAGTGTGCTTTTAGCATGCCCCTGGGTTTGATCC
 B6 GGATGGTAGGGCTTAAGTCAAGTGGTCCAGTGTGCTTTTAGCATGCCCCTGGGTTTGATCC

4-T TCAGCAACATATGCAAAAACGTAAGTAGACAGCAGACAGCAGACAGCCAGCCCCCT
 SWR TCAGCAACACATGCAAAAACGTAAGTAGACAGCAGACAGCAGACAGCCAGCCCCCT
 B6 TCAGCAACACATGCAAAAACGTAAGTAGACAGCAGACAGCAGACAGCCAGCCCCCT

4-T GTGTGGTTTGACAGCCTCTGCCTTTGACTTTTACTCTGGTGGGCACACAGAGGGCTGGAGC
 SWR GTGTGGTTTGACAGCCTCTGCCTTTGACTTTTACTCTGGTGGGCACACAGAGGGCTGGAGC
 B6 GTGTGGTTTGACAGCCTCTGCCTTTGACTTTTACTCTGGTGGGCACACAGAGGGCTGGAGC

4-T TCCTCCTCCTGACCTTCTAATGAGCCCTTCCAAGGCCACGCCTTCTTCAGGGAATCTCA
 SWR TCCTCCTCCTGACCTTCTAATGAGCCCTTCCAAGGCCACGCCTTCTTCAGGGAATCTCA
 B6 TCCTCCTCCTGACCTTCTAATGAGCCCTTCCAAGGCCACGCCTTCTTCAGGGAATCTCA

4-T GGGACTGTAGAGTTCCCAAGGCCCTGCAGCCACCTGTCTCTTCTACCTCAGCCTGGAGC
 SWR GGGACTGTAGAGTTCCCAAGGCCCTGCAGCCACCTGTCTCTTCTACCTCAGCCTGGAGC
 B6 GGGACTGTAGAGTTCCCAAGGCCCTGCAGCCACCTGTCTCTTCTACCTCAGCCTGGAGC

4-T ACTCCCTCTAACTCCCCAACGGCTTGGTACTGTACTCGCTGTGACCCCAAGTGCATGTCC
 SWR ACTCCCTCTAACTCCCCAACGGCTTGGTACTGTACTCGCTGTGATCCCAAGTGCATGTCC
 B6 ACTCCCTCTAACTCCCCAACGGCTTGGTACTGTACTGTGATCCCAAGTGCATGTCC

4-T GGGTTAGGCACTGTGAGTTGGAACAGCTGATGACATCGGTTGAAAGTCCCACCCGGAAAC
 SWR GGGTTAGGCACTGTGAGTTGGAACAGCTGATGACATCGGTTGAAAGGCCACCCGGAAAC
 B6 GGGTTAGGCACTGTGAGTTGGAACAGCTGATGACATCGGTTGAAAGGCCACCCGGAAAC

4-T AGCTGAAGCCAGCTCTTTTGCCAAAGGATTATGCCGGTTTTCTAATCAACCTGCTCCCC
 SWR AGCTGAAGCCAGCTCTTTTGCCAAAGGATTATGCCGGTTTTCTAATCAACCTGCTCCCC
 B6 AGCTGAAGCCAGCTCTTTTGCCAAAGGATTATGCCGGTTTTCTAATCAACCTGCTCCCC

4-T TAGCATGCCTGGAAGGAAAGGGTTCAGGAGACTCCTCAAGAAGCAAGTTCAGTCTCAGGT
 SWR TAGCATGCCTGGAAGGAAAGGGTTCAGGAGACTCCTCAAGAAGCAAGTTCAGTCTCAGGT
 B6 TAGCATGCCTGGAAGGAAAGGGTTCAGGAGACTCCTCAAGAAGCAAGTTCAGTCTCAGGT

4-T GCTTGGATGCCATGCTCACCATTCCACTGGATATGAACTTGGCAGAGGAGCCTAGTTGT
 SWR GCTTGGATGCCATGCTCACCATTCCACTGGATATGAACTTGGCAGAGGAGCCTAGTTGT
 B6 GCTTGGATGCCATGCTCACCATTCCACTGGATATGAACTTGGCAGAGGAGCCTAGTTGT

4-T TGCCATGGAGACTTAAAGAGCTCAGCACTCTGGAATCAAGATACTGGACACTTGGGGCCG
 SWR TGCCATGGAGACTTAAAGAGCTCAGCACTCTGGAATCAAGATACTGGACACTTGGGGCCG
 B6 TGCCATGGAGACTTAAAGAGCTCAGCACTCTGGAATCAAGATACTGGACACTTGGGGCCG

4-T ACTTGTTAAGGCTCTGCAGCATCAGACTGTAGAGGGGAAGGAACACGTCTGCCCCCTGGT
 SWR ACTTGTTAAGGCTCTGCAGCATCAGACTGTAGAGGGGAAGGAACACGTCTGCCCCCTGGT
 B6 ACTTGTTAAGGCTCTGCAGCATCAGACTGTAGAGGGGAAGGAACACGTCTGCCCCCTGGT

4-T GGCCAGTCCTGGAATGACCTCGGGCCTCCTAGGCAACAAAAGAATGAATTGGAAAGGACT
 SWR GGCCAGTCCTGGAATGACCTCGGGCCTCCTAGGCAACAAAAGAATGAATTGGAAAGGACT
 B6 GGCCCGTCTGGGATGACCTCGGGCCTCCTAGGCAACAAAAGAATGAATTGGAAAGGACT

4-T GTTCTGGGTGTGGCCTCAGCTCCTGTGCTTGTGTGGATCCCTAAAGGGTGTGCTAAGGA
 SWR GTTCTGGGTGTGGCCTCAGCTCCTGTGCTTGTGTGGATCCCTGAAAGGGTGTGCTAAGGA
 B6 GTTCTGGGTGTGGCCTCAGCTCCTGTGCTTGTGTGGATCCCTAAAGGGTGTGCTAAGGA

```

4-T  GCAATTGCACTGTGTGCTGGACAGAATTCCTGCTTATAAAATGCTTTTTTGTGTGTGTTTTG
SWR  GCAATTGCACTGTGTGCTGGACAGAATTCCTGCTTATAAAATGCTTTTTTGTGTGTGTTTTG
B6   GCAATTGCACTGTGTGCTGGACAGAATTCCTGCTTATAAAATGCTTTTTTGTGTGTGTTTTG
*****

4-T  TACTAGAGCCCTGGCTGTGTCTAGGTCTGGAGCCACCCACCCACCTCCCATCCCACC
SWR  TACTAGAGCCCTGGCTGTGTCTAGGTCTGGAGCCACCCACCCACCTCCCATCCCACC
B6   TACTAGAGCCCTGGCTG-----AGCCACCCACCCACCTCCCATCCCACC
*****

4-T  TTTACAGCCACTCTTGCAGAGAACCTGGCTATCTCCCACTTGTAGCCTGTGGATGCTGAG
SWR  TTTACAGCCACTCTTGCAGAGAACCTGGCTATCTCCCACTTGTAGCCTGTGGATGCTGAG
B6   TTTACAGCCACTCTTGCAGAGAACCTGGCTATCTCCCACTTGTAGCCTGTGGATGCTGAG
*****

4-T  GAAGCACCCAGCCAAGTAGACTCCAGGCTTGCCCTATCTCCTGCTCTGAGTCTGGCCTC
SWR  GAAGCACCCAGCCAAGTAGACTCCAGGCTTGCCCTATCTCCTGCTCTGAGTCTGGCCTC
B6   GAAACACCCAGCCAAGTAGACTCCAGGCTTGCCCTATCTCCTGCTCTGAGTCTGGCCTC
*** *****

4-T  CTCATTGTGTGTGGGAAGGAGACGGGTTCTGTCATCTCGGAAGCCACACGTGGATGT
SWR  CTCATTGTGTGTGGGAAGGAGACGGGTTCTGTCATCTCGGAAGCCACACGTGGATGT
B6   CTCATTGTGTGTGGGAAGGAGACGGGTTCTGTCATCTCGGAAGCCACACGTGGATGT
*****

4-T  GAACAATGGCTGTACTAGCTTAGACCAGCTTAGGGCTCTGCAATCAGAGGAGGGGG-GCA
SWR  AACAATGGCTGTACTAGCTTAGACCAGCTTAGGGCTCTGCAATCAGAGGAGGGGG-GCA
B6   AACAATGGCTGTACTAGCTTAGACCAGCTTAGGGCTCTGCAATCAGAGGAGGGGGAGCA
*****

4-T  GGAACAATTTGAGTGTGACCTATAACACATTCTAAAGGATGGGCAGTCCAGAATCTC
SWR  GGAACAATTTGAGTGTGACCTATAACACATTCTAAAGGATGGGCAGTCCAGAATCTC
B6   GGAACAATTTGAGTGTGACCTATAACACATTCTAAAGGATGGGCAGTCCAGAATCTC
*****

4-T  CTCCTTCAGTGTGTGTGTGTGTGTGTGTGTGTGTGTGTGTGTGTGTGTGTGTGTGTGTGTG
SWR  CTCCTTCAGTGTGTGTGTGTGTGTGTGTGTGTGTGTGTGTGTGTGTGTGTGTGTGTGTGTG
B6   CTCCTTCAGTGTGTGTGTGTGTGTGTGTGTGTGTGTGTGTGTGTGTGTGTGTGTGTGTGTG
*****

4-T  TGTGTGTGTGTGCCAGTGTGTGGAGGCCAGAGGTTGGCTTTGGGTGTGTTTGATCACT
SWR  --TGTGTGTGTGTGCCAGTGTGTGGAGGCCAGAGGTTGGCTTTGGGTGTGTTTGATCACT
B6   CATGTATGTGTGTGCCAGTGTGTGGAGGCCAGAGGTTGGCTTTGGGTGTGTTTGATCACT
*** *****

4-T  CTCAGTGTACTGAGGCAGGGCTCTCATCTGCACCCAGAGCTTGCACATTTTCTAGTCTAA
SWR  CTCAGTGTACTGAGGCAGGGCTCTCATCTGCACCCAGAGCTTGCACATTTTCTAGTCTAA
B6   CTCAGT-TACTGAGGCAGGGCTCTCATCTGTACCCAGAGCTTGCACATTTTCTAGTCTAA
*****

```

```

4-T   CTGGCTTCAGGGATCTCTGTCTGCCTATGGAGTGCTCAGGTTACAGGCAGGCTGCCATAC
SWR   CTGGCTTCAGGGATCTCTGTCTGCCTATGGAGTGCTCAGGTTACAGGCAGGCTGCCATAC
B6    CTGGCTTCAGGGATCTCTGTCTGCCTATGGAGTGCTCAGGTTACAGGCAGGCTGCCATAC
*****

4-T   CTGCCCAACATTTACATGAATACTAGAGATCTGAATTCCTGGTCTCACACTTGTAACCT
SWR   CTGCCCAACATTTACATGAATACTAGAGATCTGAATTCCTGGTCTCACACTTGTAACCT
B6    CTGCCCGACATTTACATGAATACTAGAGATCTGAATTCCTGGTCTCACACTTGTAACCT
*****

4-T   GCATTTTATCCACTAAGACATCTCTCCAAGGGCTCCCCCTTCCTATTTAATAAGTTAGTT
SWR   GCATTTTATCCACTAAGACATCTCTCCAAGGGCTCCCCCTTCCTATTTAATAAGTTAGTT
B6    GCATTTTATCCACTAAGACATCTCTCCAAGGGCTCCCCCTTCCTATTTAATAAGTTAGTT
*****

4-T   TTGAACTGGCAAGATGGCTCAGTGGGTAAGGCAGTTTGCGGACAAACCTGATGACCTGAG
SWR   TTGAACTGGCAAGATGGCTCAGTGGGTAAGGCAGTTTGCGGACAAACCTGATGACCTGAG
B6    TTGAACTGGCAAGATGGCTCAGTGGGTAAGGCAGTTTGCGGACAAACCTGATGACCTGAG
*****

4-T   TTGGATCCCTGACCATAAAGGTAGAAGAGACCTGATTCCTGCAAGTTGTCTCTGACCACC
SWR   TTGGATCCCTGACCATAAAGGTAGAAGAGACCTGATTCCTGCAAGTTGTCTCTGACCACC
B6    TTGGATCCCTGACCATAAAGGTAGAAGAGACCTGATTCCTGCAAGTTGTCTCTGACCACC
*****

4-T   ACCCCATACATGCTTCTGCATATGTGCACACATCACATTCTTGACAGACACTCACATAC
SWR   ACCCCATACATGCTTCTGCATATGTGCACACATCACATTCTTGACAGACACTCACATAC
B6    ACCCCATACATGCTTCTGCATATGTGCACACATCACATTCTTGACACACACTCACATAC
*****

4-T   CATAAATGTAATAAATTTTTTAAAAATAAATTGATTTTATTTTTTAATCATT
SWR   CATAAATGTAATAAATTTTTTAAAAATAAATTGATTTTATTTTTTAATCATT
B6    CATAAATGTAATAAATTTTTTAAA-TAAATTGATTTTATCTTTAATCATT
*****

```